THESIS

This is to certify that the

dissertation entitled

THEORETICAL AND EXPERIMENTAL
INVESTIGATION ON HYGROSCOPIC WARPING
OF WOOD COMPOSITE PANELS

presented by

DANPING XU

has been accepted towards fulfillment
of the requirements for

Ph.D. degree in FORESTRY

Major professor
Otto Suchsland

Date January 11, 1994

MSU is an Affirmative Action/Equal Opportunity Institution

O-12771

MICHIGAN STATE UNIVERSITY LIBRARIES
3 1293 01025 3627

LIBRARY
Michigan State
University

PLACE IN RETURN BOX to remove this checkout from your record.
TO AVOID FINES return on or before date due.

DATE DUE	DATE DUE	DATE DUE
052		

MSU is An Affirmative Action/Equal Opportunity Institution
c:\circ\datedue.pm3-p.1

THEORETICAL AND EXPERIMENTAL INVESTIGATION ON HYGROSCOPIC WARPING OF WOOD COMPOSITE PANELS

By

Dan Ping Xu

A DISSERTATION

Submitted to
Michigan State University
in partial fulfillment of the requirements
for the degree of

DOCTOR OF PHILOSOPHY

Department of Forestry

1994

ABSTRACT

THEORETICAL AND EXPERIMENTAL INVESTIGATION ON HYGROSCOPIC WARPING OF WOOD COMPOSITE PANELS

By

Dan Ping Xu

This thesis deals with the hygroscopic warping of laminated wood and wood composites. The theoretical analysis includes elastic, inelastic and visco-elastic approaches. Experiments were conducted on narrow cross laminated yellow-poplar beams and on two-ply beams constructed from laminas of medium-density-fiberboard and particleboard. The elastic strains and the swelling stresses that sustain warp under conditions of increasing moisture content were determined experimentally, using a specially designed restraining device.

In the case of the yellow-poplar laminates it was found that in the transverse direction (tangential) only about 25 percent of the free hygroscopic expansion is transformed into elastic strain under conditions of complete restraint. In the longitudinal direction, yellow-poplar behaves elastically. These results were used to modelling the inputs into the elastic warping equation (inelastic approach) which greatly improved the accuracy of the theoretical warping predictions.

mo

goo

bea

fou

and

two

the

In the case of laminate composites, the elastic equation without modification produced good agreements with measured warp.

The visco-elastic approach, although were time consuming produced good agreement in both cases.

A detailed discussion of the elastic warping equation for laminated beams is included. For a two-component multi-layer laminate warping is found to be a function of the ratio of the elastic moduli of the two materials, and to be proportional to the difference of the hygroscopic expansion of the two materials.

This study will allow the formulation of relative simple guidelines for the mathematical modeling of hygroscopic warping of wood based laminates.

Dedicated to my beloved Ruogong, Shen, and my dearest parents

ACKNOWLEDGMENTS

The author wishes to express her deepest appreciation to Dr. Otto Suchsland of the Department of Forestry, Michigan State University, for his guidance and encouragement in the preparation of this thesis and for his thought given throughout the course of this study. Thanks are also extended to the other members of the author's Ph. D. Degree Committee: Professors Alan Sliker of the Department of Forestry, Professor Frank Hatfield and Robert Wen of the Department of Civil and Environmental Engineering for their guidance.

She is particularly grateful to the financial support from the Michigan State University Forestry Department's Eastern Hardwood Utilization Research Program, which is funded by the USDA / Cooperative State Research Service.

Thanks are also due to Dr. Y. Feng, Dr. S. Hiziroglu and Dr. H. Xu for their help in preparing the experimental set up and sample cutting.

TABLE OF CONTENTS

TABLE OF CONTENTS (continued)

TABLE OF CONTENTS (continued)

LIST OF TABLES

LIS

Tab

Tab

Tab

Tab

Tab

Tab

Tab

Tab

Tab

Tab

Tab

Tabl

Tabl

Tabl

LIST OF TABLES (continued)

LIST OF FIGURES

LIST OF FIGURES (continued)

LIST OF FIGURES (continued)

LIST OF FIGURES (continued)

LIST OF SYMBOLS

a_i , b_i , m, D , γ : constants

C_{ijkl}: creep compliances

E: modulus of elasticity

E_θ the modulus at an angle θ from the grain direction

E_L the modulus in the grain direction

$E_\perp$ the modulus in the direction perpendicular to the grain

E_{fw} the modulus of elasticity of plywood in bending when the face grain is parallel to the span

E_{fw} the modulus of elasticity of plywood in bending when the face grain is perpendicular to the span

E' : deformation modulus

E_e : instantaneous modulus of elasticity

E_{de} : delayed modulus of elasticity

F: resultant force

I_i the moment of inertia of the i^{th} layer about the neutral plane of the plywood

I the moment of inertia of the total cross section about its center line

K: curvature of a beam

L: length of a beam

M:	resultant moment
R :	radius of curvature of a beam
S_i :	$= \sum_{1}^{i} T_i$, is a dimensional parameter
t :	time
T_i :	thickness of i^{th} layer of a beam
T	total thickness
ΔT	temperature change
W:	center deflection or warping
Y :	uniaxial swelling stress relaxation modulus
Y_{ijkl} :	relaxation moduli
x , y , z :	coordinates
α :	total free hygroscopic expansion value
α_{res}:	resultant expansion of a laminated beam
β :	hygroscopic or thermal expansion coefficient
ΔMC	the moisture content change brought about by a change in the relative humidity of the air
$\varepsilon(t)$:	time dependent strain
ε_{elast} :	elastic portion of expansion or instantaneous recovery of expansion
η_{de} =	delayed coefficient of viscosity
η_{v} =	viscous coefficient of viscosity
σ :	stress
σ_T :	thermal stress
μ :	Poisson's ratio
τ	retardation time

CHAPTER I
INTRODUCTION

1.1 The Warping Problem

This thesis deals with a significant technological problem afflicting panel materials made from solid wood or from small wooden elements laminated to form sheet materials. These sheet materials, which will be described in more detail later, may be overlaid with various thin decorative layers like veneers or other rigid or flexible layers. In this form, the laminated sheet materials are incorporated into furniture products such as tops, doors, shelves, etc.

The aforementioned problem is related to the absorption or desorption of water by these wood-based materials, which leads to dimensional changes and in certain cases to geometric distortions known as warping, cupping, or bowing. The geometric distortions can have different forms as indicated in Figure 1-1 [4].

Warping of such panels or of furniture elements made from such panels is both common and difficult to deal with. It is also a defect or characteristic which is often not repairable, and may require the replacement of the defective panel. It is difficult to deal with because it may only develop

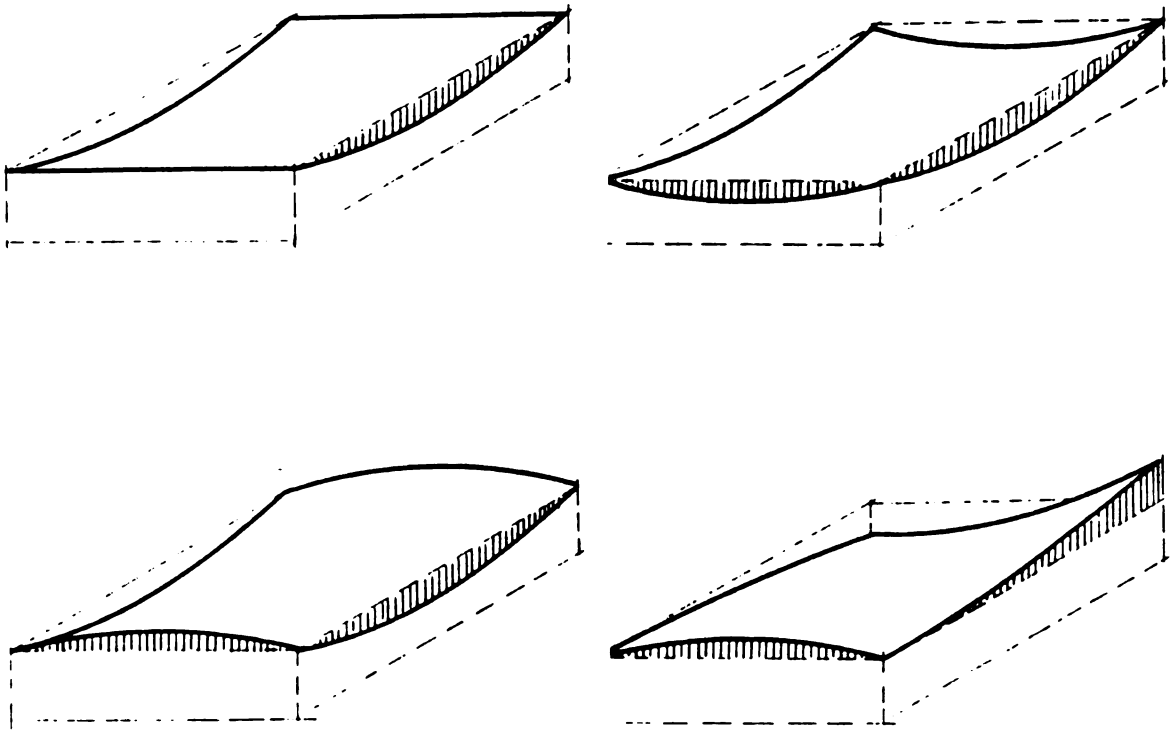

Figure 1-1 Examples of different forms of warping of flat panels [4].

long after the product has left the manufacturing plant. Thus, the warping potential of a panel can readily escape detection by standard quality control systems. It is, therefore, difficult to adjust selection and manufacturing processes and procedures in order to reduce the occurrence of panel warping.

Warping is always caused by an imbalance of forces acting in the plane of individual layers and resulting in bending moments. These forces are generated whenever the free hygroscopic expansion or shrinkage of individual layers is being restrained by adjacent layers.

Expansion or shrinkage difference between layers could be caused by a variety of factors, such as different hygroscopic equilibrium characteristics, differences in grain direction, species and other material characteristics. They may also be caused by uneven moisture uptake or loss. The inherent variability of wood material makes it almost impossible to consistently produce perfectly balanced, and thus, warp-free panels.

It would be desirable to analyze practical panel constructions with regard to their warping potentials and to assess the importance of various contributing factors. Such analysis could be based on available information on the physical and elastic properties and constants of the various materials involved but, while relatively simple, would have the disadvantage of not accounting for the distinct visco-elastic nature of wood materials, which significantly moderates internal stresses, particularly at high moisture contents.

This thesis attempts to take into consideration the visco-elastic characteristics of wood and their effect on warping tendencies of simple laminates made from veneer, wood particles, and wood fibers. The results of

such efforts, both experimental and theoretical, are then compared with results based on elastic calculations, and with measured warping of laminated beams exposed to changing relative humidities.

1.2 The Concept of Swelling Stress

The concept of swelling stress is illustrated in Figure 1-2 which shows the free and restrained axial expansion of a single layer short wood column as a result of a change in moisture content (MC) from MC_1 to MC_2 (ΔMC).

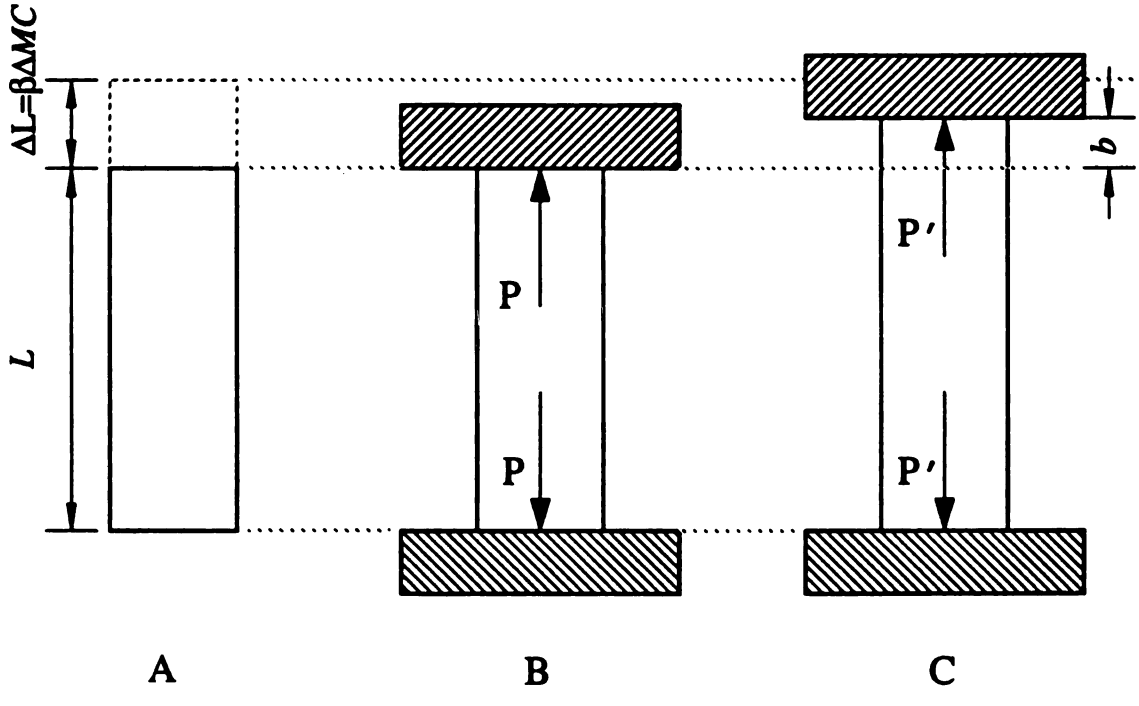

Figure 1-2 The concept of swelling stress. (A) free axial expansion; (B) completely restrained expansion; (C) partially restrained expansion.

Figure 1-2 (A) shows the free axial expansion of the column, which can be expressed as

$$\Delta L = \beta \ \Delta MC \tag{1.1}$$

where β = the axial expansion coefficient ($1/\Delta MC$)

ΔMC = the moisture content change brought about by a change in the relative humidity of the air (%).

The column after expansion is stress free.

Figure 1-2 (B) shows the same column expanding against a rigid clamp which prevents axial elongation. As a result of this restraint (in this case complete restraint) an axial swelling stress develops, which can be calculated as follows:

$$\begin{aligned} \sigma &= E \ \varepsilon \\ &= E \ \frac{\Delta L}{L} \\ &= E \ \frac{\beta \ \Delta MC}{L} \end{aligned} \tag{1.2}$$

or, for $L = 1$

$$\sigma = E \ \beta \ \Delta MC \tag{1.3}$$

where E = the modulus of elasticity in compression of the column at the end condition (MC_2), (psi).

Figure 1-2 (C) shows the same column under partial restraint, i.e. the rigid clamp allows a certain amount of free expansion, b, to occur ($b < \beta \ \Delta MC$).

The stress is now

$$\sigma' = E \ (\beta \ \Delta MC - b) \tag{1.4}$$

$$\sigma' < \sigma \tag{1.5}$$

These calculations are based on the important assumption that hygroscopic expansion converts to elastic strain.

This hygroscopic behavior of wood is analogous to the thermal behavior of metals. The equivalent thermal stress is:

$$\sigma_T = E \ \beta_T \ \Delta T \tag{1.6}$$

where $\beta_T =$ the thermal expansion coefficient ($1/°F$)

$\Delta T =$ the temperature change ($°F$).

The subject of thermal stress in metals has received considerable attention [11, 15, 18]. In many cases, equations developed for thermal stress can be applied directly to hygroscopic swelling or shrinking of wood materials [51].

Swelling stresses as depicted in Figure 1-2 can lead to buckling [51] and possibly to the destruction of slender columns or thin plates of wood composite materials by bending stress associated with buckling [16]. The typical condition leading to warping is indicated in Figure 1-3. Here, a wood material consisting of two layers having different expansion coefficients and different moduli of elasticity and being attached to one another by a rigid glue bond, is being subjected to a change in the relative humidity of the air.

Figure 1-3(A) shows the two layers and their free expansion as it would occur if the glue line did not exist. Although ΔMC is the same for both layers, their total expansion is different on account of the difference between their expansion coefficients ($\beta_2 > \beta_1$). The existence of the glue line imposes the condition of partial restraint on both layers (Figure 1-3 (B)), positive restraint in the case of layer 2 and negative restraint in the case of layer 1. The laminate expands by $\beta_{res}\Delta MC$, which causes compressive stress in layer 2 and tensile stress in layer 1, which could be expressed as follows:

$$\sigma_1 = E_1 \frac{e_1}{L+\beta_1\Delta MC} \tag{1.7}$$

or, for unit length $L = 1$

$$\sigma_1 = E_1 \frac{e_1}{1+\beta_1\Delta MC} \tag{1.8}$$

and

$$\sigma_2 = E_2 \frac{e_2}{1+\beta_2\Delta MC} \tag{1.9}$$

If both layers have the same cross-section area, then the average stress in tension and average stress in compression will be in equilibrium,

$$\sigma_1 = \sigma_2 \tag{1.10}$$

The two stresses form a bending moment which results in the warping of the laminate.

Again, the assumption here is that hygroscopic expansion transforms into elastic strain.

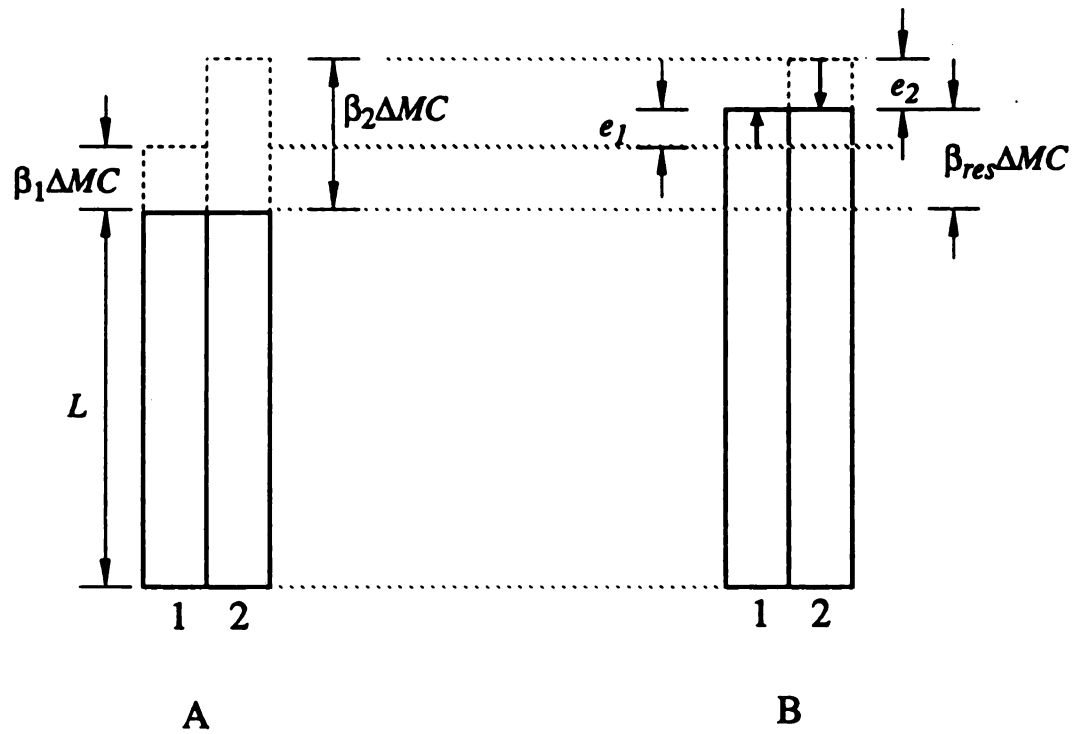

Figure 1-3 The free expansion of beam components (A) and resultant expansion of laminated two-layer beam (B).

1.3 Previous Work on Panel Warping

The elastic approach described above is essentially the approach taken by most researchers who have tried to predict the warping of various types of wood based laminates*. These studies evaluate the end conditions of the warp, i.e. the warp after all elements have reached their equilibrium moisture contents. This kind of warp is always due to some structural imbalance and will be sustained as long as the environmental end conditions are maintained.

Warp may also occur as a consequence of a transient imbalance such as the development of an unbalanced moisture content gradient. If given enough time, the moisture content gradient imbalance will disappear and the panel will flatten out again. Such warp is described by Tong and Suchsland [54]. The theoretical warp of one quadrant of a Douglas fir board having an initial moisture content of 12 percent and moisture content increases at the four identical planes of

+ 8 percent at bottom surface

+ 6 percent at 1/3 thickness from bottom surface

+ 4 percent at 2/3 thickness from bottom surface

+ 2 percent at top surface

is shown in Figure 1-4. This study was based on a finite element model.

Iwashita and Stashevski [17] measured and calculated the warping of panels consisting of various particleboard types overlaid on one side with high pressure laminates (HPL). The distortions were measured on

---

* The equation used for predicting the warp of a multi-layered laminate will be discussed in a later chapter.

approximately 90 *cm* x 90 *cm* square panels. Board substrates were 20 *mm* thick. Some had been overlaid with veneer prior to the application of HPL. Exposure conditions were:

12 percent equilibrium moisture content (65 percent relative humidity)
to 20 percent equilibrium moisture content (90 percent relative humidity)
to 12 percent equilibrium moisture content (65 percent relative humidity)
to 6 percent equilibrium moisture content (30 percent relative humidity)
to 12 percent equilibrium moisture content (65 percent relative humidity)

There was a fair agreement between computed values based on elastic assumption (see Section 2.3) and measured values in some cases. In others, real discrepancies existed.

Heebink and Haskell [13, 14] measured properties of HPL materials. This information was later utilized in a follow-up study [32] on the warping of three-ply laminates consisting of high pressure laminate (HPL) face, particleboard, and HPL backer sheet. There was a fairly good agreement between calculated and measured warping.

The warping of a veneered cabinet door was analyzed by Suchsland in 1990 [44, 45]. By applying an elastic warping model to the exact construction of the warped door, the effects of such variables as grain deviation in the veneer layers, species differences, and veneer thickness differences were investigated. The results showed warping of the same order of magnitude as that exhibited by the real door. It was also found that warping caused by imbalances in the panel construction could be amplified by large moisture content changes in the core material. The study indicated that careful monitoring of the moisture content of components at the time of assembly is

an essential prerequisite to the elimination of large moisture content differences among layers and to the manufacture of stable panels.

A study of wood-based composite sheathing materials exposed to fluctuating conditions was conducted by Hiziroglu [16]. Elastic analysis indicated that even moderate moisture content changes in the materials could lead to bending stresses exceeding the ultimate bending strength. But the experimental investigation revealed that these materials are not elastic and that relaxation at high relative humidities reduces the maximal bending stresses to about 40 to 50 percent of the bending strength. A buckled OSB beam does not return to its original straight configuration upon regaining its initial moisture content, and at the initial moisture content, the axial stress does not disappear but turns from compression into a sizable tensile stress (Figure 1-5).

Restrained hardboard columns upon moisture cycling showed similar results [51] as shown in Figure 1-6.

Suchsland and McNatt conducted a comprehensive study of the warping of laminated panels [47]. Emphasis in this study was on the theoretical evaluations of the effect of the variability of panel component properties, particularly of those of the face and back layers of multi-layered laminates on the warping of structurally balanced and unbalanced panels.

Figure 1-7 indicates the range of predicted warping during two different exposure changes as affected by a thickness imbalance and by assumed ranges of face and back veneer variability as indicated by their coefficients of variation. Figure 1-8 shows the predicted warping of the same panel without thickness imbalance. These warping values seem to be

extremely high (up to 5 in. center deflection over 48 in. span). It must be concluded that this warping response to a relatively small relative humidity change would be greatly reduced in a real panel by considerable creep and stress relaxation across the grain of face and back veneers.

Warping along the grain, on the other hand, again due to assumed variation of lamina characteristics, is much smaller (Figure 1-9). Here the elastic approach produces much more realistic results because the expansion values along the grain are very small and the modulus of elasticity very high, a combination resulting in more elastic behavior. This does not mean that the practical or real panel shows no warping tendencies along the face grain. The real panel does warp, because of its great sensitivity to even small grain deviations from the true longitudinal orientation (Figure 1-10).

A study of the warping of overlaid particleboard was conducted by Suchsland, Feng and Xu [42]. These laminates, consisting of different particleboard substrates and of various types of plastic overlays, both in 2-ply and 3-ply constructions, were exposed to one moisture cycle, and the warp was measured and also calculated based on elastic assumptions. Residual warping at the end of the cycle indicated viscoelastic behavior, at least on the part of the particleboard substrates (Figure 1-11 and Figure 1-12).

A recent study by H. Xu [57] developed a visco-elastic plate theory, taking into account the effects of changing moisture contents over time, and applies this theory with good results to the prediction of the warp of a two-ply yellow-poplar laminate (Figure 1-13).

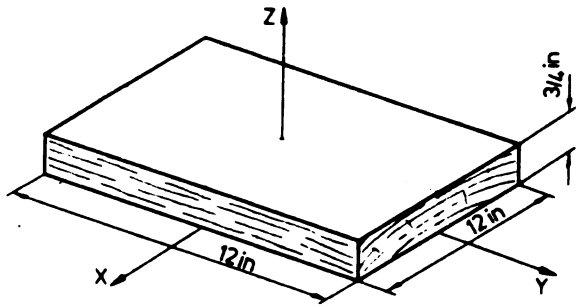

a) Douglas-fir plate used as an example for finite element approximation of panel warping.

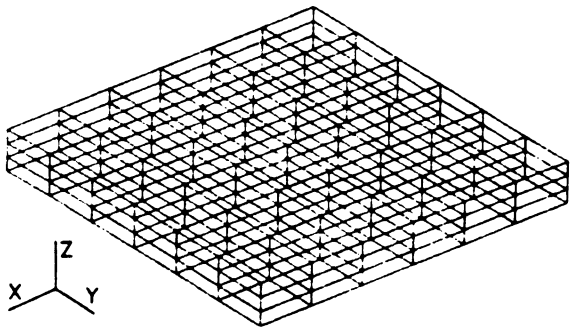

b) Finite element mesh representing 6in by 6in quadrant of Douglas-fir plate. Horizontal planes are planes of equal moisture content change.

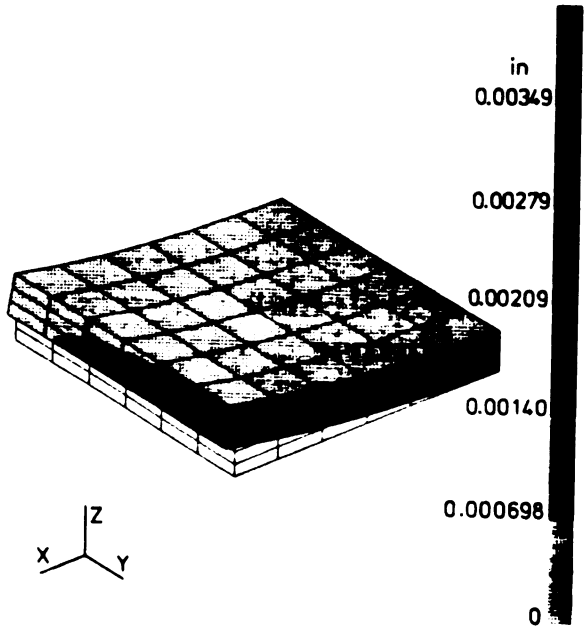

c) Warping of 6in by 6in quadrant of Douglas-fir plate. Displacement in Y-direction is indicated by shading. Maximum u_y (0.00349in) occurs at bottom surface of lower corner.

Figure 1-4 Warping of solid wood panel [54].

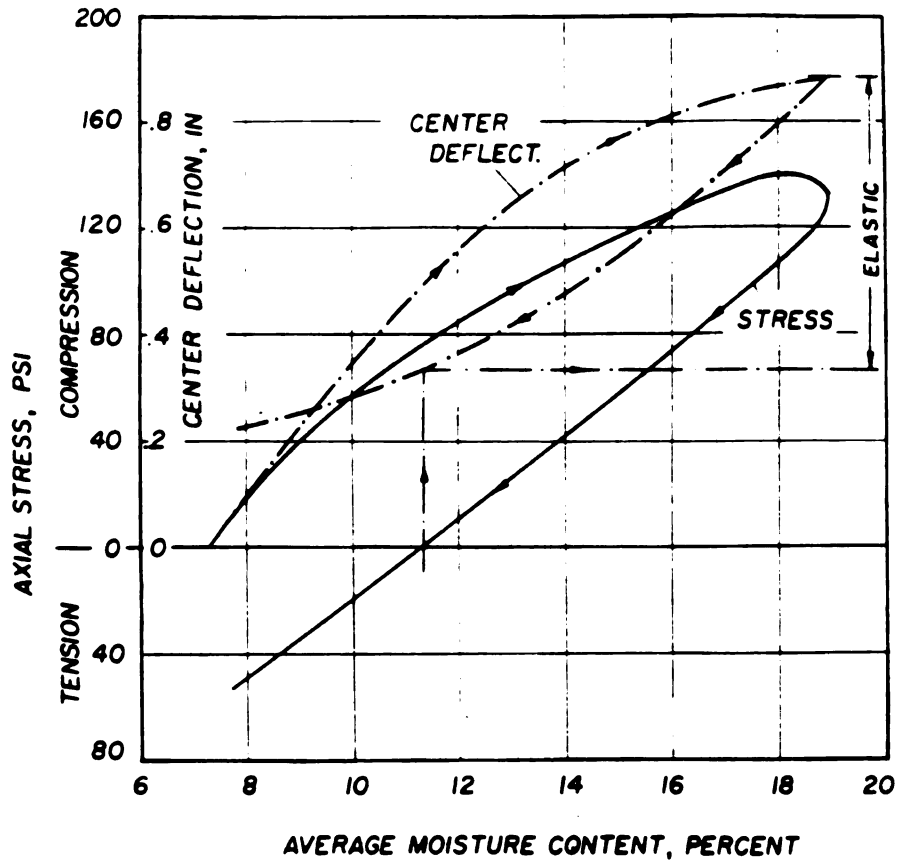

Figure 1-5 Stresses in axially restrained wood composite. Results of one exposure cycle (36% to 93% to 36% RH). Graph indicates axial stress and center deflection as functions of average MC. Upon reversal of exposure condition (93% to 36% RH), center deflection does not fully recover [16].

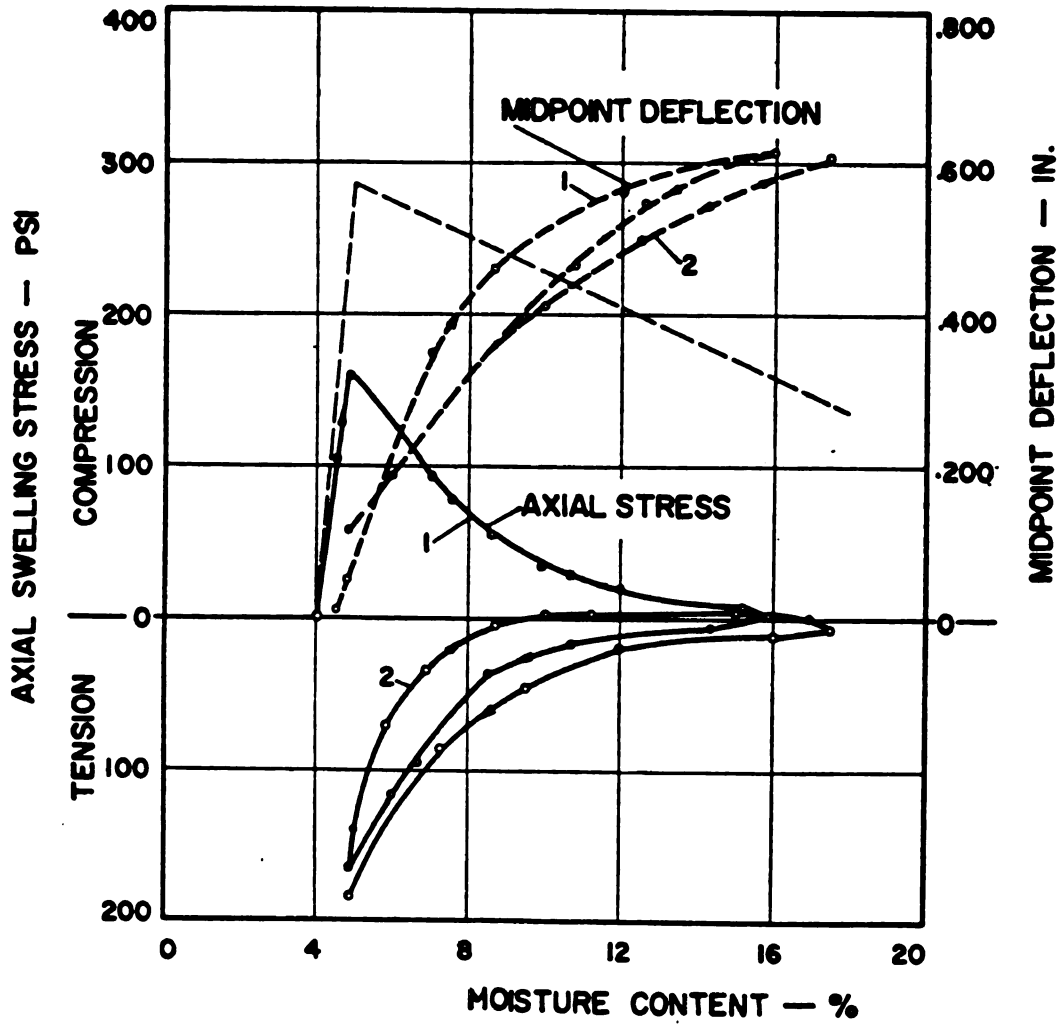

Figure 1-6 Axial stresses and midpoint deflection of axially restrained hardboard strips as function of moisture content (clamped dry). Number 1 and 2 indicate sequence of exposure cycles. Dashed line represents theoretical stresses [51].

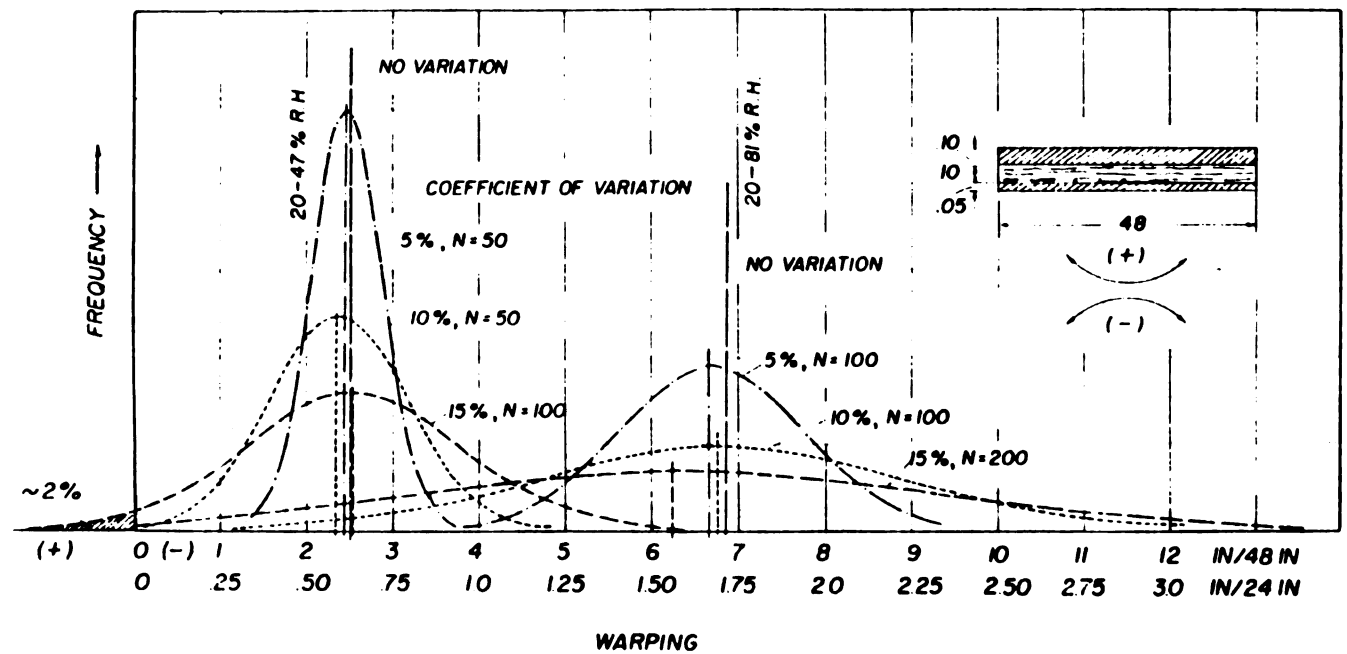

Figure 1-7 Warping across face grain of unbalanced, 24 in. long three-ply loblolly pine beams after exposure to two different relative humidity intervals. The normal variation of the results about the average values are due to assumed variability of input variables of face layers [46].

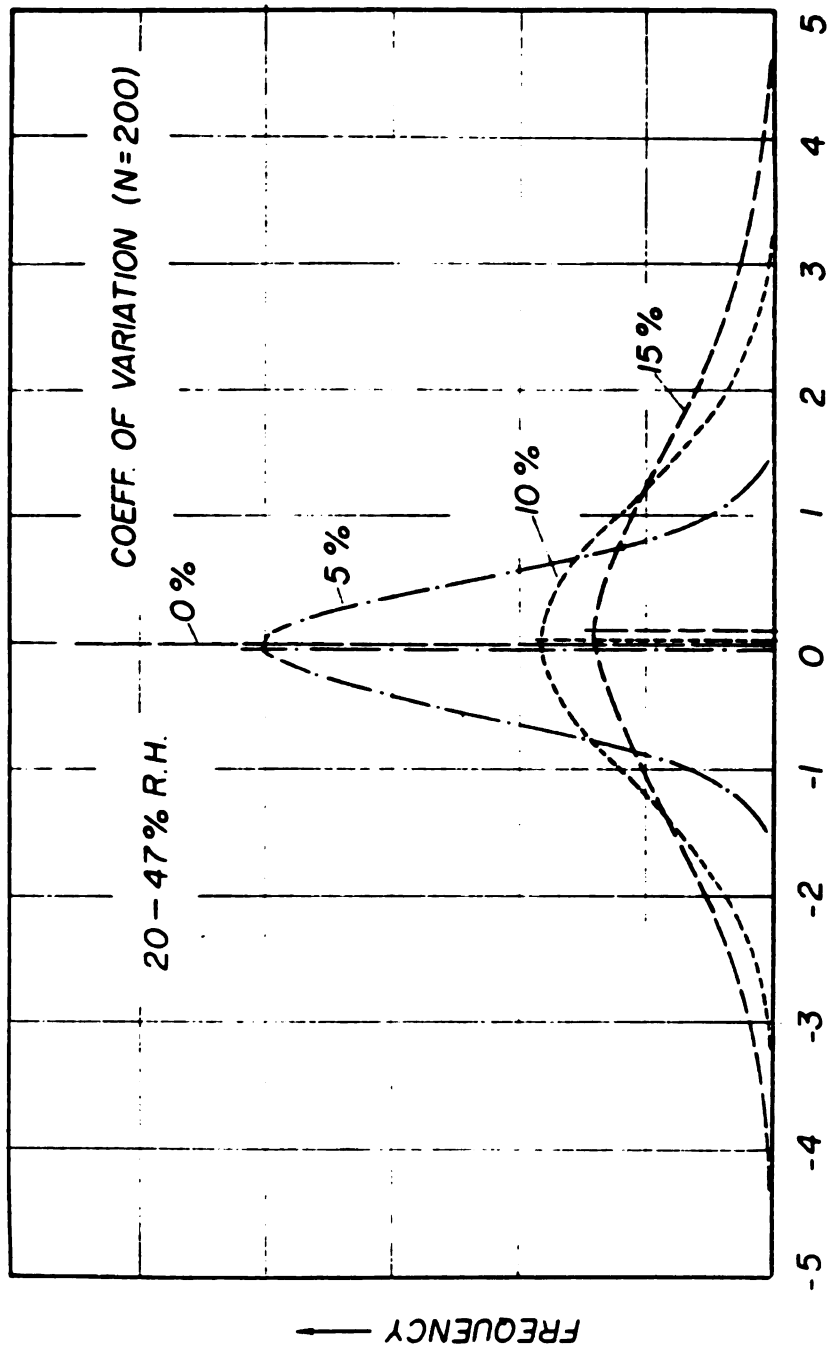

Figure 1-8 Warping across face grain of balanced loblolly pine beams after exposure to relative humidity intervals. Variability of input variables of face layers causes warping in both directions [47].

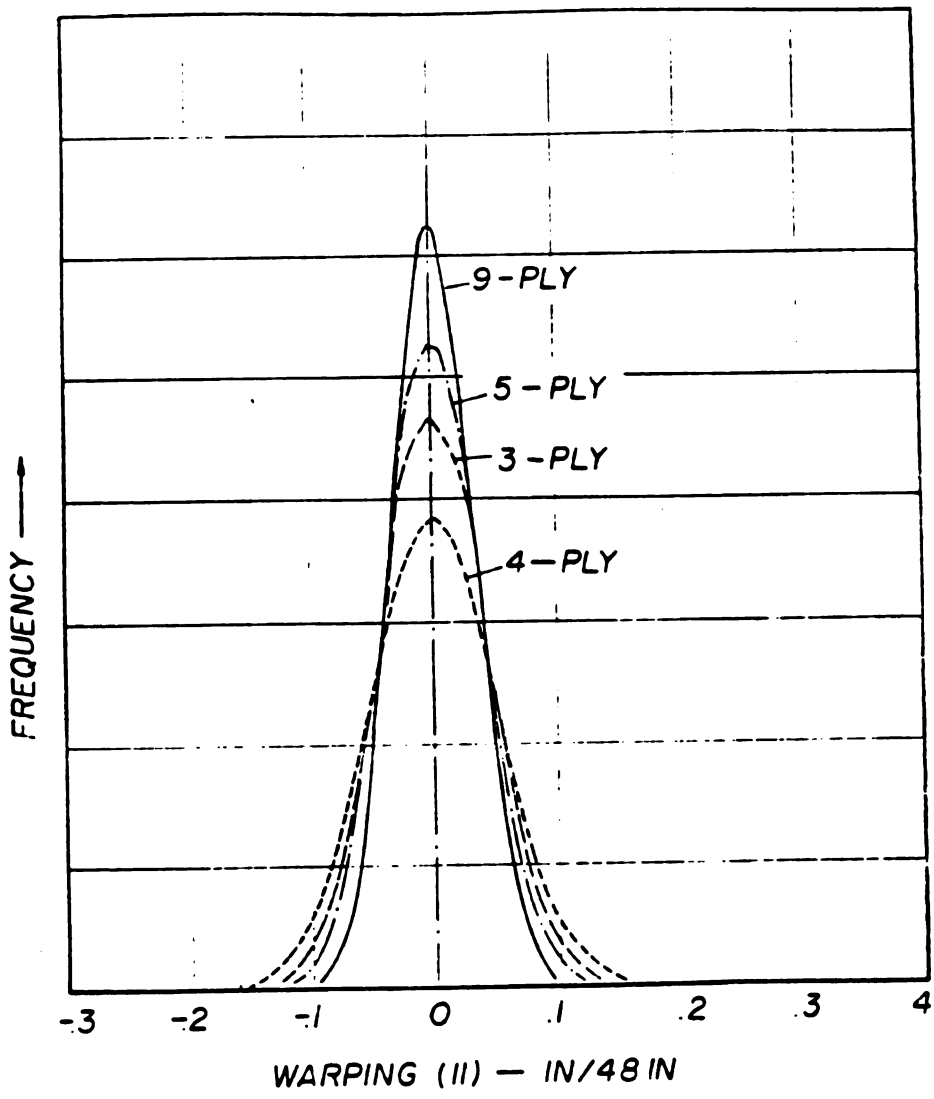

Construction:
3-ply: 1/6, 1/6, 1/6
4-ply: 1/8 (1/8, 1/8) 1/8
5-ply: (1/10) x 5
9-ply: (1/45) x 9

Figure 1-9 Effect of construction on warping along face grain of 1/2 in. loblolly pine plywood [47].

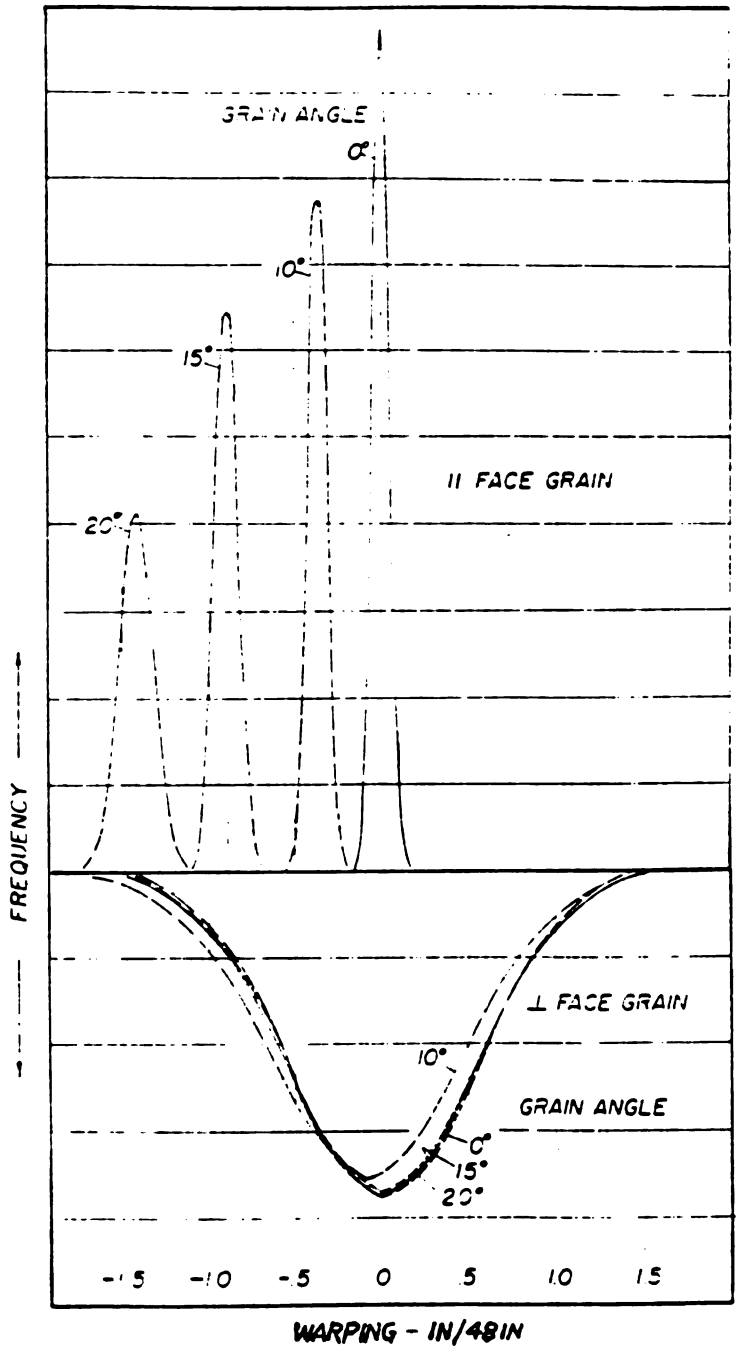

Figure 1-10 Effect of cross grain in top veneer on warping of 1/2 in., 3-ply loblolly pine plywood [47].

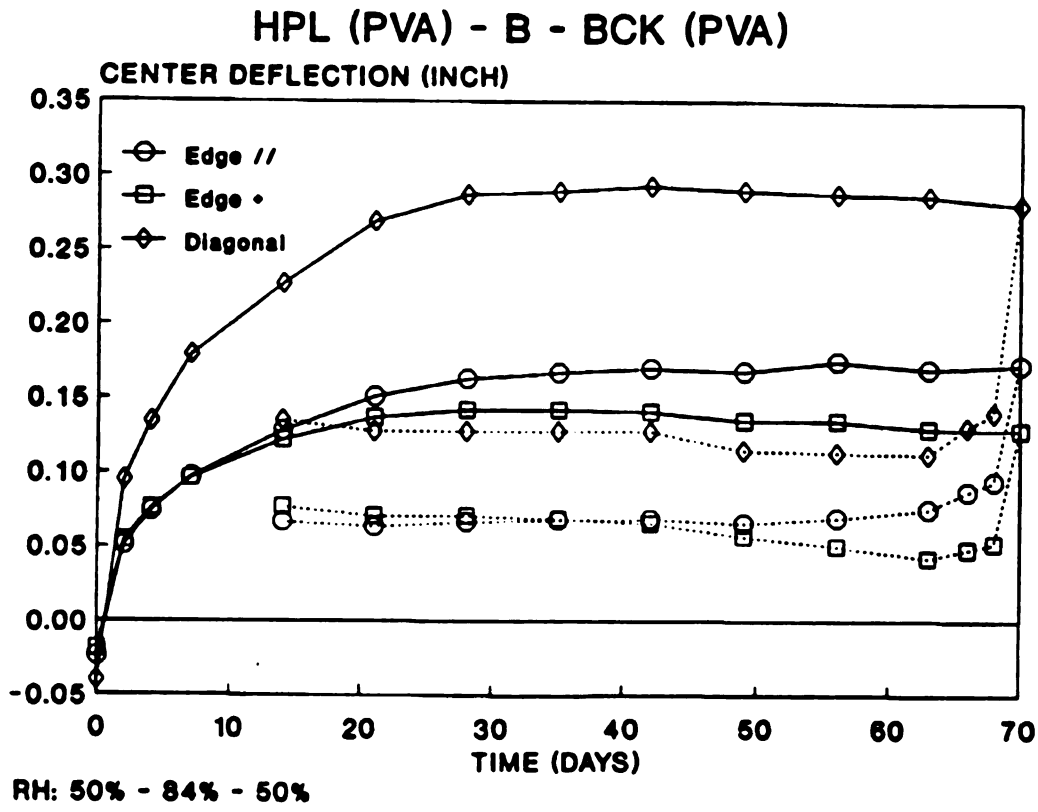

Figure 1-11 Warping record of particleboard with HPL and backer laminate. Exposure interval is 50% to 84% to 50% RH [42].

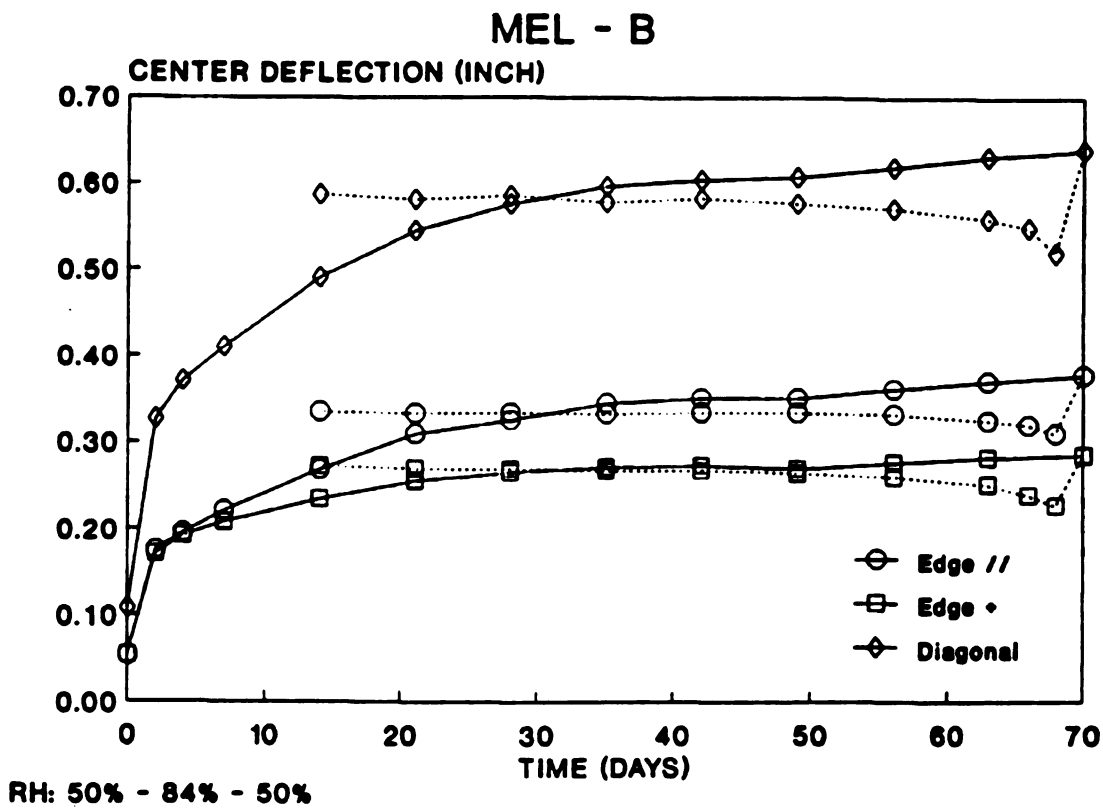

Figure 1-12 Warping record of particleboard with melamine laminate. Exposure interval is 50% to 84% to 50% RH [42].

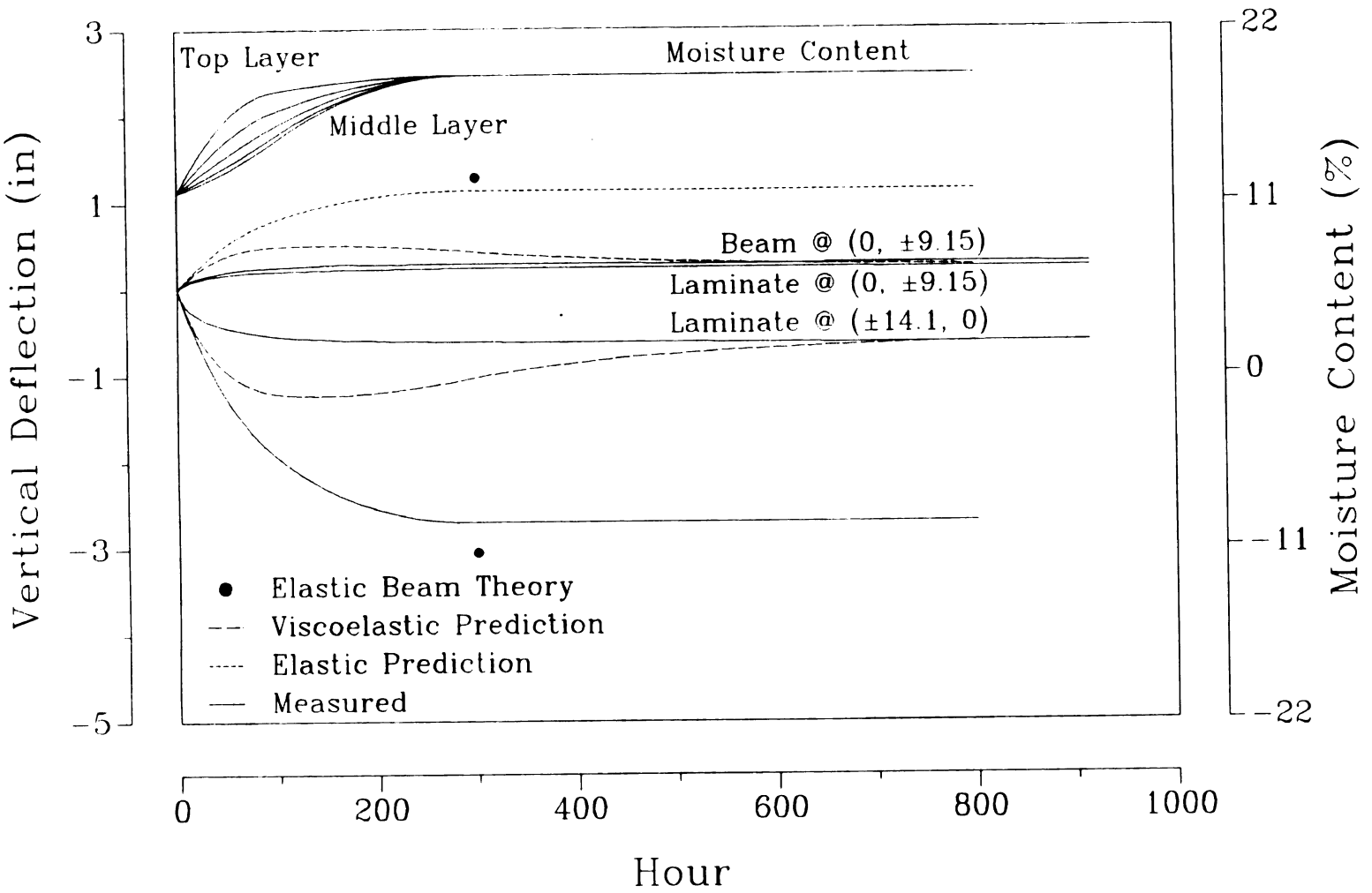

Figure 1-13 **Theoretical predictions vs. measured vertical deflections of yellow-poplar laminate and beam [57]**

1.4 Need for More Sophisticated Approach

As can be seen from the previous studies, estimating of warping based on elastic assumptions has certain limitations.

Wood is known to be a visco-elastic material with a plastic response component that will become significant at high stress levels and high moisture contents. Therefore, stress relaxation is an important factor in the mechanics of warping of laminated wood panels.

Keylwerth experimentally investigated the free and restrained swelling of wood and reported his findings in a series of articles in 1962 [21, 22]. He measured the development of compressive stresses in both radial and tangential directions in small uniaxially restrained specimens of beech wood as the moisture content increased. The swelling stresses quickly reached a maximum value, but due to the increasing plastic deformation of the restrained specimen, stress levels were considerably lower than would be calculated under assumptions of elasticity (Figure 1-14 and 1-15). The free expansion in the radial or tangential directions was then divided into elastic, visco-elastic and plastic components as illustrated in Figure 1-16. This separation was obtained by releasing the completely restrained specimens at certain time intervals and measuring their immediate and time dependent expansion, and comparing them to the total free expansion measured on unrestrained control specimens. In Figure 1-16, the upper portion shows deformation in the tangential direction, which is also the direction of restraint. The lower portion represents the radial direction. Restrained swelling of various wood species of different specific gravities is summarized

in Table 1-1. The exposure time for beech and pine was 24 hours, but it was extended for bongossi to 48 hours because the diffusion in bongossi wood is slower than in pine or beech.

It is interesting to note that the elastic component of the total restrained expansion in each of the two directions is fairly constant in relative terms, regardless of the species tested and of the moisture content range. There is also a fair correlation between the maximum swelling stress and the static modulus of elasticity measured at the initial condition.

It is clearly this elastic component of the restrained swelling which determine the stress level and which sustain the potential warp. It should be used to modify the elastic equation for panel warping.

This was attempted by Suchsland and McNatt [47] for the case of a three layer plywood model in which the "deformation modulus" as formulated by Keylwerth [21],

$$E' = \frac{\sigma'}{\varepsilon_{elast}} \tag{1.11}$$

where E' = the deformation modulus

σ' = the swelling stress measured when axially restrained specimen has reached equilibrium with air condition

ε_{elast} = the elastic portion of total swelling

was substituted for the static modulus of elasticity across the grain of the veneer, and ε_{elast} for the free expansion across the grain of the veneer.

It was not deemed necessary to make such modification in the

longitudinal direction of the veneer.

This modification of the input parameters produced more realistic predictions than the elastic approach but still left considerable discrepancies. This may be due to a rather unsophisticated method of determining swelling stresses [48].

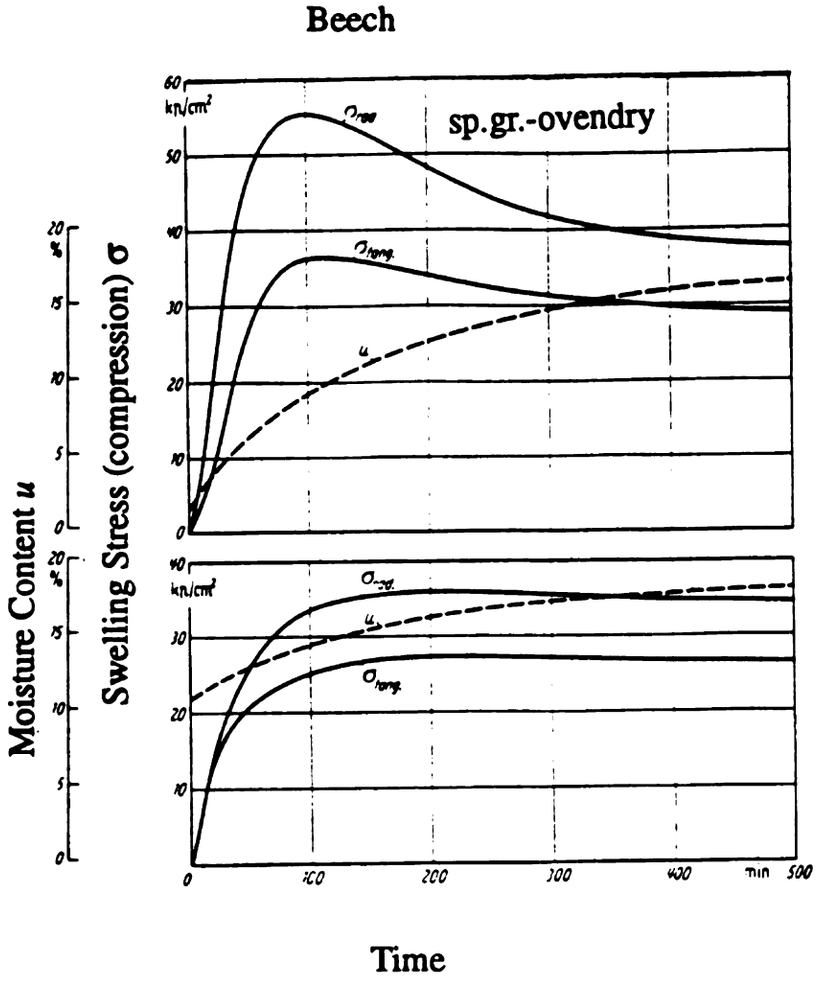

Figure 1-14 Time function of average axial swelling stress (compression) for two different moisture content intervals [21].

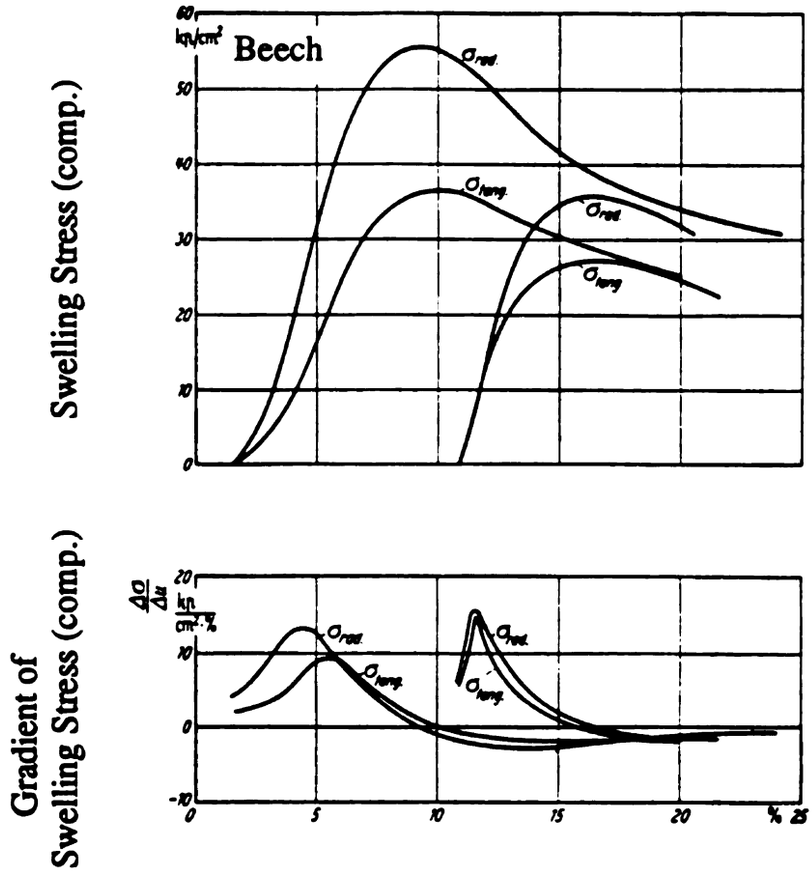

Figure 1-15 Radial and tangential swelling stress (compression) for two different moisture content intervals (upper figure), and stress gradients (lower figure) [21].

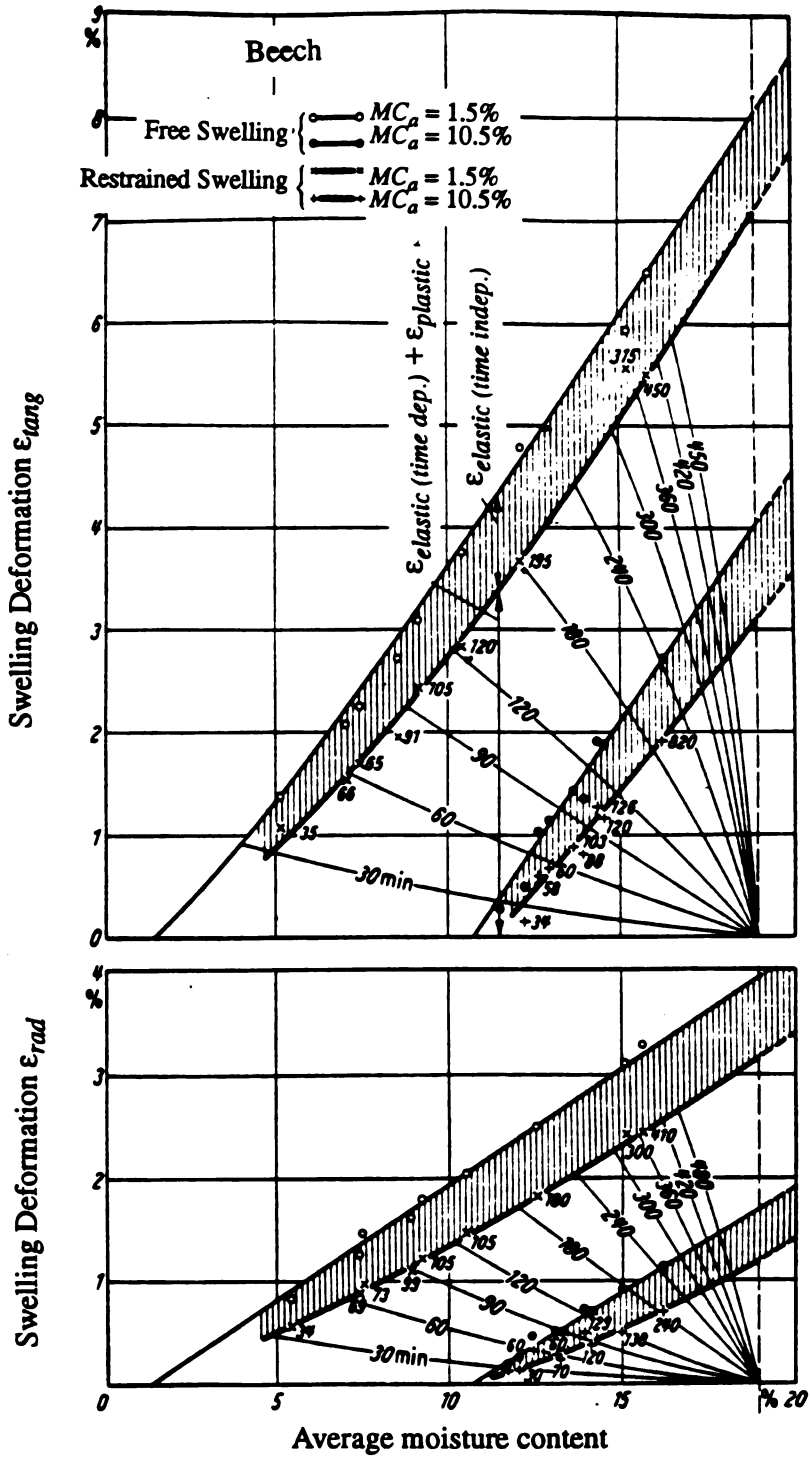

Figure 1-16 Free and restrained swelling deformations of beech as function of two different moisture content intervals [21].

Table 1-1 Swelling stresses (compression) in various species under total axial restraint as functions of increasing average moisture content [21]

Species	Moisture Content MC_a at beginning of restraint swelling	Direction of restraint	Static Modulus of Elasticity at MC_a	Maximum Stress σ_{max} before plastic flow	Average free expansion per 1% ΔMC	Elastic Strain Component ε_{elas} at end of test $MC \sim 20\%$	Deformation Modulus at end of test $E = \sigma / \varepsilon_{elas}$ $MC \sim 20\%$
	(%)		kip / cm^2	kip / cm^2	% /%	%	kip / cm^2
Beech	1.5	radial	14500	55.5	0.22	0.77	3870
$r_0 = 0.68\ g/cm^3$	1.5	tangential	6500	36.5	0.38	1.03	2200
	8	radial	-	50	0.22	0.6	5700
	8	tangential	-	36	0.38	1.07	2500
	10.5	radial	12500	35.5	0.22	0.46	6450
	10.5	tangential	5500	27	0.38	0.96	2400
Pine	8	radial	11000	33.5	0.19	0.64	2500
$r_0 = 0.59\ g/cm^3$	8	tangential	7000	37	0.32	1.02	2100
Bongossi	8	radial	27500	105	0.31	0.71	13500
$r_0 = 1.00\ g/cm^3$	8	tangential	17500	79	0.40	0.99	7300

CHAPTER II
THE MECHANICS OF
WARPING OF HYGROSCOPIC LAMINATES

2.1 Hygroscopic Behavior of Solid Wood and of Wood Composites

Solid Wood

Wood and all products derived from wood are hygroscopic. These materials absorb and desorb water according to some functional relationship between the relative humidity of the air and the materials moisture content (Figure 2-1). This water resides in the cell wall as "bound" water. As the relative humidity approaches 100 percent (approximately 30 percent moisture content), water begins to appear in liquid form in the cell cavity. The bound water causes cell walls to expand which results in gross dimensional changes of the wood or wood products. Thus, changes in relative humidity translate directly into dimensional changes. Increasing moisture content to above 30 percent (fiber saturation point) does not cause further swelling. The moisture content - relative humidity relationship of solid wood is reversible, at least for most practical purposes. So is the relationship between moisture content and dimensional change of wood (Figure 2-2).

The dimensional changes of solid wood in response to moisture content changes are highly directional. They are greatest in the transverse direction (radial and tangential) and smallest in the longitudinal direction as shown in Table 2-1. The relationship between moisture content and dimensional change is fairly linear so that it can be expressed as the product of the dimensional change coefficient (change per 1 percent moisture content change) and the moisture content change.

Wood Composites

Conventional wood composite are sheet material composed of small woody elements held together by an adhesives bond. The size and shape of the element are the most important characteristics of the materials, ranging from veneer sheets (plywood) to individual fibers (fiberboard). Most composite sheet manufacturing processes have in common a randomization of the grain direction in the plane of the sheet. This is accomplished by cross lamination in the case of plywood and by random deposition of elements in the case of particleboard and fiberboard. The distinction between fiberboard and particleboard is in the size of the elements, fibers generally being much smaller than particles, the former being derived from wood by a pulping process, the latter by a mechanical cutting or milling operation.

Plywood is a glued wood panel made up of relatively thin layers of veneer with the grain of adjacent layers at right angles. Each layer consists of a single thin sheet, or ply. The usual constructions have an odd number of layers. The outside plies are called faces or face and back plies, the inner

plies are called cores or centers.

Particleboard is a generic term for a panel manufactured from pieces of wood smaller than veneer sheets but larger than wood fibers, combined with a synthetic resin or other suitable binder and bonded together under heat and pressure in a hot press by a process in which the interparticle bond is created by the added binder. Densities range from 30 lb/ft^3 to 60 lb/ft^3 . Special types of particle panel products are flakeboard, waferboard and oriented strand board (OSB) as shown in Figure 2-3.

Medium-density fiberboard is a dry formed panel product manufactured from lignocellulosic fibers rather than particle combined with a synthetic resin or other suitable binder. The panels are compressed to a density of 31 lb/ft^3 to 55 lb/ft^3 by the application of heat and pressure by a process in which the interfiber bond is substantially created by the added binder.

High-density fiberboard (about 55 to 70 lb/ft^3) is called hardboard [46].

Wood composition boards have some very desirable characteristics: availability in large sheets, smooth surfaces, uniformity in properties from sheet to sheet, and freedom from localized defects. However, some of the products have been largely excluded from primary structural uses because they have been unable to approach the longitudinal stiffness, dimensional stability and long-term load-carrying ability of sawn lumber.

Wood composite sheet materials such as particleboard and fiberboard derive their important characteristics from solid wood. Their gross mechanical and physical properties are similar to those of solid wood but are

modified because of the more or less randomized disposition in the plane of the board of the individual particle or fiber elements.

Their hygroscopic behavior differs from that of solid wood in several respects:

- The isotherm is lower and has a distinct hysteresis (Figure 2-1).
- The expansion and shrinkage in the plane of the sheet is the same in all directions. It is relatively small compared with the transverse dimensional change of solid wood (Figure 2-2 (a)).
- Thickness swelling is large due to the effects of densification to higher densities in manufacturing (Figure 2-2 (b)).
- Both linear dimensional change and thickness swelling show hysteresis which is particularly strong in thickness swelling.

Composition boards are often overlaid with either veneer or plastic overlays such as melamine impregnated paper, high pressure laminates (resin impregnated paper laminate), vinyl and veneer. Such overlaid panels are common in the furniture, kitchen and store fixture industries. In many cases the overlaid sheets are of an unbalanced construction potentially leading to warping problems in service [29, 44, 45, 46].

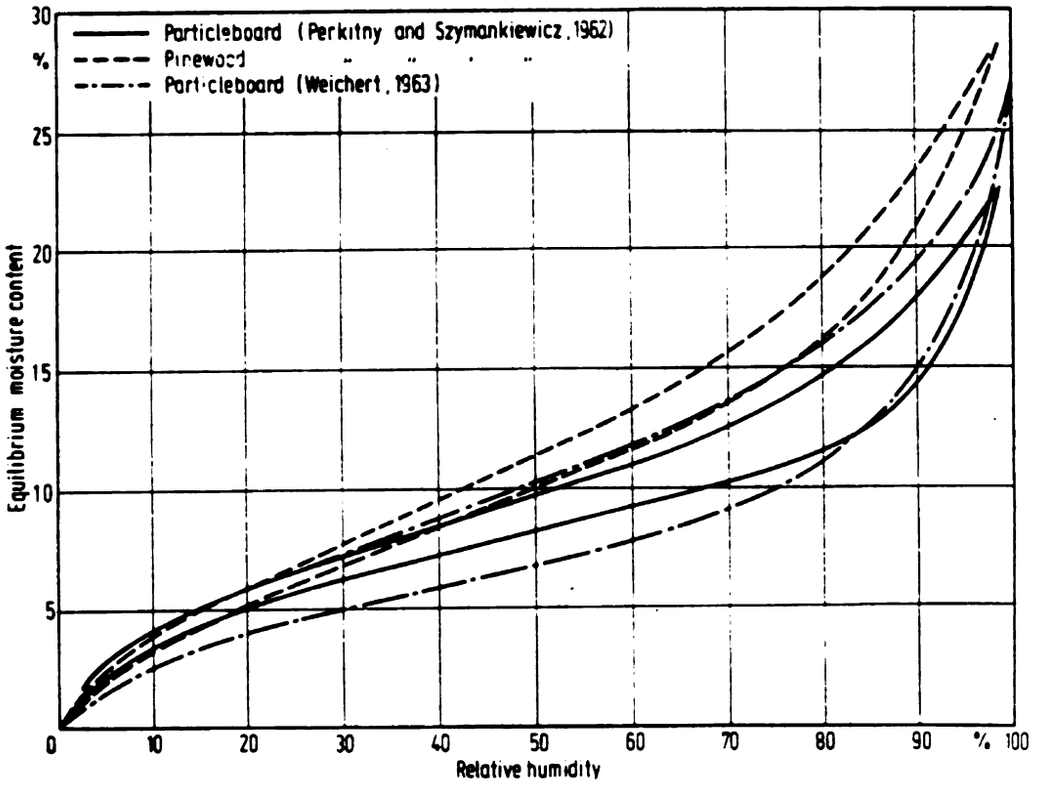

Figure 2-1 Hygroscopic isotherms for wood and particleboard [23].

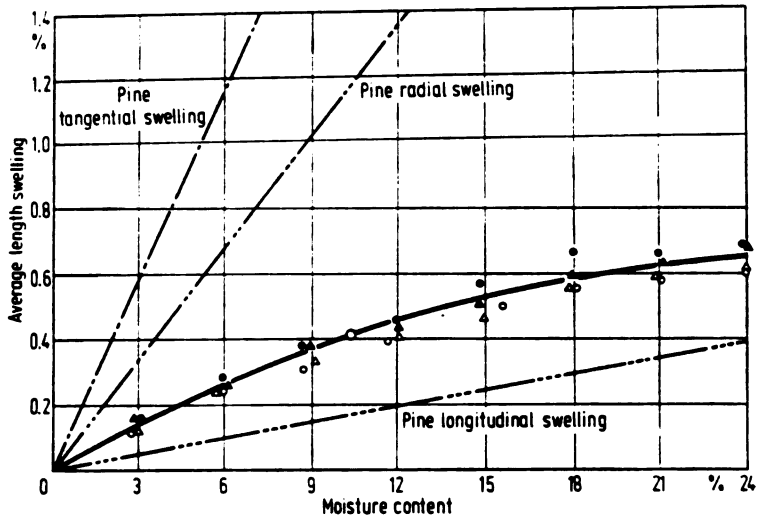

(a). change in length

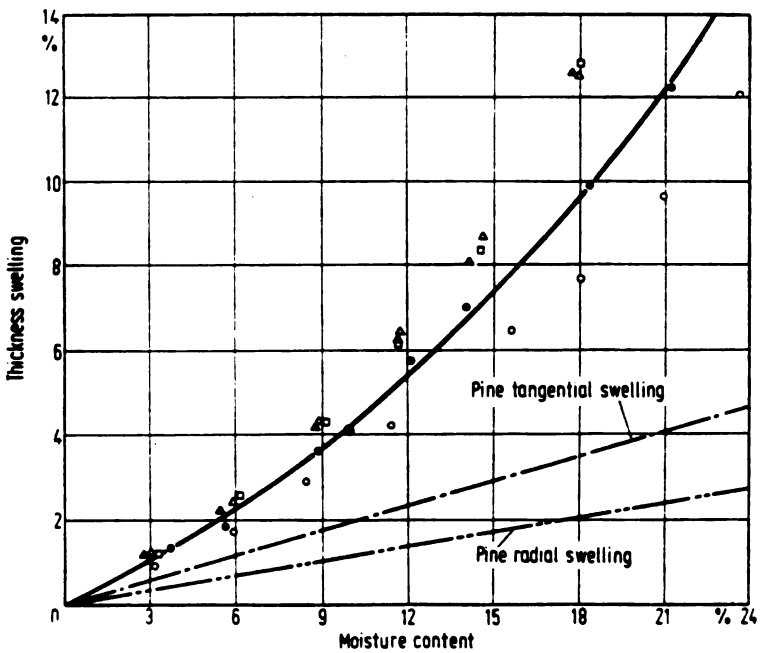

(b). change in thickness

Figure 2-2 Dimensional changes in solid pine wood and particleboard (heavy line) versus moisture content [23].

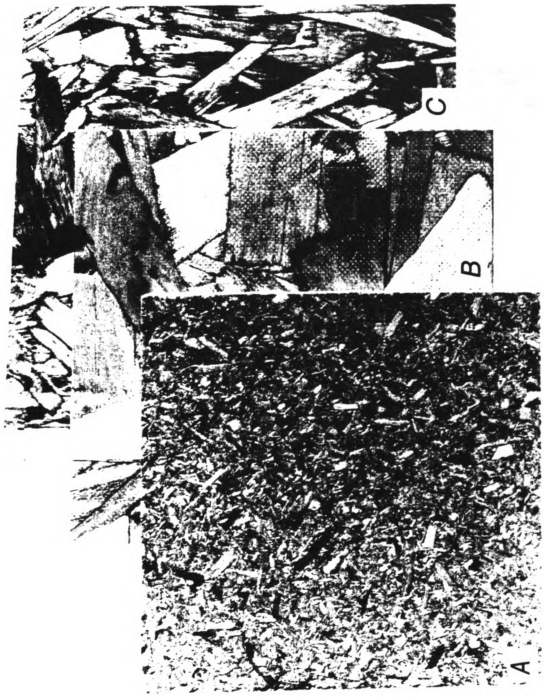

Figure 2-3 Basic particle panel products: *A* particleboard, *B* waferboard, and *C* oriented strand board [10].

Table 2-1 Dimensional change of domestic woods [10]

Species	Shrinkage from green to ovendry moisture content[1]		
	Radial	Tangential	Volumetric
	Percent		
HARDWOODS			
Alder, red	4.4	7.3	12.6
Ash:			
Black	5.0	7.8	15.2
Blue	3.9	6.5	11.7
Green	4.6	7.1	12.5
Oregon	4.1	8.1	13.2
Pumpkin	3.7	6.3	12.0
White	4.9	7.8	13.3
Aspen:			
Bigtooth	3.3	7.9	11.8
Quaking	3.5	6.7	11.5
Basswood, American	6.6	9.3	15.8
Beech, American	5.5	11.9	17.2
Birch:			
Alaska paper	6.5	9.9	16.7
Gray	5.2	—	14.7
Paper	6.3	8.6	16.2
River	4.7	9.2	13.5
Sweet	6.5	9.0	15.6
Yellow	7.3	9.5	16.8
Buckeye, yellow	3.6	8.1	12.5
Butternut	3.4	6.4	10.6
Cherry, black	3.7	7.1	11.5
Chestnut, American	3.4	6.7	11.6
Cottonwood:			
Balsam poplar	3.0	7.1	10.5
Black	3.6	8.6	12.4
Eastern	3.9	9.2	13.9
Elm:			
American	4.2	9.5	14.6
Cedar	4.7	10.2	15.4
Rock	4.8	8.1	14.9
Slippery	4.9	8.9	13.8
Winged	5.3	11.6	17.7
Hackberry	4.8	8.9	13.8
Hickory, Pecan	4.9	8.9	13.6
Hickory, True:			
Mockernut	7.7	11.0	17.8
Pignut	7.2	11.5	17.9
Shagbark	7.0	10.5	16.7
Shellbark	7.6	12.6	19.2
Holly, American	4.8	9.9	16.9
Honeylocust	4.2	6.6	10.8
Locust, black	4.6	7.2	10.2
Madrone, Pacific	5.6	12.4	18.1
Magnolia:			
Cucumbertree	5.2	8.8	13.6
Southern	5.4	6.6	12.3
Sweetbay	4.7	8.3	12.9
Maple:			
Bigleaf	3.7	7.1	11.6
Black	4.8	9.3	14.0
Red	4.0	8.2	12.6
Silver	3.0	7.2	12.0
Striped	3.2	8.6	12.3
Sugar	4.8	9.9	14.7
Oak, red:			
Black	4.4	11.1	15.1
Laurel	4.0	9.9	19.0
Northern red	4.0	8.6	13.7
Pin	4.3	9.5	14.5
Scarlet	4.4	10.8	14.7
Southern red	4.7	11.3	16.1
Water	4.4	9.8	16.1
Willow	5.0	9.6	18.9
Oak, white:			
Bur	4.4	8.8	12.7
Chestnut	5.3	10.8	16.4
Live	6.6	9.5	14.7
Overcup	5.3	12.7	16.0
Post	5.4	9.8	16.2
Swamp chestnut	5.2	10.8	16.4
White	5.6	10.5	16.3

Table 2-1 (continued)

Species	Shrinkage from green to ovendry moisture content[1]		
	Radial	Tangential	Volumetric
	Percent		
HARDWOODS—continued			
Persimmon, common	7.9	11.2	19.1
Sassafras	4.0	6.2	10.3
Sweetgum	5.3	10.2	15.8
Sycamore, American	5.0	8.4	14.1
Tanoak	4.9	11.7	17.3
SOFTWOODS			
Baldcypress	3.8	6.2	10.5
Cedar:			
Alaska-	2.8	6.0	9.2
Atlantic white-	2.9	5.4	8.8
Eastern redcedar	3.1	4.7	7.8
Incense-	3.3	5.2	7.7
Northern white-	2.2	4.9	7.2
Port-Orford-	4.6	6.9	10.1
Western redcedar	2.4	5.0	6.8
Douglas-fir:[2]			
Coast	4.8	7.6	12.4
Interior north	3.8	6.9	10.7
Interior west	4.8	7.5	11.8
Fir:			
Balsam	2.9	6.9	11.2
California red	4.5	7.9	11.4
Grand	3.4	7.5	11.0
Noble	4.3	8.3	12.4
Pacific silver	4.4	9.2	13.0
Subalpine	2.6	7.4	9.4
White	3.3	7.0	9.8
Hemlock:			
Eastern	3.0	6.8	9.7
Mountain	4.4	7.1	11.1
Hemlock (con.):			
Western	4.2	7.8	12.4
Larch, western	4.5	9.1	14.0
Pine:			
Eastern white	2.1	6.1	8.2
Jack	3.7	6.6	10.3
Loblolly	4.8	7.4	12.3
Lodgepole	4.3	6.7	11.1
Longleaf	5.1	7.5	12.2
Pitch	4.0	7.1	10.9
Pond	5.1	7.1	11.2
Ponderosa	3.9	6.2	9.7
Red	3.8	7.2	11.3
Shortleaf	4.6	7.7	12.3
Slash	5.4	7.6	12.1
Sugar	2.9	5.6	7.9
Virginia	4.2	7.2	11.9
Western white	4.1	7.4	11.8
Redwood:			
Old-growth	2.6	4.4	6.8
Young-growth	2.2	4.9	7.0
Spruce:			
Black	4.1	6.8	11.3
Engelmann	3.8	7.1	11.0
Red	3.8	7.8	11.8
Sitka	4.3	7.5	11.5
Tamarack	3.7	7.4	13.6
Tupelo:			
Black	5.1	8.7	14.4
Water	4.2	7.6	12.5
Walnut, black	5.5	7.8	12.8
Willow, black	3.3	8.7	13.9
Yellow-poplar	4.6	8.2	12.7

[1] Expressed as a percentage of the green dimension.

[2] Coast Douglas-fir is defined as Douglas-fir growing in the States of Oregon and Washington west of the summit of the Cascade Mountains. Interior West includes the State of California and all counties in Oregon and Washington east of but adjacent to the Cascade summit. Interior North includes the remainder of Oregon and Washington and the States of Idaho, Montana, and Wyoming.

2.2 Elastic Characteristics of Solid Wood and Wood Composites

Wood

Wood is linearly elastic within certain load and load duration limits, and follows Hooke's law, that is, stress is linearly related to strain in direct proportion.

As an orthotropic materials, wood has twelve constants. These are:

three moduli of elasticity: E_L , E_R , E_T

three shear moduli: G_{TR} , G_{LR} , G_{LT}

six Poisson's ratios: μ_{LT} , μ_{TL} , μ_{TR} , μ_{RT} , μ_{LR} , μ_{RL} .

The subscripts refer to the three principal directions in wood. L , T , R denote longitudinal, tangential and radial directions respectively. For the Poisson's ratios the first subscript refer to the direction of the applied stress and the second subscript to the direction of the lateral strain. There is a set of three equations relating some of the elastic constants, so that the number of independent constants is reduced to nine. The equations are [10]:

$$\frac{\mu_{LT}}{E_L} = \frac{\mu_{TL}}{E_T} \quad ; \quad \frac{\mu_{TR}}{E_T} = \frac{\mu_{RT}}{E_R} \quad ; \quad \frac{\mu_{LR}}{E_L} = \frac{\mu_{RL}}{E_R} \qquad (2.1)$$

The state of strain can be expressed as a function of the state of stress by

$$\begin{Bmatrix} \varepsilon_{LL} \\ \varepsilon_{TT} \\ \varepsilon_{RR} \\ \gamma_{TR} \\ \gamma_{LR} \\ \gamma_{LT} \end{Bmatrix} = \begin{bmatrix} \frac{1}{E_L} & -\frac{\mu_{TL}}{E_T} & -\frac{\mu_{RL}}{E_R} & 0 & 0 & 0 \\ -\frac{\mu_{LT}}{E_L} & \frac{1}{E_T} & -\frac{\mu_{RT}}{E_R} & 0 & 0 & 0 \\ -\frac{\mu_{LR}}{E_L} & -\frac{\mu_{TR}}{E_T} & \frac{1}{E_R} & 0 & 0 & 0 \\ 0 & 0 & 0 & \frac{1}{G_{TR}} & 0 & 0 \\ 0 & 0 & 0 & 0 & \frac{1}{G_{LR}} & 0 \\ 0 & 0 & 0 & 0 & 0 & \frac{1}{G_{LT}} \end{bmatrix} \begin{Bmatrix} \sigma_{LL} \\ \sigma_{TT} \\ \sigma_{RR} \\ \tau_{TR} \\ \tau_{LR} \\ \tau_{LT} \end{Bmatrix} \qquad (2.2)$$

The elastic modulus in the longitudinal or the grain direction, E_L , is much higher and those in the transverse directions are lower. In any directions relative to the grain direction, the modulus can be approximately obtained from Hankinson-type formula as [10]

$$E_\theta = \frac{E_L E_\perp}{E_L (\sin\theta)^n + E_\perp (\cos\theta)^n} \qquad (2.3)$$

in which E_θ = the modulus at an angle θ from the grain direction

E_L = the modulus in the grain direction

$E_\perp$ = the modulus in the direction perpendicular to the grain

n = an empirically determined constant, ranging from 1.5 to 2 for most wood species [10].

The modulus in any direction expressed as a fraction of the one in the grain direction plotted against the angle θ is shown in Figure 2-4.

The modulus of elasticity of solid wood is also affected by changes in moisture content below the fiber saturation point. It increases with decreasing moisture content and can be expressed as follows [10]

$$E = E_{12}\left(\frac{E_{12}}{E_{gr}}\right)^{-\left(\frac{MC-12}{MC_P-12}\right)} \tag{2.4}$$

where E = the modulus of elasticity

MC = moisture content in percent

MC_P = the moisture content at which the mechanical property changes due to drying are first observed, usually around 20 to 30 percent depending on the wood species.

E_{12} = the modulus of elasticity at 12 percent moisture content

E_{gr} = the modulus of elasticity for all moisture contents greater than MC_P (green condition).

Wood Composites

Wood composites, due to the rearranging or randomization of wood elements, leave elastic properties less directional or more uniform than those of solid wood.

The elastic properties of plywood are orthotropic. As compared with

solid wood, the chief advantage of plywood is an equalization of elastic properties in the plane of the panel. The strength along the grain of the face veneers is of course remarkably reduced. Board such as particleboard or fiberboard are generally considered to be transversely isotropic, which means that there are only insignificant differences between machine direction and cross-machine direction, but the elastic-mechanical properties in the plane of the board are generally different from those in the direction of the thickness.

The modulus of elasticity of plywood is equal to the weighted average of the moduli of elasticity of all plies [10]. In edgewise tension or compression,

$$E_W \text{ or } E_X = \frac{1}{T} \sum_{1}^{n} E_i T_i \qquad (2.5)$$

where T = the thickness of plywood

T_i = the thickness of the veneer in the i^{th} ply

E_i = the modulus of elasticity of the veneer in the i^{th} ply

E_W and E_X is the modulus of elasticity of plywood parallel and perpendicular to the face-grain respectively.

Modulus of elasticity at any angles to the face-grain direction is given approximately by [10]

$$\frac{1}{E_\theta} = \frac{1}{E_W}(\cos\theta)^4 + \frac{1}{E_X}(\sin\theta)^4 + \frac{1}{G_{WX}}(\sin\theta)^2(\cos\theta)^2 \qquad (2.6)$$

where E_θ = the modulus of elasticity at an angle θ to the face grain

G_{WX}= the shear modulus under edge-wise shear.

The relation of E_θ/E_X is also plotted in Figure 2-4 for two different veneer ratios.

The modulus of elasticity in flexure of plywood is equal to the average of the moduli of elasticity parallel to the span of the various plies weighted according to their moment of inertia about the neutral plane. That is

$$E_{fw} \text{ or } E_{fx} = \frac{1}{I} \sum_{1}^{n} E_i I_i$$

where E_{fw} = the modulus of elasticity of plywood in bending when the face grain is parallel to the span

E_{fw} = the modulus of elasticity of plywood in bending when the face grain is perpendicular to the span

E_i = the modulus of elasticity of the i^{th} layer in the span direction

I_i = the moment of inertia of the i^{th} layer about the neutral plane of the plywood

I = the moment of inertia of the total cross section about its center line

The important elastic strength properties of particleboard and fiberboard include static bending, tensile strength parallel to the surface and perpendicular to the surface (internal bond), compression strength and bending strength parallel and perpendicular to the surface, etc. These properties depend largely on the species of the material, the density, resin

content, resin type and the moisture content of the board.

Boards with higher density have higher mechanical strength. Figure 2-5 shows the general trend of such relationship. Although the most important species variable governing board properties is the density of the wood raw material itself, the lower-density woods are widely used in the manufacturing today. Their strength properties appear to be superior to the higher-density species. This is because lower-density woods provide larger volume of wood chips compared to the higher-density woods to make the same density of the board. Therefore, a better bond among the chips occurs as the board is compressed to its final thickness. In order to achieve a certain mechanical strength of the board, the use of a higher-density wood will lead to a board being much heavier.

The moisture content of the board has less effects on the strength of the particleboard than on solid wood as indicated in Figure 2-6.

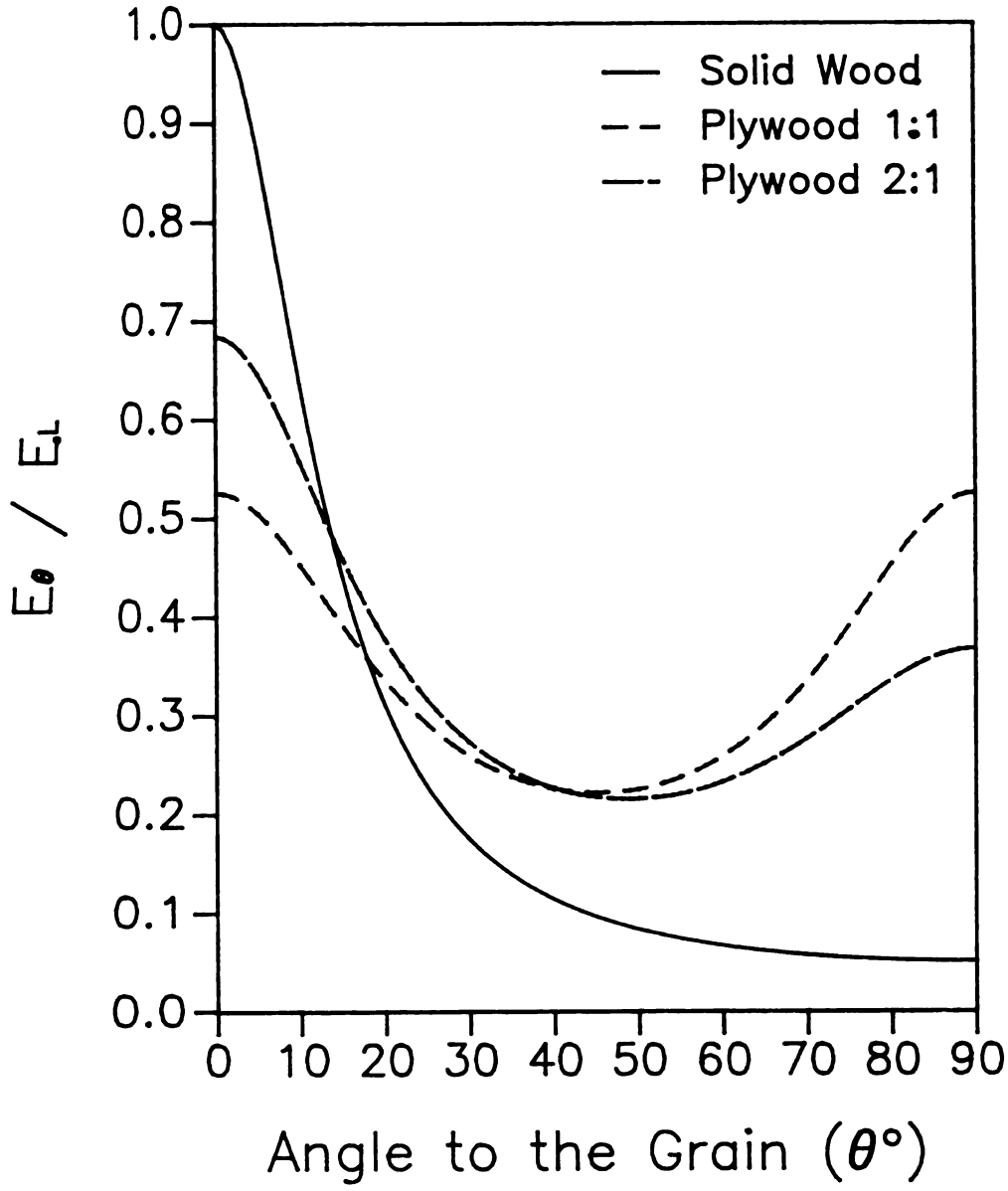

Figure 2-4 The modulus (tension or compression) as function of grain angle.

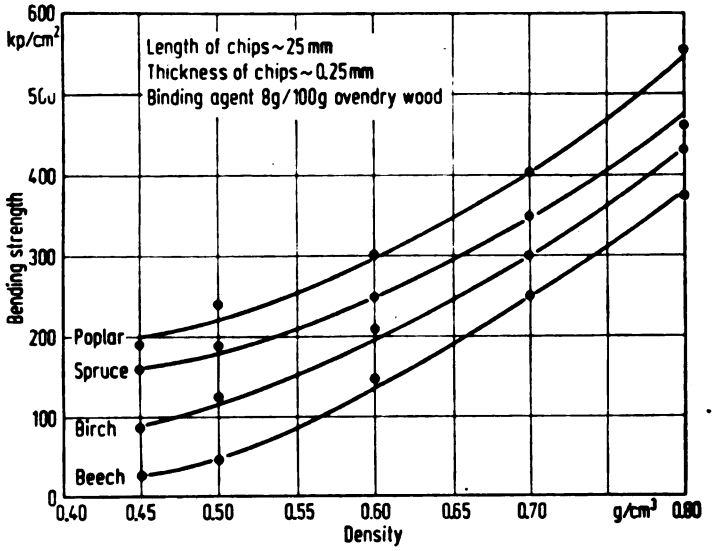

Figure 2-5 Effects of wood species on bending strength in relation to density of particleboard [23].

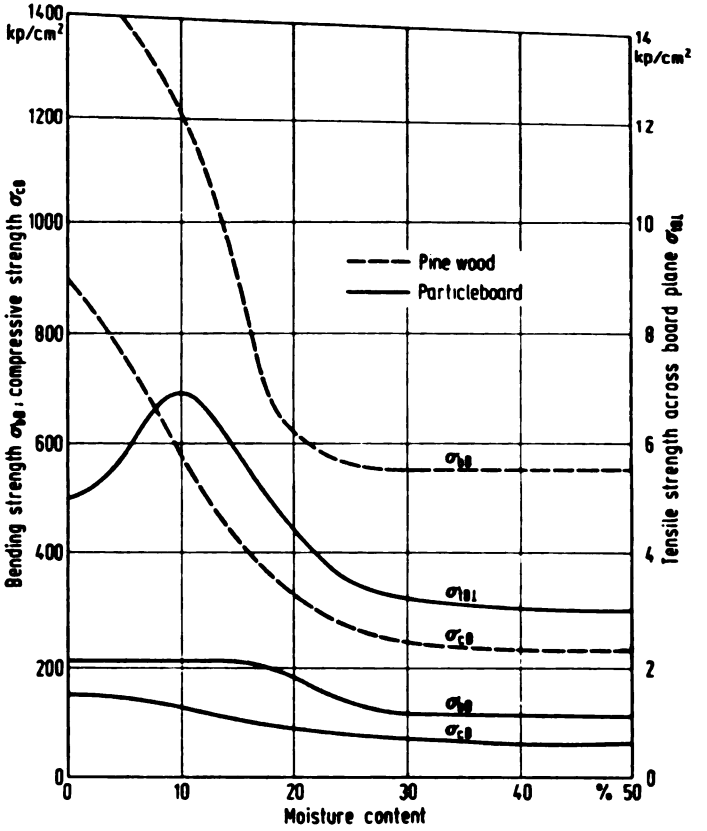

Figure 2-6 Effects of moisture content on various strength properties of solid pine and of particleboard [23].

2.3 Prediction of Warping of Wood Laminates Based on Elasticity

Figure 2-7 shows a laminated beam with n layers. The differences between the resultant expansion and free expansion $(\alpha_{res} - \alpha)$ indicate the compressive or tensile strains which are proportional to the corresponding forces that develop in the individual layers. These forces can give rise to bending moments about the neutral axis of the beam. Only when these bending moments are balanced, does the beam remain flat. The following derivation of the warping equation is based on an article by C.B. Norris [32].

If the radius of curvature is assumed as R, the total stress σ in any point can be determined as

$$\sigma = (\alpha_{res} - \alpha) E - \frac{y}{R} E \tag{2.7}$$

where α_{res} = the resultant expansion of the beam.

The force resultant on a cross section of the beam can be found by integrating the stress over the thickness as follows

$$F = \int \sigma dy = \int (\alpha_{res} - \alpha) E dy - \int \frac{y}{R} E dy \tag{2.8}$$

and the bending moment resultant on a cross section of the beam is determined by

$$M = \int \sigma y dy = \int (\alpha_{res} - \alpha) E y dy - \int \frac{y^2}{R} E dy \tag{2.9}$$

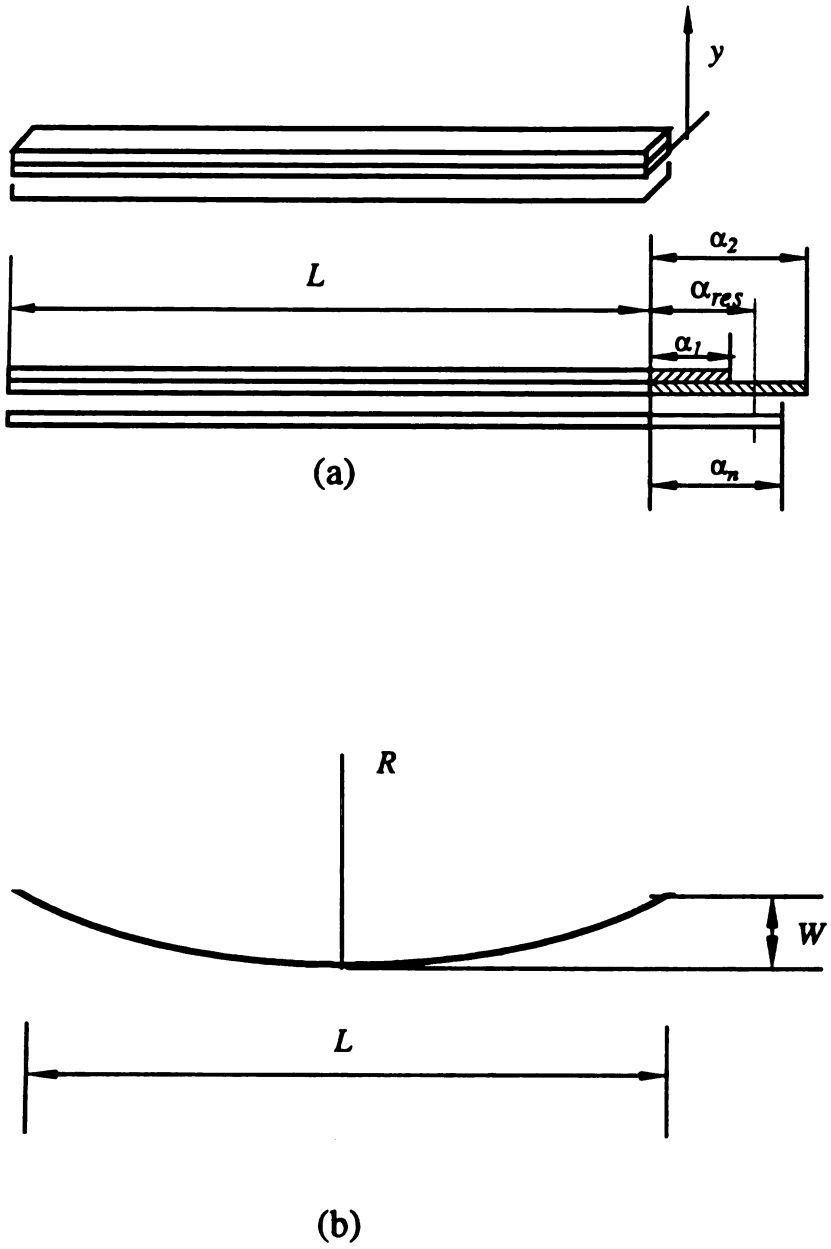

Figure 2-7 A laminated beam with n layers showing individual free expansion, α_i, and resultant expansion, α_{res}, (a), and illustration of relationship between radius of curvature, R, base length, L, and center deflection, W, of warped beam (b).

If it is assumed that there is no external force and moment on the beam, Equations (2.8) and (2.9) can be integrated over each layer by using summation

$$\alpha_{res}\sum_{1}^{n}E_iT_i-\sum_{1}^{n}\alpha_iE_iT_i-\frac{1}{2R}\sum_{1}^{n}E_i(S_i^2-S_{i-1}^2)\ =\ 0 \qquad (2.10)$$

and

$$\frac{\alpha_{res}}{2}\sum_{1}^{n}E_i(S_i^2-S_{i-1}^2)-\frac{1}{2}\sum_{1}^{n}\alpha_iE_i(S_i^2-S_{i-1}^2)-\frac{1}{3R}\sum_{1}^{n}E_i(S_i^3-S_{i-1}^3)\ =\ 0 \qquad (2.11)$$

The radius of curvature of the beam R can then be determined from these two equations as

$$R=\frac{\dfrac{2\sum_{1}^{n}E_i(S_i^3-S_{i-1}^3)}{3\sum_{1}^{n}E_i(S_i^2-S_{i-1}^2)}-\dfrac{\sum_{1}^{n}E_i(S_i^2-S_{i-1}^2)}{2\sum_{1}^{n}E_iT_i}}{\dfrac{\sum_{1}^{n}\alpha_iE_i(S_i^2-S_{i-1}^2)}{\sum_{1}^{n}E_i(S_i^2-S_{i-1}^2)}-\dfrac{\sum_{1}^{n}\alpha_iE_iT_i}{\sum_{1}^{n}E_iT_i}} \qquad (2.12)$$

where $S_i\ =\ \sum_{1}^{i}T_i\ \ (in)$, is the cumulated thickness (see Figure 2-8)

$\alpha_i\ =$ the expansion value of the i^{th} layer (in/in) over the range of

moisture change anticipated

E_i = the modulus of elasticity of the i^{th} layer (psi) at the end condition

T_i = the thickness of the i^{th} layer (in).

The center deflection or the warping W (Figure 2-7) is given by

$$W = \frac{L^2}{8R} = \frac{L^2}{8} \frac{\dfrac{\sum_1^n \alpha_i E_i (S_i^2 - S_{i-1}^2)}{\sum_1^n E_i (S_i^2 - S_{i-1}^2)} - \dfrac{\sum_1^n \alpha_i E_i T_i}{\sum_1^n E_i T_i}}{\dfrac{2\sum_1^n E_i (S_i^3 - S_{i-1}^3)}{3\sum_1^n E_i (S_i^2 - S_{i-1}^2)} - \dfrac{\sum_1^n E_i (S_i^2 - S_{i-1}^2)}{2\sum_1^n E_i T_i}} \qquad (2.13)$$

where L = the length of the beam.

The radius of curvature of the beam, R, or the center deflection, W, may have positive or negative values. We will define warp being positive if the curve is concave when viewed from above as shown in Figure 2-7(b).

For a two-layer beam, it can be shown (see Appendix A) that W is a function of the moduli ratio E_1/E_2, the thickness ratio T_1/T_2, and the absolute value of thickness T_2, and is proportional to the difference of the expansion values of the two layers:

$$W = f(E_1/E_2, T_1/T_2)\frac{(\alpha_1 - \alpha_2)L^2}{T_2} \qquad (2.14)$$

For a given E_1/E_2 ratio, maximum warping W_{max} occurs when

$$E_1/E_2 = (T_2/T_1)^2 \qquad (2.15)$$

Equations (2.14) and (2.15) are true only for two-layer laminated beams.

Figure 2-9 is the plot of center deflection or warping W vs. various E_1/E_2, and T_1/T_2 ratios. The thickness of the second layer T_2 was set to be 1 *inch*, $\alpha_1 - \alpha_2$ was set to be 0.01 *in/in* (1 percent) and the span is 48 *inches*. The numerical results are listed in Table 2-2.

For any two layer laminate with arbitrary thickness of $T_2 = T_2'$, expansion difference of $\alpha'_1 - \alpha'_2$, and length of $L = L'$, the theoretical corresponding warping value

$$W' = W\frac{(\alpha'_1 - \alpha'_2)L'^2}{48^2 \times T_2'} \times 100 \qquad (2.16)$$

where W is the value from Figure 2-9 or Table 2-2.

Equation (2.14) indicates that a larger difference $(\alpha_1 - \alpha_2)$ leads to larger warping, but that larger T_2 leads to smaller warping providing that T_1/T_2 and other parameters remain the same.

The resultant expansion α_{res} of a multi-layered beam can be calculated by

$$\alpha_{res} = \frac{\sum_{1}^{n} \frac{\alpha_i E_i T_i}{(1+\alpha_i)}}{\sum_{1}^{n} \frac{E_i T_i}{(1+\alpha_i)}} \tag{2.17}$$

if the curvature of the beam is negligible. Otherwise, the resultant expansion α_{res} should be determined by solving Equation (2.10) using known R.

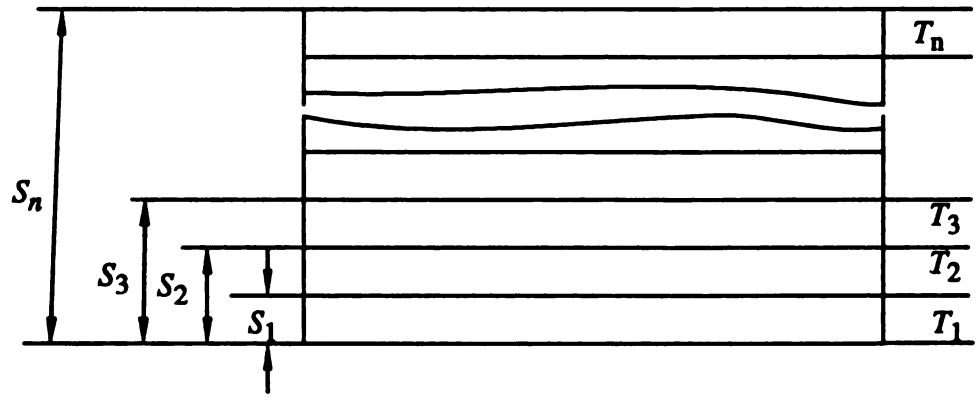

Figure 2-8 Illustration of dimensional variables of n -layer beam

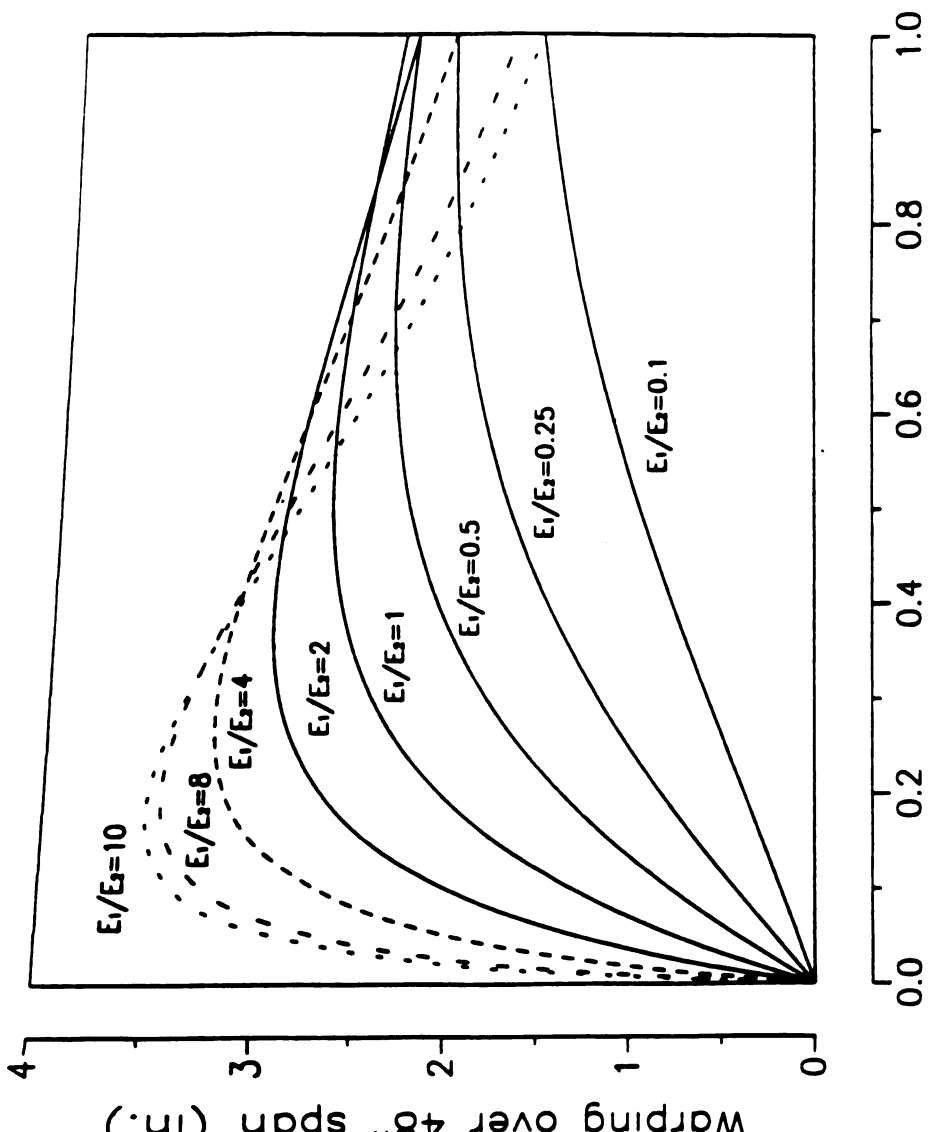

Figure 2-9 Center deflection of two layer laminate ($T_2 = 1$ in. $\alpha_1 - \alpha_2 = 0.01$ in./in. L = 48 in.)

Table 2-2 Center deflection of two layer laminate ($T_2 = 1$ in. $\alpha_1 - \alpha_2 = 0.01$ in./in. L = 48 in.)

	E_1/E_2							
T_1/T_2	**10**	**8**	**4**	**2**	**1**	**0.5**	**0.25**	**0.1**
0.001	0.1663	0.1341	0.0681	0.0343	0.0172	0.0086	0.0043	0.0017
0.01	1.2413	1.0539	0.6006	0.3228	0.1677	0.0855	0.0432	0.0174
0.025	2.1725	1.9352	1.2515	0.7333	0.4012	0.2105	0.1079	0.0438
0.5	2.8749	2.6639	1.9488	1.2679	0.7464	0.4095	0.2152	0.0888
0.1	3.3642	3.2228	2.6607	1.9714	1.2983	0.7714	0.4258	0.1817
0.2	3.4909	3.4280	3.1220	2.6328	2.0000	1.3496	0.8176	0.3746
0.3	3.3214	3.3071	3.1633	2.8505	2.3596	1.7495	1.1520	0.5688
0.4	3.0507	3.0761	3.0542	2.8738	2.5190	2.0040	1.4184	0.7549
0.5	2.7429	2.8022	2.8800	2.8022	2.5600	2.1488	1.6168	0.9253
0.6	2.4324	2.5189	2.6789	2.6829	2.5313	2.2151	1.7542	1.0746
0.8	1.8732	1.9923	2.2670	2.3910	2.3704	2.2035	1.8865	1.3008
1.0	1.4340	1.5620	1.8937	2.0945	2.1600	2.0945	1.8937	1.4340

2.4 Nonelastic Behavior of Solid Wood and Wood Composites

2.4.1 General

As has been pointed out in the first chapter of this study, the assumption of elasticity in calculating the warping of wood based laminates does not always lead to satisfactory results.

The non-elastic behavior shall therefore be briefly reviewed. This will be followed by the analysis of a visco-elastic beam under stress. Finally, the experimental approach used in the study shall be developed and the objective shall be outlined.

2.4.2 Wood as Visco-elastic Material

Wood and wood-based materials are known as viscoelastic materials in that they exhibit elastic as well as viscous strain properties. In wood, this behavior is a consequence of its amorphous and crystalline components [33, 21, 1]. Wood is known to be a complex heterogenous material composed mainly of cellulose, hemicelluloses, and lignin. Cellulose has both highly arranged crystalline and rather disorganized amorphous regions in its structure while lignin is mainly amorphous and hemicelluloses. Crystalline materials usually are highly elastic and show little time-dependent strain response to load over time. Amorphous materials normally have low elasticity and a high time-dependent strain response to constant load as indicated by Miller and Benicak [28].

Creep is defined as the time-dependent deformation exhibited by a material under constant load. In contrast, if a displacement is applied instantaneously and held constant over time, the stress will subside with time. This phenomenon is called relaxation, the change in resistance to forces in a material subjected to a constant deformation. The simplest type of time-dependent behavior to observe is creep. A relaxation test usually requires more specialized equipment [3]. Frequently the measurement of force depends on the displacement of the sensing element. Consequently, force measurements while displacement is presumably held constant can be subject to error: although the change in displacement may be small, it may be incorrect to assume that the sample is in a state of constant strain.

2.4.3 Creep Behavior

Figure 2-11 illustrates the characteristic deformation-time relationship for visco-elastic materials during sustained loading and relaxation [1, 46, 3]. Unlike elastic material as shown in Figure 2-10, the deformation of visco-elastic materials does not recover completely upon unloading. "In outlining the curve, starting at the origin, the application of load at time t_0 produces an instantaneous elastic deformation OA, on maintaining the load to t_1, the deformation increases at a decreasing rate, this increment is defined as creep. With removal of the load at time t_1, an instantaneous recovery BC occurs which is approximately equal in magnitude to the initial elastic deformation OA. As time elapses, there is a partial recovery CD of the creep deformation at a decreasing rate until time t_2, where it becomes constant. Thus, the amount of creep that occurred during loading is composed of a recoverable

component which is time-dependent and displays delayed elastic deformation and an irrecoverable component which is permanent and is due to plastic or viscous flow" [1].

Apart from the viscoelastic cell wall components, it was pointed out [25, 24, 31] that factors affecting the amount of creep are mainly the magnitude and duration of loading, moisture content and temperature as illustrated in Figure 2-12.

The study of the time effect indicates that the deformation increases very quickly following initial loading and slows down to a more or less constant rate thereafter. Beyond some point in time, known as the "point of inflection", deformation increases at an increasing rate until rupture (failure) occurs.

Creep deflection increases, and time to failure decreases with increasing level of stress. Beyond a given stress level, creep deflection increases at a rapid rate and failure is imminent. The range for which creep of solid wood can be assumed to be linear, i.e., proportional to stress, varies from approximately 30 percent [31] to up to 50 and even 75 percent [38] of ultimate strength.

The increase in creep deflection caused in wood by increasing in moisture content or temperature is well documented, as indicated in the literature reviewed by Schniewind [38]. Increases in these properties have the effect of plasticizers that lower the viscosity of the matrix and allow increased deformation to occur at a given stress level [41]. The effect of a change in moisture content is much higher than that resulting from a change in temperature.

Bodig and Jayne reported that in composites adhesive bonds between fiber and between wood particles tend to weaken and may even rupture when exposed to high relative humidity [3]. The rate of flexural creep of particleboard was found to accelerate above approximately 75 percent relative humidity according to Haygreen et al [12].

Cyclic relative humidity conditions have a greater effect on creep properties of particleboard than steady state conditions, as reported by McNatt and Hunt, Laufenberg [27, 25].

2.4.4 Modelling of Creep

Numerous models have been utilized in the literature to describe the creep behavior of wood and wood-derived composite board. Essentially, these fall into two categories: empirical curve fitting and mechanical analogies in the form of linear viscoelastic models.

The power law model is most widely used in empirical curve fitting of the creep response of wood materials. The equation takes the form:

$$\varepsilon(t) = \varepsilon_0 + at^m \tag{2.18}$$

where: $\varepsilon(t)$ = time dependent strain

ε_0 = elastic strain

t = time

a, m = constants

Constants a and m can be determined by transforming the function to a linear relationship by rearranging and taking common logarithms:

$$\log(\varepsilon - \varepsilon_0) = \log a + m \log t \tag{2.19}$$

The power function is derived by taking the antilog of the linear equation.

The power model is simple and describes the creep response of wood and wood-derived materials well. Other possible empirical curve fitting options are illustrated in Table 2-3 [3].

The viscoelastic behavior, as shown in Figure 2-11 could also be simulated by mechanical analogies, i.e., a combination of springs and dashpots. Springs are used to simulate the elastic component, where stress is directly proportional to strain; and dashpots —— pistons moving in cylinders filled with a viscous fluid —— are used to represent the plastic or viscous components, where stress is directly proportional to the rate of strain.

The simplest linear model which has been used successfully for wood and wood derived materials is the four-element or Burger model as shown in Figure 2-13 [46, 1]. It is comprised of the Maxwell body and Kelvin body connected in series. The Maxwell body consists of a spring and a dashpot joined in series and accounts for elastic and viscous behavior, respectively. The Kelvin body represents delayed elastic behavior (visco-elastic) and consists of a parallel arrangement of spring and a dashpot. Together the two models with the four elements account for the principal features of the time-

dependent behavior of wood and wood composites.

In Figure 2-13, element A would respond instantly in accordance with its modulus of elasticity E_e , elements B and C cannot respond instantly because of the "sluggishness" of the dashpots. They both will deflect, however, with time (creep). Upon load removal, element A will recover instantaneously and completely, element B will slowly but completely contract to its original condition because of the restoring force of the spring. Element C will remain extended (permanent plastic deformation).

The theoretical formula of the Burger model expresses the total strain developed under stress with respect to time as the sum of the elastic, viscoelastic, and viscous components [9]:

$$\varepsilon(t) = \sigma\left(\frac{1}{E_e} + \frac{1}{E_{de}}(1 - e^{-t/\tau}) + \frac{1}{\eta_v}t\right) \qquad (2.20)$$

where: $\varepsilon(t)$ = time dependent strain

$\frac{\sigma}{E_e}$ = instantaneous elastic strain

$\frac{\sigma}{E_{de}}(1 - e^{-t/\tau})$ = delayed elastic strain, $\tau = \frac{\eta_{de}}{E_e}$ is retardation time

$\frac{\sigma}{\eta_v}$ = viscous flow

E_e = instantaneous modulus of elasticity

E_{de} = delayed modulus of elasticity

η_{de} = delayed coefficient of viscosity

η_v = viscous coefficient of viscosity

t = time

$\frac{1}{E_e}+\frac{1}{E_{de}}(1-e^{-t/\tau})+\frac{1}{\eta_v}t$ in Equation (20) is called creep compliance. For uniaxial loading, it can be used to define relaxation modulus by inverting the creep compliance.

An example of these parameters for commercial sheathing plywood and laboratory waferboard at three environmental conditions, and hardboard at two moisture content levels are shown in Table 2-4.

2.4.5 Visco-elastic Beam Theory

The constitutive equations for classic linear viscoelastic anisotropic material in a three dimensional state of stress can be written in a concise form using tensor notation [37, 7, 57]

$$\varepsilon_{ij}(t) = \int_{0^-}^{t} C_{ijkl}(t-\tau)\frac{\partial \sigma_{kl}}{\partial \tau}d\tau \qquad i,j = 1,2,3 \qquad (2.21)$$

The inverse of the above equation may be written as

$$\sigma_{ij}(t) = \int_{0^-}^{t} Y_{ijkl}(t-\tau)\frac{\partial \varepsilon_{kl}}{\partial \tau}d\tau \qquad i,j = 1,2,3 \qquad (2.22)$$

where C_{ijkl}, Y_{ijkl}, ε_{ij}, and σ_{ij} are defined to be the creep compliances, relaxation moduli, strains, and stresses, respectively. The stresses and strains in Equations (2.21) and (2.22) are functions of coordinate position as well as time.

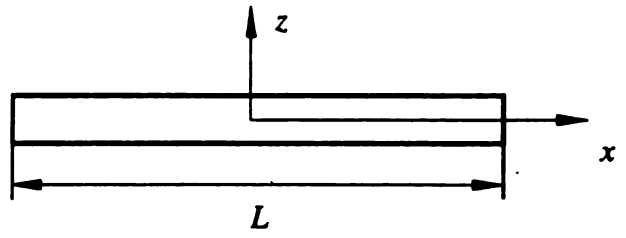

Figure 2-14 Uniaxial beam element.

For an uniaxial beam element (Figure 2-14), Equations (2.21) and (2.22) can be considerably simplified. Since the transverse shear strains are negligible, therefore the transverse deformation in the axial direction is a linear function of the z coordinate, and can be written as [19]

$$u = u_0 - z\frac{dw}{dx} \tag{2.23}$$

If the displacement w in the z direction is assumed to follow quadratic curve, The curvature of the beam is

$$K = -\frac{d^2w}{dx^2} \tag{2.24}$$

The signs of w and K follow the classic laminated theory.

The total axial strain which causes swelling stress due to hygroscopic expansion (ε^h) is in the form [35, 11, 57]

$$\varepsilon = \frac{du_0}{dx} + z\left(-\frac{d^2w}{dx^2}\right) = (\varepsilon^o - \varepsilon^h) + zK \tag{2.25}$$

where $(\varepsilon^o - \varepsilon^h)$ = the transverse strain.

The total axial time-wise stress is then determined by

$$\sigma^m(t) = \int_{0^-}^{t} Y(t-\tau)\,(\frac{d}{d\tau}\varepsilon^o(\tau) - \frac{d}{d\tau}\varepsilon^h(\tau) + z\frac{d}{d\tau}K(\tau))\,d\tau \qquad (2.26)$$

$$= \int_{0}^{t} Y(t-\tau)\,(\frac{d}{d\tau}\varepsilon^o(\tau) + z\frac{d}{d\tau}K(\tau) - \frac{d}{d\tau}\varepsilon^h(\tau))\,d\tau$$

where $Y(t-\tau)$ = the relaxation modulus in the axial direction

z = the distance between the neutral axis and the point considered

$\varepsilon^o(\tau)$ = the resultant strain at time τ

$K(\tau) = \frac{1}{R(\tau)}$, $R(\tau)$ is the radius of curvature of the beam at time τ

$\varepsilon^h(\tau)$ = the hygroscope free expansion due to change in moisture content at time τ .

Similar to the elastic theory, the total axial force over all layers is

$$N^m(t) = \int_{-\frac{h}{2}}^{\frac{h}{2}} \sigma^m(t)\,dz$$

$$= \int_{0}^{t}\sum_{k=1}^{n}\int_{h_{k-1}}^{h_k} Y(t-\tau)_k\,(\frac{d}{d\tau}\varepsilon^o(\tau) + z\frac{d}{d\tau}K(\tau) - \frac{d}{d\tau}\varepsilon^h(\tau)_k)\,dz\,d\tau \qquad (2.27)$$

$$= \int_{0}^{t} Q_{11}(t-\tau)\,\varepsilon'^o(\tau)\,d\tau + \int_{0}^{t} Q_{12}(t-\tau)\,K'(\tau)\,d\tau - \int_{0}^{t} N^h(t-\tau)\,d\tau$$

and the moment at the end of the beam is

$$M^m(t) = \int_{-\frac{h}{2}}^{\frac{h}{2}} \sigma^m(t)\, z dz$$

$$= \int_0^t Q_{21}(t-\tau)\,\varepsilon'^o(\tau)\,d\tau + \int_0^t Q_{22}(t-\tau)\,K'(\tau)\,d\tau - \int_0^t M^h(t-\tau)\,d\tau \qquad (2.28)$$

where $\varepsilon'^o(\tau) = \frac{d}{d\tau}\varepsilon^o(\tau)$

$$K'(\tau) = \frac{d}{d\tau}K(\tau)$$

and Q_{11}, Q_{12}, Q_{21}, and Q_{22} are functions of dimension and of relaxation moduli $Y(\tau)$. N^h and M^h are force and moment determined by dimension, relaxation moduli $Y(\tau)$ and the hygroscope free expansion $\varepsilon^h(\tau)$

$$Q_{11}(t-\tau) = \sum_{k=1}^{n} Y(t-\tau)_k (S_k - S_{k-1}) \qquad (2.29)$$

$$Q_{12}(t-\tau) = \sum_{k=1}^{n} \frac{1}{2} Y(t-\tau)_k (S_k^2 - S_{k-1}^2) = Q_{21}(t-\tau) \qquad (2.30)$$

$$Q_{22}(t-\tau) = \sum_{k=1}^{n} \frac{1}{3} Y(t-\tau)_k (S_k^3 - S_{k-1}^3) \qquad (2.31)$$

$$N^h(t-\tau) = \sum_{k=1}^{n} Y(t-\tau)_k (S_k - S_{k-1})\,\varepsilon'^h(\tau)_k \qquad (2.32)$$

$$M^h(t-\tau) = \sum_{k=1}^{n} \frac{1}{2} Y(t-\tau)_k (S_k^2 - S_{k-1}^2)\,\varepsilon'^h(\tau)_k \qquad (2.33)$$

The first derivative of $\varepsilon^h(\tau)$ can be approximated by

$$\varepsilon'^h(\tau_{i-1}) = \frac{\Delta\alpha(\tau_{i-1})}{(\tau_i - \tau_{i-1})} \tag{2.34}$$

where $\Delta\alpha(\tau_{i-1})$ = the hygroscope free expansion value between time τ_{i-1} and τ_i.

Equation (2.27) and (2.28) can be combined in matrix form

$$\begin{bmatrix} N^m(t) \\ M^m(t) \end{bmatrix} = \int_0^t \begin{bmatrix} Q_{11}(t-\tau) & Q_{12}(t-\tau) \\ Q_{21}(t-\tau) & Q_{22}(t-\tau) \end{bmatrix} \begin{bmatrix} \varepsilon'^o(\tau) \\ K'(\tau) \end{bmatrix} d\tau - \int_0^t \begin{bmatrix} N^h(t-\tau) \\ M^h(t-\tau) \end{bmatrix} d\tau \tag{2.35}$$

If there is no external force and moment, $N^m(t) = M^m(t) = 0$, Equation (2.35) becomes

$$\int_0^t \begin{bmatrix} N^h(t-\tau) \\ M^h(t-\tau) \end{bmatrix} d\tau = \int_0^t \begin{bmatrix} Q_{11}(t-\tau) & Q_{12}(t-\tau) \\ Q_{21}(t-\tau) & Q_{22}(t-\tau) \end{bmatrix} \begin{bmatrix} \varepsilon'^o(\tau) \\ K'(\tau) \end{bmatrix} d\tau \tag{2.36}$$

Using numerical analysis method,

$$\sum_{i=1}^{m} \begin{bmatrix} N^h(t-\tau_{i-1}) \\ M^h(t-\tau_{i-1}) \end{bmatrix} (\tau_i - \tau_{i-1})$$

$$= \sum_{i=1}^{m} \begin{bmatrix} Q_{11}(t-\tau_{i-1}) & Q_{12}(t-\tau_{i-1}) \\ Q_{21}(t-\tau_{i-1}) & Q_{22}(t-\tau_{i-1}) \end{bmatrix} \begin{bmatrix} \varepsilon'^o(\tau_{i-1}) \\ K'(\tau_{i-1}) \end{bmatrix} (\tau_i - \tau_{i-1}) \tag{2.37}$$

Taking $\tau_i - \tau_{i-1}$ = constant, and $\tau_m = t$, $\tau_0 = 0$, the above equation can be written as

$$\begin{bmatrix} \varepsilon'^o(\tau_{m-1}) \\ K'(\tau_{m-1}) \end{bmatrix} = \begin{bmatrix} Q_{11}(t-\tau_{m-1}) & Q_{12}(t-\tau_{m-1}) \\ Q_{21}(t-\tau_{m-1}) & Q_{22}(t-\tau_{m-1}) \end{bmatrix}^{-1}$$
$$\left(\sum_{i=1}^{m} \begin{bmatrix} N^h(t-\tau_{i-1}) \\ M^h(t-\tau_{i-1}) \end{bmatrix} - \sum_{i=1}^{m-1} \begin{bmatrix} Q_{11}(t-\tau_{i-1}) & Q_{12}(t-\tau_{i-1}) \\ Q_{21}(t-\tau_{i-1}) & Q_{22}(t-\tau_{i-1}) \end{bmatrix} \begin{bmatrix} \varepsilon'^o(\tau_{i-1}) \\ K'(\tau_{i-1}) \end{bmatrix} \right) \quad (2.38)$$

Obviously, once the relaxation modulus and the hygroscopic expansion are defined, all the parameters can be determined. The deformation rate $\begin{bmatrix} \varepsilon'^o \\ K' \end{bmatrix}$ at final time $t = \tau_m$ can therefore be obtained according to Equation (2.38).

The normal strain and the curvature $\begin{bmatrix} \varepsilon^o(\tau_m) \\ K(\tau_m) \end{bmatrix}$ can subsequently be found by

$$\begin{bmatrix} \varepsilon^o(\tau_m) \\ K(\tau_m) \end{bmatrix} = \begin{bmatrix} \varepsilon'^o(\tau_{m-1}) \\ K'(\tau_{m-1}) \end{bmatrix} (\tau_m - \tau_{m-1}) + \begin{bmatrix} \varepsilon^o(\tau_{m-1}) \\ K(\tau_{m-1}) \end{bmatrix}$$

$$= \sum_{i=1}^{m} \begin{bmatrix} \varepsilon'^o(\tau_{i-1}) \\ K'(\tau_{i-1}) \end{bmatrix} (\tau_{m-i+1} - \tau_{m-i}) + \begin{bmatrix} \varepsilon^o(\tau_0) \\ K(\tau_0) \end{bmatrix} \quad (2.39)$$

The deflection at any time t can be derived by setting the initial values being zero: $w(0,0) = 0$ and $w'(0,0) = 0$, and calculated by

$$w(x,t) = \frac{1}{2} K(t) x^2 \quad (2.40)$$

The center deflection can be obtained by substituting $x = \frac{L}{2}$

$$w_{max}(t) = \frac{1}{8} K(t) L^2 \qquad (2.41)$$

The final center deflection is the summation of center deflections determined for each time interval.

A program written in FORTRAN was generated for the calculation of w_{max} (Appendix B).

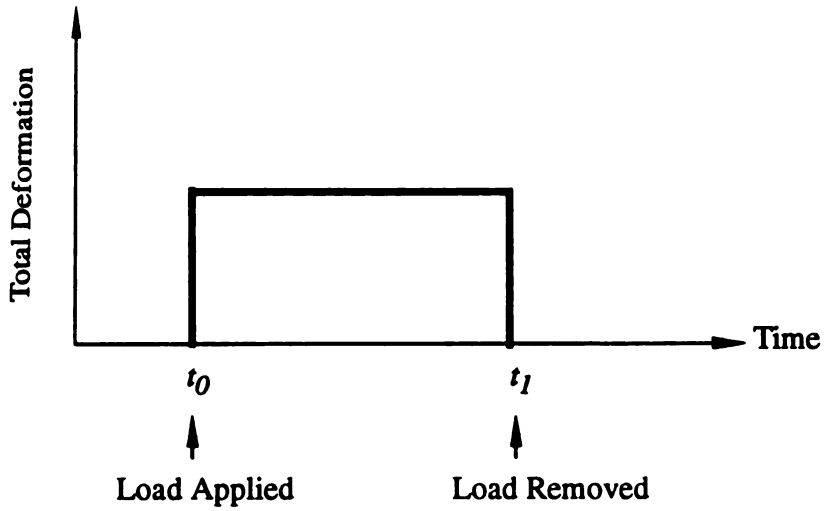

Figure 2-10 Deformation response curve to constant load of elastic materials.

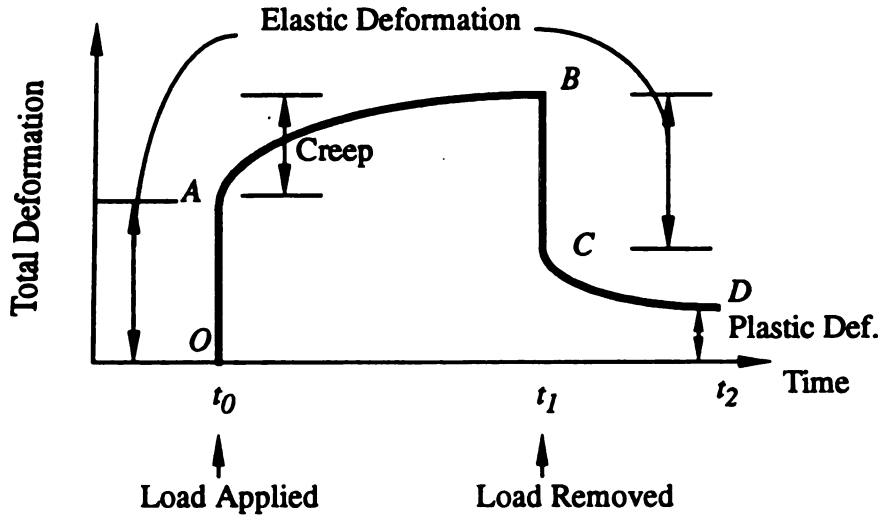

Figure 2-11 Deformation response curve to constant load of visco-elastic materials.

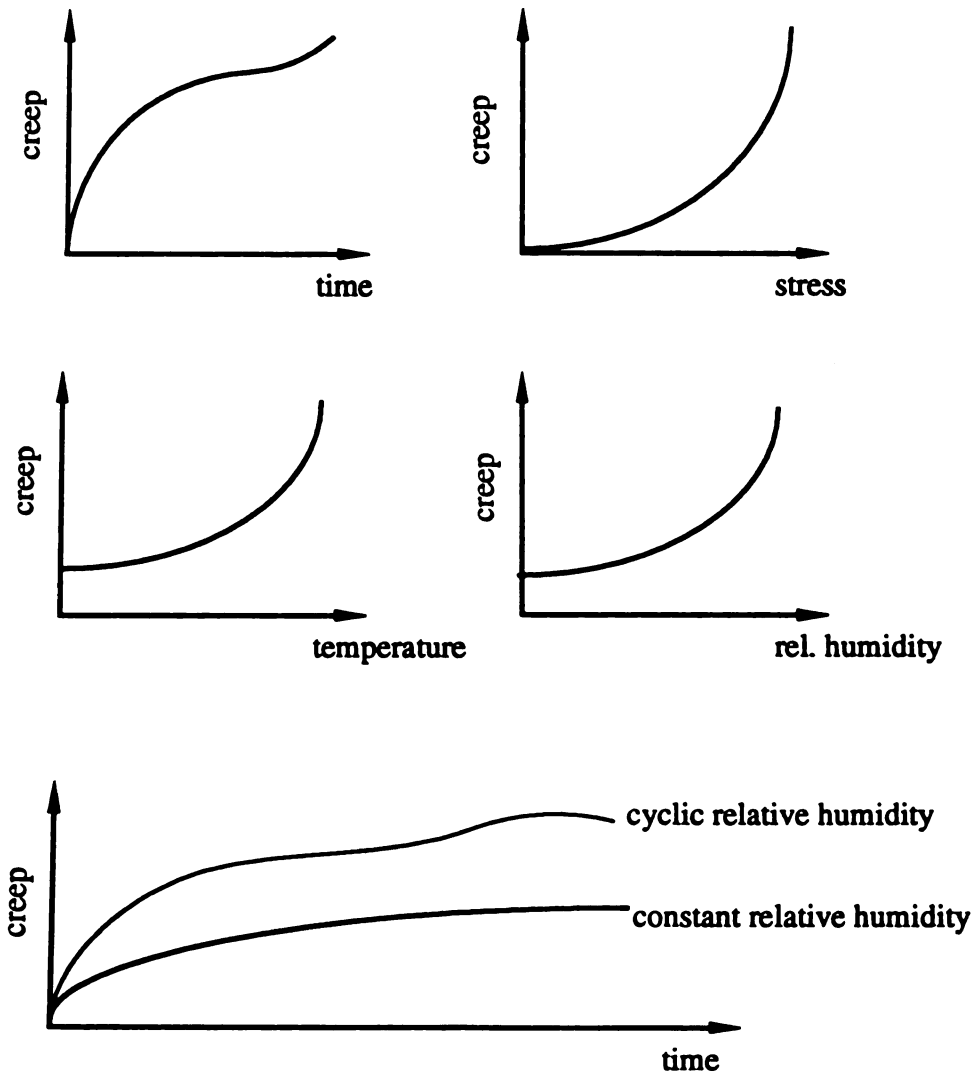

Figure 2-12 Effect of external factors on creep.

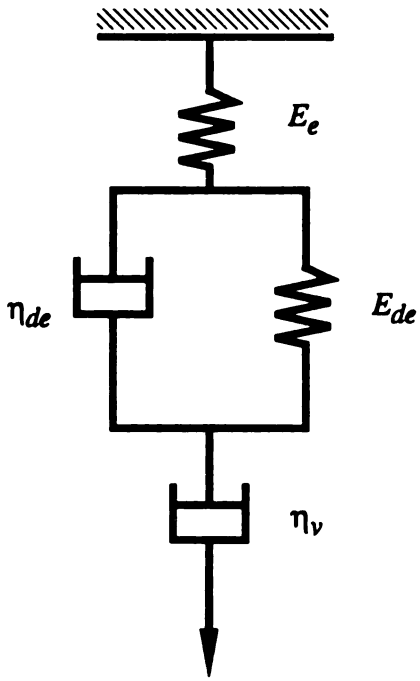

A. elastic element

B. delayed elastic element

C. plastic element

Figure 2-13 Burger's four-element visco-elastic model.

Table 2-3 Most often used empirical creep equations [3]

Name	Equation	Constants
Parabolic (power law)	$\varepsilon(t) = \varepsilon_0 + at^m$	a, m
Andrade one third law	$\varepsilon(t) = \varepsilon_0 (1 + at^{1/3}) e^{mt}$	a, m
Logarithmic	$\varepsilon(t) = a + b \log t$	a, b
Hyperbolic sine	$\varepsilon(t) = a + b \sinh ct^m$	a, b, c, m
deLacombe	$\varepsilon(t) = \varepsilon_0 + at^m + bt^n$	a, b, m, n
McVetty	$\frac{d\varepsilon}{dt} - \frac{d\varepsilon_0}{dt} = ae^{-bt}$	a, b
Marin-Pao	$\varepsilon(t) = \frac{\sigma}{E} + a\sigma^m (1 - be^{-nt}) + c\sigma^p t$	a, b, c, m, n, p
Garofalo	$\varepsilon(t) = \varepsilon_0 + \varepsilon_1 (1 - e^{-mt}) + \frac{d\varepsilon_2}{dt} t$	m
Ploynomial	$\varepsilon(t) = a + bt^{1/n} + ct^{2/n} + dt^{3/n}$	a, b, c, d, n

Table 2-4 Flexural creep parameters of wood composite boards [1], [30]

Parameter		Environmental Conditions							
		30 °C, 65%RH		20 °C, 65%RH		30 °C, 90%RH		8.42%*MC*	17.48%*MC*
		Plywood	Waferboard	Plywood	Waferboard	Plywood	Waferboard	Hardboard[1)]	
σ	(MPa)	3.71	3.51	3.53	3.51	3.75	3.50	2.42	2.42
E_e	(MPa)	7,924	5,108	7,965	5,219	7,696	5,131	882	588
E_{de}	(MPa)	65,269	27,912	51,105	20,211	34,024	11,372	-	-
η_{de}	(MPa-hrs)	177,736	66,518	111,780	50,849	87,455	27,856	-	-
τ	(hrs)	2.7231	2.3831	2.1873	2.5160	2.5704	2.4496	-	4.03
η_v	(MPa-hrs)	124,477,942	38,122,144	78,128,831	12,238,263	24,602,119	5,330,570	119,241	2,724
Elastic Strain									
ε_e	($\times 10^{-3} mm/mm$)	.471	.692	.475	.684	.495	.721	.555	1.005
Elastic Strain Recovery									
ε'_e	($\times 10^{-3} mm/mm$)	.465	.679	.461	.651	.480	.660	-	.855
Creep strain									
ε_t	($\times 10^{-3} mm/mm$)	.094	.246	.130	.526	.308	1.189	.180	1.74
Irrecoverable Strain									
ε_p	($\times 10^{-3} mm/mm$)	.040	.133	.064	.366	.205	.913	-	1.56

1) Data are approximated and interpreted from the figures of Moslemi's study [30]

Note: 1 MPa = 145 psi

2.5 Development of Experiment on Restrained Swelling

The experiment is based on the supposition that the warping of a laminated panel can be predicted better by replacing two of the three inputs (E_i , T_i , α_i) for each layer with parameters that allow for the viscoelastic characteristics of wood. Instead of using α_i which is the total free expansion of the lamina for a given moisture content interval, we will use only the "elastic portion" of it, i.e., that part which is actually transformed into elastic strain. And instead of using E_i which is the statically determined modulus of elasticity as a function of moisture content, we will use a "deformation modulus" defined as the maximum measured swelling stress divided by the elastic portion of the free expansion

$$E' = \frac{\sigma'}{\varepsilon_{elast}} \tag{1.11}$$

The thickness, T_i , of course remains unaffected. Both σ'_i and ε_{ielast} must be determined by experiment.

As has been pointed out before, solid wood behaves sufficiently elastically in the longitudinal direction, so that the above modification need only be applied to layers stressed in the transverse direction (radial or tangential).

This approach is illustrated in Figure 2-15 for the special case of a two-ply laminate in which one lamina has a large hygroscopic expansion and a low modulus of elasticity while the other has no or very little hygroscopic

expansion and a very high modulus of elasticity. This would be typical of a two-ply solid wood cross laminate.

The figure shows the free expansion in the horizontal axis and the elastic portion of this expansion which will sustain the swelling stress under complete restraint on the vertical axis.

One could view the condition of complete restraint of one lamina by the other as the moisture content increases from one level to another as being equivalent to the condition where the expanding lamina was allowed to move freely and was then compressed back to its original length.

In a visco-elastic material, only a portion of this compressive strain e_2 would be converted to elastic strain. In Figure 2-15 this portion is shown as ε_{2elast}. It is that portion of the completely restrained hygroscopic expansion which sustains a swelling stress at the end condition (hygroscopic equilibrium). The graph assumes that this portion ε_{2elast} increases linearly from zero.

This elastic portion of the total compressive strain can be readily measured for any end condition involving moisture content increase. The condition of a shrinking laminate involving tensile strain is very similar, but the experimental determination of the elastic strain portion would be much more difficult. The experiments are therefore limited to moisture content increases.

The elastic ε_{2elast} is thus substituted for the free expansion in the warping formula. And instead of the modulus of elasticity E, measured at the end condition by static test, the more realistic ratio of the swelling stress at the end condition divided by ε_{2elast} is used (deformation modulus). The

swelling stress is determined in the same experiment used for the determination of ε_{2elast} .

Lamina I in Figure 2-15 is assumed to be elastic and requires no substitution.

Upon increase in moisture content from the initial condition, the length change of lamina I and therefore of the whole laminate is practically zero. The free expansion α_2 is being completely restrained ($\alpha_2 = e_2$). Rather than using $e_2 \times E_2$ for the calculation of the compression stress at stress balance, we shall use $\varepsilon_{2elast} \times E'_2$, where ε_{2elast} is the instantaneously recovered axial compression deformation after completely restrain α_2 to moisture content equilibrium

$$E'_2 = \frac{\sigma'}{\varepsilon_{2elast}} \qquad (2.42)$$

where σ' = the measured axial compression stress at complete restraint of α_2 at moisture content equilibrium.

Inputs for layer I would be E_1 and α_1 since E_1 is very large and α_1 very low that the elastic assumptions are justified.

The measurement of ε_{2elast} and E'_2 requires a test apparatus capable of continuous measurement of specimen weight, development of axial swelling stress, and upon releasing of the restraint at moisture content equilibrium, of the instantaneous recovery of the restrained expansion, ε_{2elast} . Additionally, the free expansion would also be measured. This apparatus will be described in detail below.

We will now consider the more general case of a two-ply laminate in

which both layers expand and have moderate moduli of elasticity. This is the case presented in the introductory chapter (see Figure 1-3).This more general case is illustrated in Figure 2-16. Both layers will be considered to be visco-elastic.

The two layers have unequal free expansion ($\alpha_2 > \alpha_1$) and unequal moduli ($E_1 \neq E_2$). The elongation of the laminate after moisture content increase is based on stress balance ($\sigma_1 = \sigma_2$). This final elongation (α_{res}) lies somewhere between α_1 and α_2 , which means that layer I will be extended (tensile stress) and layer II be compressed (compression stress).

In analogy to the previous example the stress balance for the two layers will be calculated as

$$\sigma_1 = \varepsilon'_{1elast} \; E'_1 \tag{2.43}$$

and

$$\sigma_2 = \varepsilon'_{2elast} \; E'_2 \tag{2.44}$$

at stress balance

$$\sigma_1 = \sigma_2 \tag{2.45}$$

or

$$\varepsilon'_{1elast} \; E'_1 = \varepsilon'_{2elast} \; E'_2 \tag{2.46}$$

Here however the values ε'_{1elast} and ε'_{2elast} are not the measured

recovered compression strain after complete axial restraint but only a certain portion of that depending on the extent of the final remain restraint which is equal to e_2 in the case of layer II and e_1 in the case of layer I. These portions are indicated within the shaded triangles.

It should be noted that layer I is not being restrained in a positive sense (compression) but in a negative sense (tension). This would require that ε_{1elast} be determined by a tension test. However, such tension tests are much more difficult to conduct and, therefore, the important assumption was made that ε_{1elast} as determined by compression test is a valid approximation of the corresponding value found by tension test.

The point of stress balance is found in Figure 2-16 as the point of intersection of the two lines representing $\varepsilon'_{1elast} \times E'_1$ and $\varepsilon'_{2elast} \times E'_2$. Determination of the point of intersection will yield ε'_{1elast} and ε'_{2elast}, the desired inputs for the warping equation. E'_1 and E'_2 are determined as described above.

The expression of e_1, e_2, ε'_{1elast} and ε'_{2elast} can be written in terms of known values ε_{1elast}, ε_{2elast}, α_1, α_2, E'_1 and E'_2 as follows

$$e_1 = \frac{\varepsilon_{2elast} E'_2 (\alpha_2 - \alpha_1)}{\alpha_2 \left(\varepsilon_{1elast} \frac{E'_1}{\alpha_1} + \varepsilon_{2elast} \frac{E'_2}{\alpha_2} \right)} \qquad (2.47)$$

$$e_2 = \frac{\varepsilon_{1elast} E'_1 (\alpha_2 - \alpha_1)}{\alpha_1 \left(\varepsilon_{1elast} \frac{E'_1}{\alpha_1} + \varepsilon_{2elast} \frac{E'_2}{\alpha_2} \right)} \qquad (2.48)$$

$$\varepsilon'_{1elast} = \frac{\varepsilon_{1elast}\varepsilon_{2elast}E'_2(\alpha_2 - \alpha_1)}{\varepsilon_{1elast}E'_1\alpha_2 + \varepsilon_{2elast}E'_2\alpha_1} \tag{2.49}$$

$$\varepsilon'_{2elast} = \frac{\varepsilon_{1elast}\varepsilon_{2elast}E'_1(\alpha_2 - \alpha_1)}{\varepsilon_{1elast}E'_1\alpha_2 + \varepsilon_{2elast}E'_2\alpha_1} \tag{2.50}$$

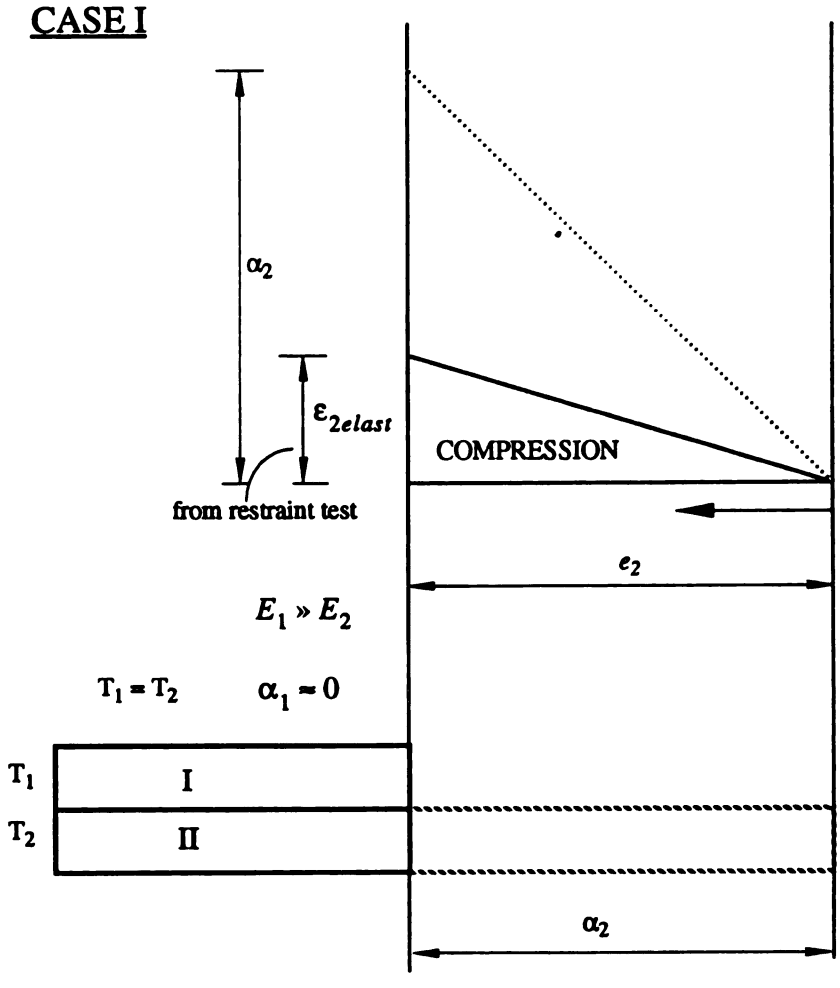

Input into warping equation: E_1, α_1

$$E'_2 = \frac{\sigma'}{\varepsilon_{2elast}} \quad , \quad \varepsilon_{2elast}$$

Figure 2-15 Case I: Complete restraint.

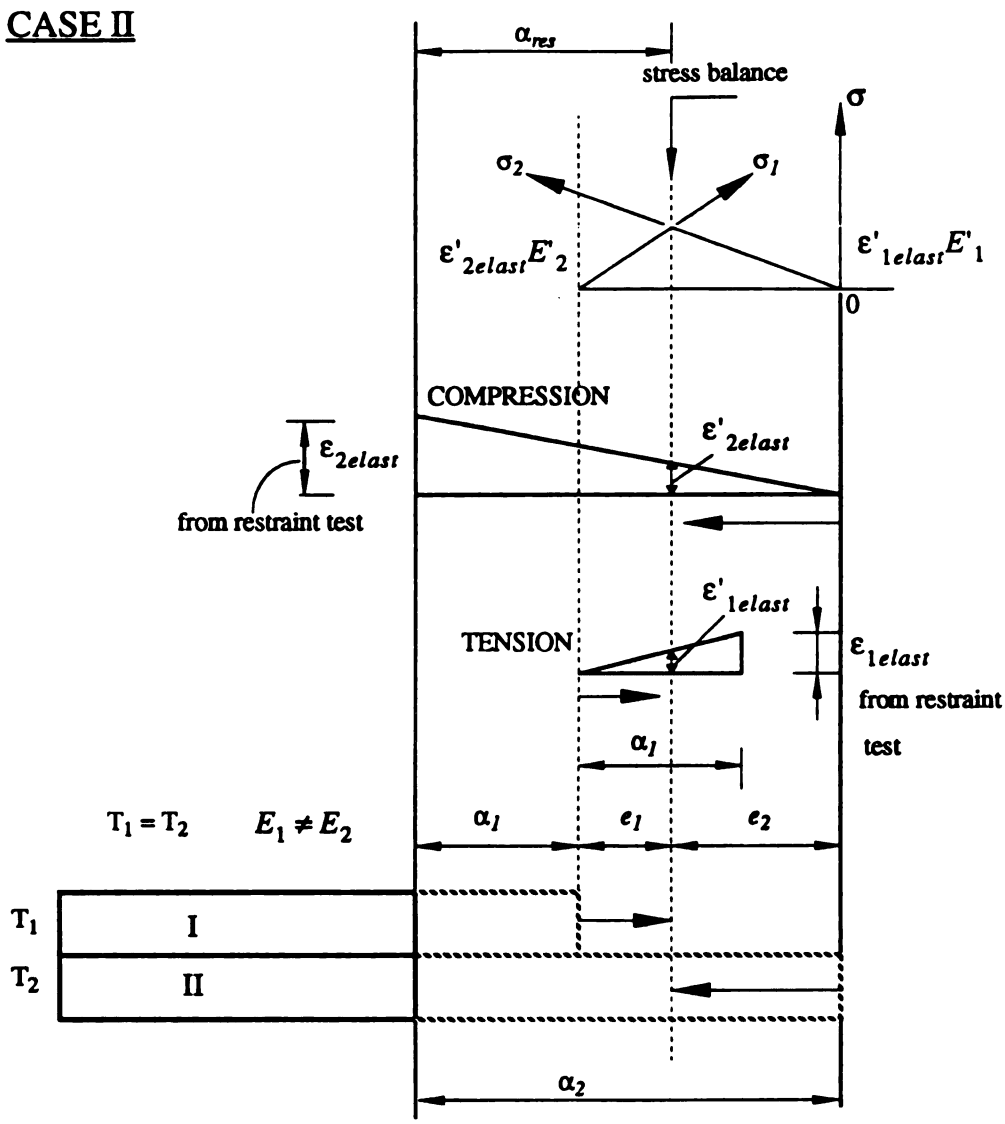

Input into warping equation: E'_1, ε'_{1elast}

E'_2, ε'_{2elast}

Figure 2-16 Case II: Partial restraint.

2.6 Objectives and Scope of the Study

A qualitative understanding of the mechanics of panel warping is needed if we are to improve the performance of wood and wood composite products such as laminated wood, plywood or laminated wood composite panels.

The main objective of this study is to demonstrate the theoretical analysis of the warping problem, elastically and non-elastically; to investigate various factors involved in the hygroscopic warping; to evaluate and compare the prediction power of different theories or approaches; and to see the possibility of improving the existing theory by using alternative inputs.

Theoretical analysis can be classified as elastic theory and visco-elastic theory. Beyond the theoretical analysis, it is desirable to conduct some simple but practical warping experiments using various materials with different hygroscopic characteristics and conditions. This will allow verification of analytical prediction.

The scope of the experiment is limited to narrow laminated beams, since the results from beams can be used to simulate the maximum deformation of a corresponding plate.

The secondary objective of this study is to experimentally investigate the measurement of true swelling stresses on wood and wood composite materials upon hygroscopic expansion. A specially designed device will be used for this study. These experiments will also provide the inputs for the theoretical treatments.

CHAPTER III

EXPERIMENTAL METHODS

3.1 General

The experiments were designed to provide the following

- hygroscopic and mechanical characteristics of the laminating materials to be used as input into warping equations
- warping measurements on laminated beams of various combination and exposed to a variety of relative humidity intervals.

It was essential that the specimens used for the determination of hygroscopic and mechanical characteristics were truly representative of the characteristics of the laminas used for the manufacture of the laminated beams. This was especially critical in the case of the solid wood beams because solid wood often shows considerable variation of its properties between specimens coming from the same source.

The warping of the beams was observed over a number of different relative humidity intervals (always increasing humidity). This required that hygroscopic and mechanical tests were conducted at various levels of relative

humidity equilibrium and over various relative humidity intervals.

For the solid wood laminated beams, the warping was measured over these intervals of relative humidity exposure:

66 - 81%

66 - 93%

and for the composite beams these intervals were

30 - 81%

50 - 81%

30 - 93%

50 - 93%

The testing program essentially breaks down into these elements:

- Determination of modulus of elasticity in tension and compression at the above relative humidity levels and determination of hygroscopic expansion over the above relative humidity intervals
- Determination of the elastic portion of the free expansion and determination of the actual swelling stress of restrained specimens. This work required special apparatus which will be described later.

Three types of wood materials were used throughout the study, namely, solid wood, yellow-poplar (*Liriodendron tulipifera*), medium-density-fiberboard (MDF), and particleboard (PB).

Tangentially sawn yellow-poplar lumber 4- to 6- *inch* wide, 1-*inch* thick and 6-*ft* long was purchased from a local sawmill. Its average density was 0.483 g/cm^3 when moisture content is about 9 percent.

4-*ft* by 4-*ft* panels of MDF and PB of 1-*inch* thickness were cut from commercially manufactured panels provided by Georgia Pacific Corporation. Both types of product had 8 percent average moisture content and the density was 0.85 g/cm^3 for MDF and 0.82 g/cm^3 for the PB.

3.2 Specimen Preparation

3.2.1 Yellow-Poplar

In order to test the warping equation to the plywood structure, a yellow-poplar board with only tangential and longitudinal direction in the plane of the board was manufactured in the laboratory. The specimen preparation and the experimental design were established based on the preliminary study and experiments and is described in the following:

Clear and straight grained lumber were jointed and planned to 0.75-*inch* thickness. The boards were then cut into 1-*inch* wide and 5-*ft* long strips on a table saw.

After conditioning these strips at the initial condition of 66 percent *RH* at 70°*F*, 26 strips which had perfect flat grain and were straight were carefully selected and edge-glued to a panel as illustrated in Figure 3-1 using epoxy resin (Duro$_{TM}$ Master Mend^{TM} TM61). The dimension of the panel at this point was 25-*inch* by 60-*inch* with a thickness of 0.75-*inch*.

The panel was then trimmed down to a size of 24-*inch* by 48-*inch* and planned to a thickness of 0.25-*inch*. All the test specimens were cut from this sheet (see Figure 3-2) and are described as follows:

Hygroscopic expansion specimens (24-*inch* by 1-*inch* by 0.25-*inch*):

E-L (longitudinal)

E-T (tangential)

Beam lamina (24-*inch* by 1-*inch* by 0.25-*inch*):

L1, L2, L3, L4 (longitudinal)

T1, T2, T3, T4 (tangential)

These laminas were used to construct three types of unbalanced cross-laminated beams as shown in Figure 3-3 and as described in Section 3.3.3.

Tension test specimens (10-*inch* by 0.25-*inch* by 0.25-*inch*):

L1-T1, L1-T2..... L4-T1, L4-T2 (longitudinal)

It will be noted that these specimens correspond directly and are part of strips L1 to L4 used for the laminated beams

Compression test specimens (4-*inch* by 1-*inch* by 0.75-*inch*)

Comp1, Comp2, Comp3 (tangential)

These three strips dimensioned 24-*inch* by 1-*inch* by 0.25-*inch* were laminated to form a 1-*inch* wide and 0.75-*inch* thick beam, which is later cut into 4-*inch* long specimens (see Section 3.3.5).

Restraint test specimens (2-*inch* by 1-*inch* by 0.25-*inch*)

R1, R2, E1, E2 (tangential)

These four strips dimensioned 24-*inch* by 1-*inch* by 0.25-*inch* were used to make restraint specimens (2-*inch* by 1-*inch* by 0.25-*inch*). Half of them were used for restrained swelling test specimens, and the other half were used for hygroscopic

expansion test specimens as matched samples as described in Section 3.3.6.

It will be noted that a special effort was made to characterize the strips used for beam construction in terms of their important properties as closely as possible by appropriate specimen selection from the edge glued panel.

For complete listing of test specimens see Table 3.1

3.2.2 Wood Composite Board

A similar experiment was conducted with wood composite board. Again the warping was evaluated on two ply laminated beams. Since wood composition boards are orthotropic in the plane of the board, the hygroscopic and mechanical imbalance was created by laminating two dissimilar board materials, one being an MDF board and the other a particleboard.

Most wood composite boards have a pronounced density variation over their cross-section (thickness). This density variation is generally balanced with higher density in the faces and lower density in the center.

In order to eliminate possible effects of this density variation on beam balance, the beam laminas and all other specimens were cut from the full thickness of the board (1 *inch*). The width of each specimens (0.25-*inch*) became the thickness of the lamina (see upper right corner of Figure 3-4).

The cutting scheme of specimens from MDF and PB is presented in Figure 3-4. A board was first cut into four equal size pieces to provide four replications with randomization. On each piece, specimens were cut along

the machine direction of the board according to the cutting schedule shown in Figure 3-4 and described as follows

Hygroscopic expansion specimens (12-*inch* by 1-*inch* by 0.25-*inch*):

E1-1, E1-2, E2-1, E2-2,..., E4-1, E4-2

Laminated beam lamina (30-*inch* by 1-*inch* by 0.25-*inch*):

B1, B2, B3, B4

These laminas cut from MDF and PB were laminated to construct four two-ply unbalanced laminated beams.

Tension test specimens (10-*inch* by 1-*inch* by 0.25-*inch*):

MT1-1, MT1-2,..., MT4-1, MT4-2

Only specimens cut from MDF were tested.

Compression test specimens (4-*inch* by 1-*inch* by 1-*inch*):

C1-1, C1-2, C1-3, C1-4,..., C4-1, C4-2, C4-3, C4-4

Only specimens cut from PB were tested.

Restraint test specimens (2-*inch* by 1-*inch* by 0.25-*inch*):

As in the case of yellow-poplar, some of them were used as restrained swelling test specimens, and the rest were used as matched samples for hygroscopic expansion test and weight gain control samples as described in Section 3.3.6.

For complete listing of test specimens see Table 3.1.

Table 3-1 Test specimen outline

Yellow-Poplar

Specimen ID	Test	Size (in)	Exposure Condition (%RH)	Replication
E - T	Tangential hygroscopic expansion	1 x .25 x 24	66 - >81 -> 93	1
E - L	Longitudinal hygroscopic expansion	1 x .25 x 24	66 - >81 -> 93	1
L1-T1, L1-T2	Longitudinal tension from L1	.25 x .25 x 10	66, 81 , 93	2
L2-T1, L2-T2	Longitudinal tension from L2	.25 x .25 x 10	66, 81 , 93	2
L3-T1, L3-T2	Longitudinal tension from L3	.25 x .25 x 10	66, 81 , 93	2
L4-T1, L4-T2	Longitudinal tension from L4	.25 x .25 x 10	66, 81 , 93	2
Cut from Comp1,2,3	Tangential compression	1 x .75 x 4	66, 81 , 93	5
Cut from R1	Tangential restrained swelling	1 x .25 x 2	66 ->81	5
Cut from R2	Tangential restrained swelling	1 x .25 x 2	66 ->93	5
Cut from E1	Short column, free expansion	1 x .25 x 2	66 ->81	5
Cut from E2	Short column, free expansion	1 x .25 x 2	66 ->93	5
T1, T2, T3, T4	Tangential beam lamina	1 x .25 x 24	66 - >81 -> 93	
L1, L2, L3, L4	Longitudinal beam lamina	1 x .25 x 24	66 - >81 -> 93	

Table 3-1 (continued)

MDF & PB

Specimen ID	Test	Size (in)	Exposure Condition (%RH)	Replication
MDF	Tension	1 x .25 x 10	81, 93	8
MDF	Hygroscopic free expansion	1 x .25 x 12	30 -> 50 -> 81 -> 93	8
MDF	Restrained swelling, free expansion	1 x .25 x 2	30 -> 81	6 - 8
MDF	Restrained swelling, free expansion	1 x .25 x 2	50 -> 81	6 - 8
MDF	Restrained swelling, free expansion	1 x .25 x 2	30 -> 93	6 - 8
MDF	Restrained swelling, free expansion	1 x .25 x 2	50 -> 93	6 -8
PB	Compression	1 x .25 x 4	30, 50, 81, 93	4
PB	Hygroscopic free expansion	1 x .25 x 12	30 -> 50 -> 81 -> 93	8
PB	Restrained swelling, free expansion	1 x .25 x 2	30 -> 81	6 - 8
PB	Restrained swelling, free expansion	1 x .25 x 2	50 -> 81	6 - 8
PB	Restrained swelling, free expansion	1 x .25 x 2	30 -> 93	6 - 8
PB	Restrained swelling, free expansion	1 x .25 x 2	50 -> 93	6 -8
MDF, PB	Beam lamina	1 x .25 x 30	30 -> 81	
MDF, PB	Beam lamina	1 x .25 x 30	50 -> 81	
MDF, PB	Beam lamina	1 x .25 x 30	30 -> 93	
MDF, PB	Beam lamina	1 x .25 x 30	50 -> 93	

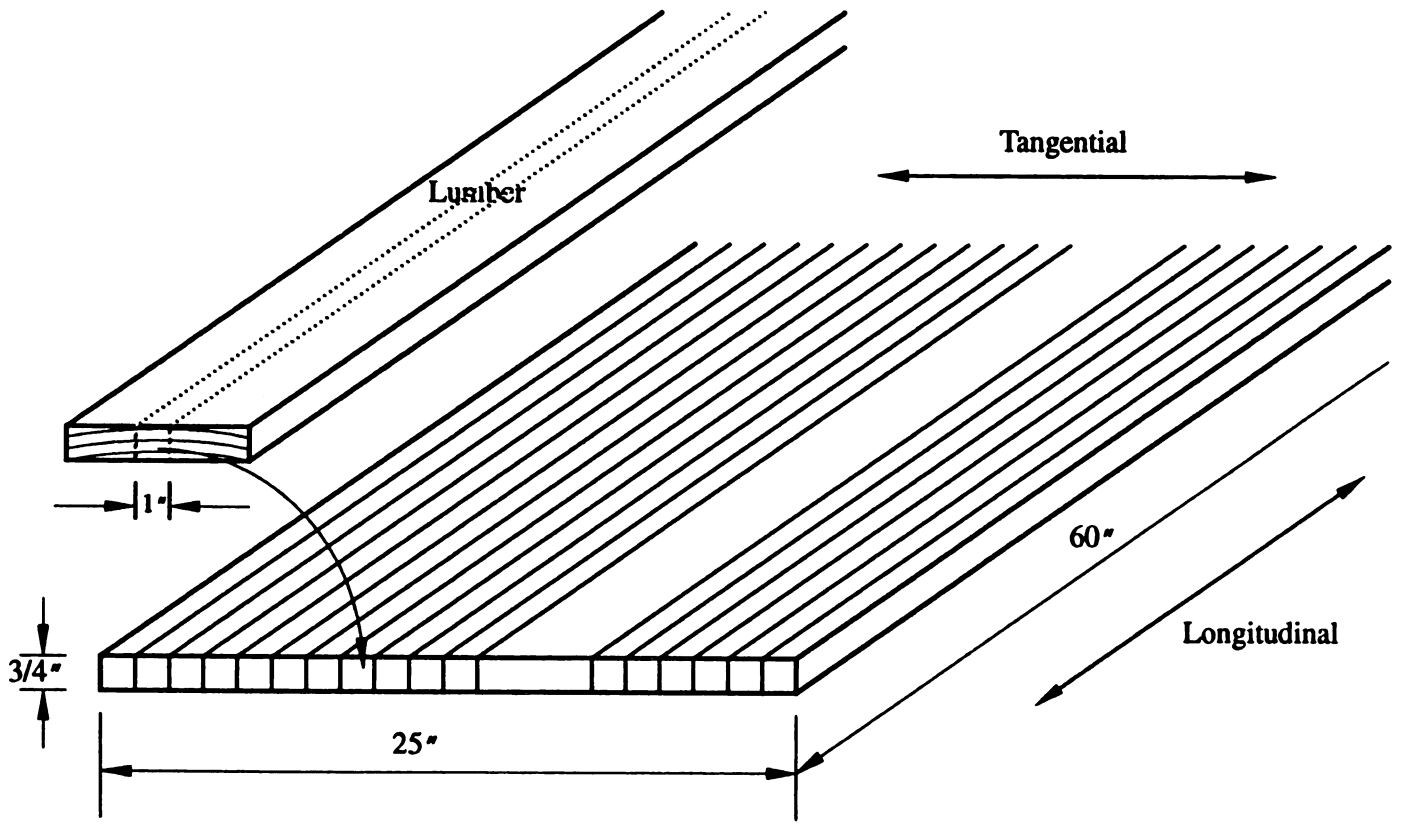

Figure 3-1 Designing of yellow-poplar board.

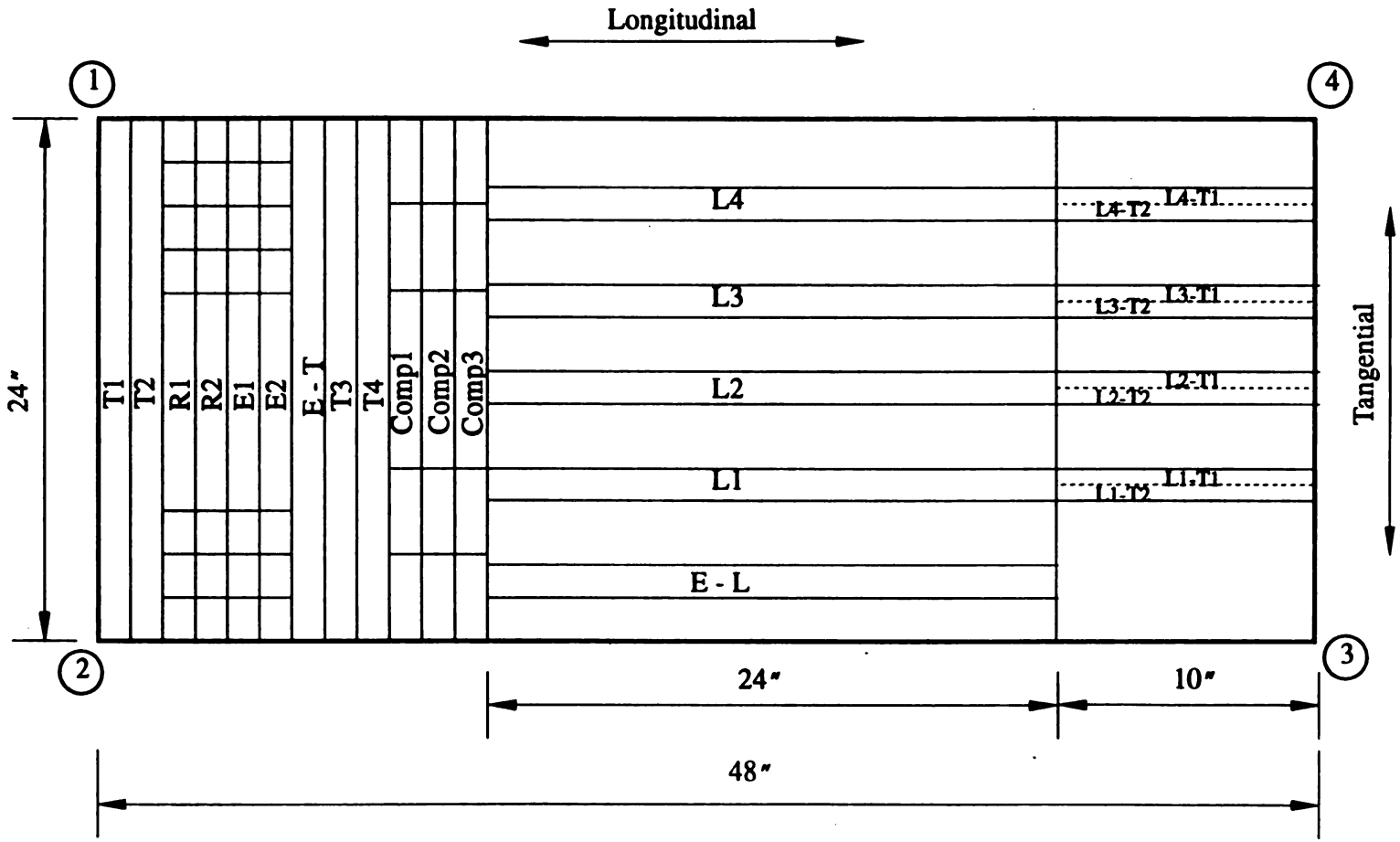

Figure 3-2 Specimen arrangement on the yellow-poplar panel.

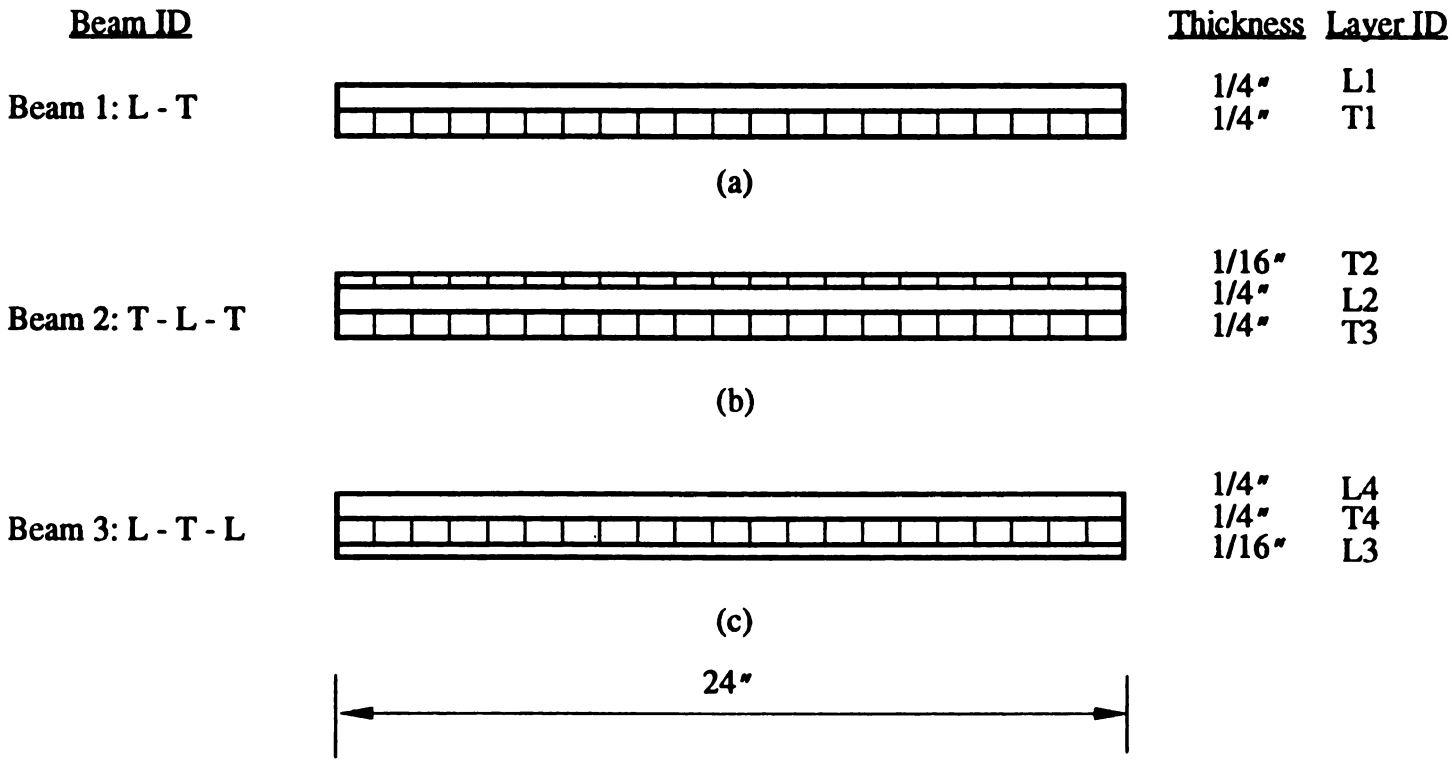

Figure 3-3 Designing of unbalanced yellow-poplar laminated beams. Upon increasing in relative humidity, beams warp concavely upward.

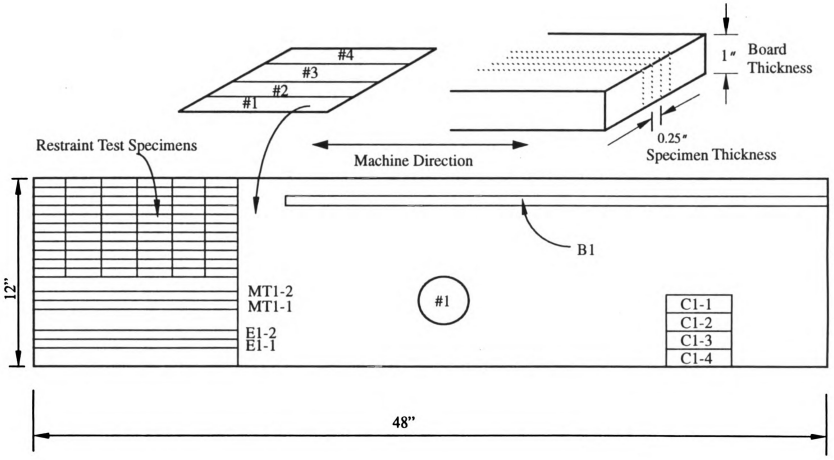

Figure 3-4 Cutting diagram for 1-inch thick MDF and PB boards

3.3 Test Methods

3.3.1 Relative Humidity Condition

To provide the various relative humidity conditions a conditioning chamber was used to obtain 30 and 50 percent relative humidity, while different types of saturated salt solutions were employed for 66, 81, and 93 percent relative humidity: Sodium Nitrite, $NaNO_2$, for 66%, Ammonium Sulfate, $(NH_4)_2SO_4$, for 81%, and Mono Ammonium Phosphate, $NH_4H_2PO_4$, for 93%.

The conditioning chamber shown in Figure 3-5, which has a volumetric capacity of 20-ft^3, was manufactured by Parameter Generation Company. It is equipped with solid-state controls for precise adjustments and provides constant temperatures ranging from $4°C$ to $88°C$ and constant relative humidities ranging from 10 percent to 98 percent.

A series of tanks 12 x 30 x 12.5-*inch* in size charged with different saturated salt solutions were used to condition the larger specimens. Saturated salt solutions were maintained in two plastic trays placed in each tank. Specimens were supported on a plexiglass frame. Each tank was equipped with a fan to supply air circulation, as exhibited in Figure 3-6.

In addition to the tanks, several laboratory desiccators were also used for conditioning the smaller specimens, and two stainless steel desiccators were used for restraint tests.

3.3.2 Measurement of Hygroscopic Expansion

The hygroscopic free expansion is calculated by using the following equation

$$\alpha = \frac{(L_2 - L_1)}{L_1} \qquad (in/in)$$

where L_1 and L_2 are the initial and the final length of the specimen, respectively.

Determination of hygroscopic expansion was carried out using two different measurement methods, namely a dial gage and an optical comparator.

Yellow-poplar specimens were tested by a dial gage fixed on an aluminum frame as illustrated in Figure 3-7. The dial gage has an accuracy of 0.001 *inch* being equivalent to 0.004% of the 24-*inch* long specimen. Both specimens (longitudinal and tangential) were measured after exposure to sequential *RH* levels of 66 percent, 81 percent and 93 percent.

Measurements were taken at each relative humidity condition after the specimens had reached their equilibrium moisture contents. These conditions were the same as those at which the laminated beams were conditioned. The results were used as inputs to the warping equation.

Hygroscopic expansion of MDF and PB were determined on an optical comparator as described by Suchsland [50] and shown in Figure 3-8. Specimens were cut to 12-*inch* length, 1-*inch* width and 0.25-*inch* thickness. Gage length was 10.000 *inches*.

After an initial storage at 30 percent RH, specimens were sequentially conditioned at 50 percent, 81 percent and 93 percent relative humidity. These conditions were different from those used for the conditioning of yellow-poplar specimens. However, they were the same as the conditions used for the laminated beams of MDF and PB as explained in the following section.

3.3.3 Measurement of Warping of the Laminated Beams

In order to compare the analytical predictions with the experimental results, several laminated beams with material or structural unbalance were fabricated from yellow-poplar, MDF and PB strips.

Yellow-Poplar

Three types of yellow-poplar laminated beams were made introducing structural and material unbalance (see Figure 3-3). These were:

L - T beam: a two-ply beam with longitudinal and tangential strips cut from the yellow-poplar sheet. Each strip was 24-*inch* long and 1-*inch* wide and approximately 1/4-*inch* thick.

T - L - T beam: a three-ply beam with an additional 1/16-*inch* thick tangential lamina added to the above L-T beam.

L - T - L beam: a three-ply beam with an additional 1/16-*inch* thick longitudinal lamina attached to the above L-T beam.

The thinner laminas in beams T-L-T and L-T-L were originally 0.25-

inch thick. Their thickness was reduced by planning after the beams had been assembled.

MDF and PB

Four identical two-ply wood composite beams with 30-*inch* length and 1-*inch* width were laminated using MDF and PB. Each layer was cut from the board as indicated in Figure 3-4. The laminas were 1-*inch* wide and 0.25-*inch* thick.

Laminating and Conditioning Procedure

For all the yellow-poplar beams and MDF/PB beams, the strips or lamina were first conditioned at the initial condition, then they were glued together to the various combinations as explained previously by an epoxy glue. The purpose of using the epoxy glue was to avoid the addition of water. After glue lines were set, the beams were kept in the initial condition until equilibrium was reached again. The initial warping (center deflection) of the beams over the span was monitored on a device equipped with a dial gage having an accuracy of 0.001 *inch* as shown in Figure 3-9. The beams were then brought to the next higher *RH* atmosphere. The warping and the weight change were measured thereafter until the measurements remained constant and the beam was considered to have equalized. The effective measured warping W_m is the difference between the final and the initial center deflection.

All three yellow-poplar beams were exposed at the sequential relative humidity levels of 66 percent, 81 percent and 93 percent.

For MDF and PB laminated beams, two pairs were initially conditioned at 30 percent and 50 percent relative humidity levels respectively. After they reached equilibrium moisture content, one of each pair was exposed to 81 percent while the other was conditioned at 93 percent relative humidity (see Figure 3-10).

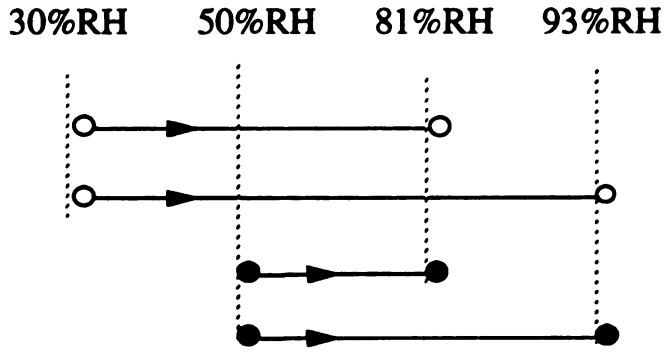

Figure 3-10 Relative humidity conditions for MDF/PB laminated beams.

3.3.4 Tension Test

Static tension tests were performed for those laminas which would be subjected to tensile stress during warping. In the case of yellow-poplar those laminas are the longitudinal laminas, and in the case of the composites they

are the MDF laminas, because MDF has a lower hygroscopic expansion than PB, putting it in tension during moisture uptake.

Yellow-Poplar

Tension specimens of yellow-poplar were cut from the end of the strips that were used as laminas for the unbalanced laminated beam as shown in Figure 3-2. Two specimens were used from each lamina with a cross-sectional area of 0.25-*inch* x 0.25-*inch* . The obtained modulus of elasticity (*MOE*) represents the *MOE* of the lamina, and would be appropriate as input for the tension layer in the elastic warping equation.

The dimensions and the construction of the tension specimens are illustrated in Figure 3-11 (a). The ends of the specimen were reinforced with two angled pieces of wood. Holes drilled through the center of these assembles allowed load transfer by means of steel shafts. The axis of the hole was aligned perfectly perpendicular to the axis of the specimen to prevent the development of a bending moment during loading.

The tensile force was applied by dead load. An 1-*inch* strain gage extensometer was mounted at the center part of the specimen. Readings were recorded by using a 3800 Strain Indicator manufactured by Measurements Group, Instruments Division with 1/63000 *inch* of precision over the 1-*inch* span. After conditioning to equilibrium at 66 percent relative humidity, a specimen was loaded by a 10 *lb* weight, initially. Increments of 10- *lb* loads were added thereafter until the total load would develop a stress of 1/3 of the proportional limit of the material. Therefore, the loading was always

within the elastic range of the material. The specimens were retested using the same procedure after exposure to equilibrium at 81 percent and 93 percent relative humidity levels, respectively.

Only the MOE values in tension at the end conditions, 81% RH and 93% RH, were subsequently used as the inputs in the elastic warping equation.

All specimens were tested in an environment of 66 percent relative humidity and 70°F. The specimens conditioned at the higher relative humidity levels may have lost some moisture during the testing. But these losses were considered to be insignificant and were disregarded.

MDF

MDF tensile specimens were tested in a similar way. They were randomly selected from the board. Six samples were tested. The full cross-sectional area of the board was utilized as shown in Figure 3-11 (b). The relative humidity conditions to which the specimens were exposed were 81 percent and 93 percent.

3.3.5 Compression Test

Compression tests were carried out for the materials which would be under compression in an expanding unbalanced beam. That is, yellow-poplar in the tangential direction and particleboard.

Yellow-Poplar

Three 1-*inch* wide and 24-*inch* long strips in the tangential direction were cut from the yellow-poplar sheet as explained previously. In order to avoid buckling during the compression tests, three strips were glued together to form a thick laminated strip by using epoxy glue. This thick laminated strip was then cut into five 4-*inch* long specimens. In order to mount a strain gage extensometer to the specimen, one of the vertical edges was chamfered to provide an approximately 1/5 *inch* wide bearing area.

An Instron universal testing machine was employed to supply the loading for the compression test. The deformation within an 1 *inch* gage length was monitored by a strain gage extensometer connected to a strain indicator.

The specimens were first tested with a continuously increasing load within the elastic limit of the material at an initial relative humidity level of 66 percent, and then were retested after conditioning at 81 percent and 93 percent relative humidity levels, respectively. Loading speed was 0.015 *in / min.*

The average of the *MOE* s thus obtained would represent the properties of those strips in the tangential direction used in the beams, and were subsequently used as inputs for those layers in the elastic warping equation.

Particleboard

Sixteen specimens of particleboard 1 *inch* by 1 *inch* in cross section and 4 *inches* long were randomly selected from the board. The loading direction was parallel to the surface of the board. Specimens were tested on the Instron universal machine after conditioning at relative humidity levels of 30 percent, 50 percent, 81 percent and 93 percent with four replications at each condition. Loading speed was 0.02 *in / min*

3.3.6 Restrained Swelling Test

This is the test that determined the elastic portion of the restrained swelling and the actual swelling stress of the specimens expanding under complete axial restraint. The tests were conducted on short columns which after initial conditions at a low reference relative humidity were mounted in a rigid clamp which prevented any axial expansion during exposure to higher levels of relative humidity. When the specimens reached equilibrium at the higher relative humidity, the clamp was opened and the instantaneous recovery measured and expressed as a fraction of the free expansion of control specimens expanding without restraint under the same test conditions. Incorporated in the clamping device was a load cell which measured the developing swelling stress throughout the test.

The restraining device (see Figure 3-12) was specially designed and built for this study. It consists of two stainless steel ball bearing guide blocks fastened to a rigid aluminum beam and riding on two precision ground

stainless steel shafts. These shafts were fastened to a lower and an upper horizontal steel plate. The position of the aluminum beam and guide blocks could be finely adjusted by means of a spindle threaded through the center of the upper horizontal plate, and connected to the aluminum beam. A spherical depression was machined into the center of the upper aluminum beam. A steel ball was placed between the beam and the spindle. A miniature load cell was attached to the bottom face of the aluminum beam, its center coinciding exactly with the center of the adjustment spindle (see Figure 3-12)

To reduce the possibility of eccentric loading which is almost unavoidable with one small column, the test was conducted on two identical columns, each two *inches* long, one *inch* wide, and 0.25 *inch* thick and spaced two *inches* apart (Figure 3-13 (a)). The two columns were cut to exactly the same length and were then glued between two aluminum blocks which were notched to assure the exact spacing of the specimens.

An attached clip gage extensometer measured the distance between the aluminum blocks, i.e., the length of the two columns. The entire assembly was placed in a stainless steel desiccator in which the relative humidity could be adjusted by means of saturated salt solutions maintained in shallow trays. The air within the desiccator was continuously circulated by means of a small electronic fan. Figure 3-14 shows two such desiccators, each with a restraint device as described above. Measurements from load cell and clip gage were recorded by electronic data acquisition equipment shown in left of Figure 3-14.

The above mentioned control specimens were also mounted between two aluminum blocks. Their hygroscopic expansion was not restrained in any

way and was measured continuously by a clip gage extensometer (Figure 3-13 (b)). An additional control specimen was suspended from a miniature cantilever load cell, which continuously measured weight gain during the test.

The test proceeded as follows:

Five identical short columns were conditioned at the low reference relative humidity (66 percent for yellow-poplar, 30 and 50 percent for MDF and PB). Two were then mounted between the aluminum blocks and placed in the restrained device. A minimal load was applied by twisting the spindle to assure seating of the load cell and to remove all slack. The clip gage was attached to pins projecting from the two aluminum blocks. Two more short columns were mounted between another set of aluminum blocks. A clip gage was attached and the assembly placed in the desiccator. A fifth column was hung on the cantilever load cell within the desiccator. Salt solution were put into place, the desiccator was closed, the fan started.

A sample record of a test is shown in Figure 3-15. Such test were performed on tangential yellow-poplar columns for these test intervals:

66 - 81% relative humidity

66 - 93% relative humidity

They were performed on MDF and PB for these test intervals:

30 - 81% relative humidity

50 - 81% relative humidity

30 - 93% relative humidity

50 - 93% relative humidity

In these cases, the columns were 0.25 *inch* thick cross-sections of the 1-*inch* thick board. Their length was 2.0 *inch* .

Five test replications were used for each of two condition of yellow-poplar specimens, and six to eight replications were used for each of the four conditions of MDF and PB, respectively.

Figure 3-5 Conditioning chamber used for conditioning of specimens.

THIS PHOTOGRAPH
WAS PRODUCED BY
MSU / INSTRUCTIONAL
MEDIA CENTER
(517) 353-3960
MSU is an
Affirmative Action /
Equal Opportunity
Institution.

Figure 3-6 Conditioning tank used for conditioning of specimens.

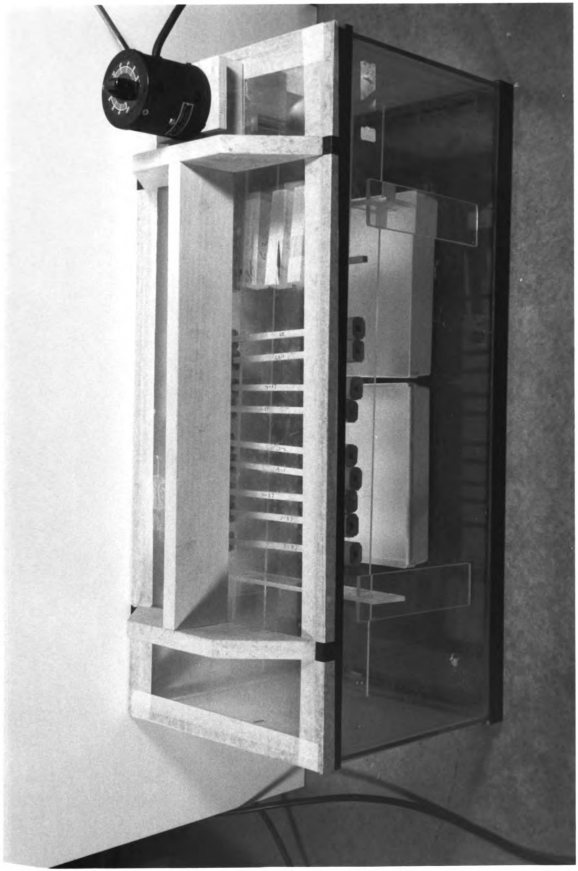

THIS PHOTOGRAPH
WAS PRODUCED BY
MSU / INSTRUCTIONAL
MEDIA CENTER
(517) 353-3960
MSU is an
Affirmative Action /
Equal Opportunity
Institution.

Figure 3-7 A dial gage fixed on an aluminum frame used to measure hygroscopic expansion of yellow-poplar.

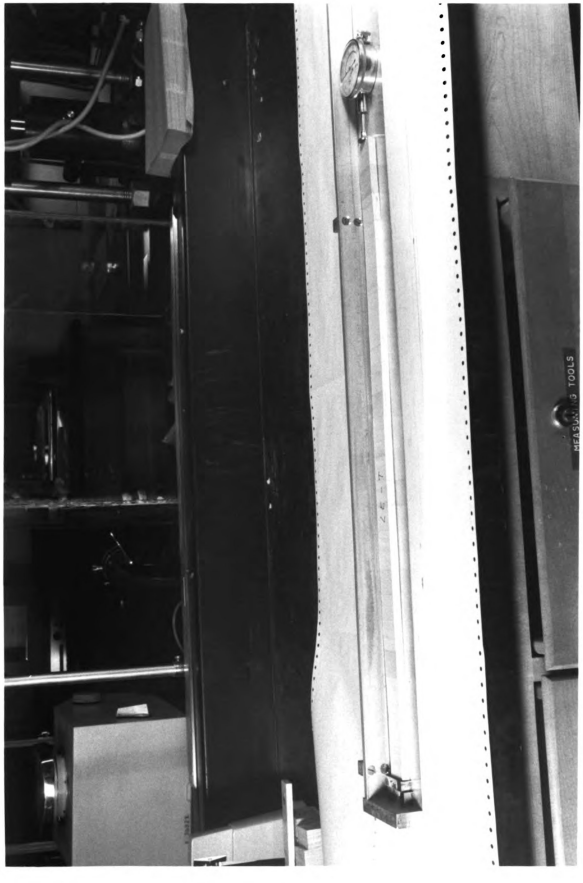
24"
MEASURING TOOLS

THIS PHOTOGRAPH
WAS PRODUCED BY
MSU / INSTRUCTIONAL
MEDIA CENTER
(517) 353-3960
MSU is an
Affirmative Action /
Equal Opportunity
Institution.

Figure 3-8 Optical comparator [50] used for hygroscopic expansion determination.

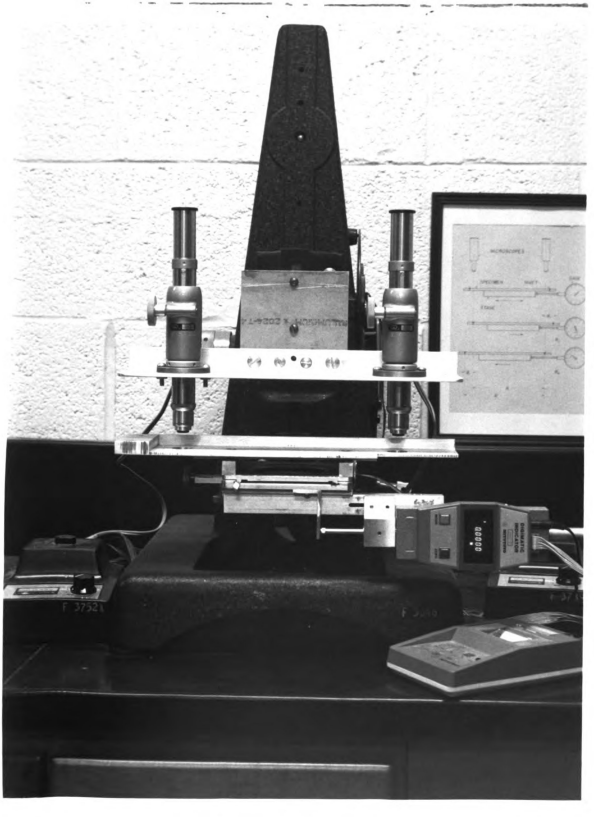

THIS PHOTOGRAPH
WAS PRODUCED BY
MSU / INSTRUCTIONAL
MEDIA CENTER
(517) 353-3960
MSU is an
Affirmative Action /
Equal Opportunity
Institution.

Figure 3-9 A dial gage fixed on an aluminum frame used to measure warping of yellow-poplar laminated beam.

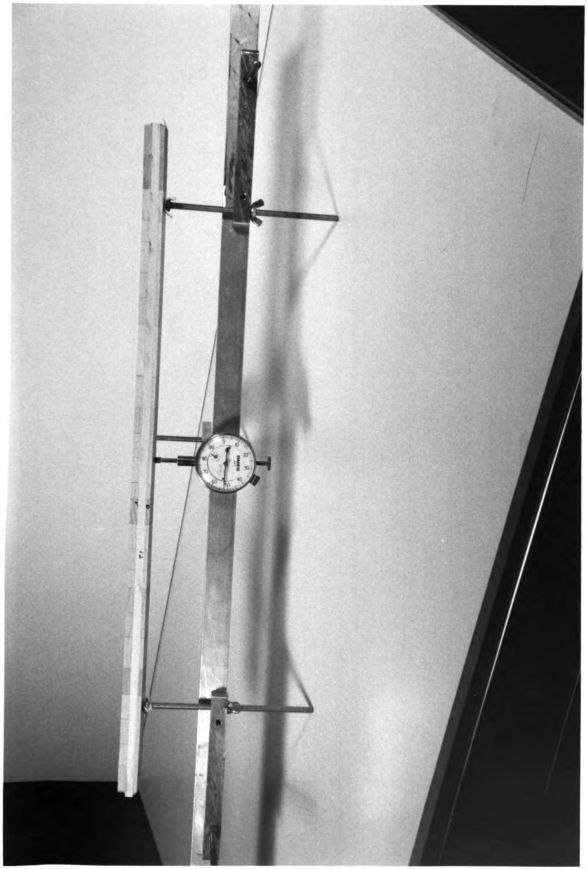

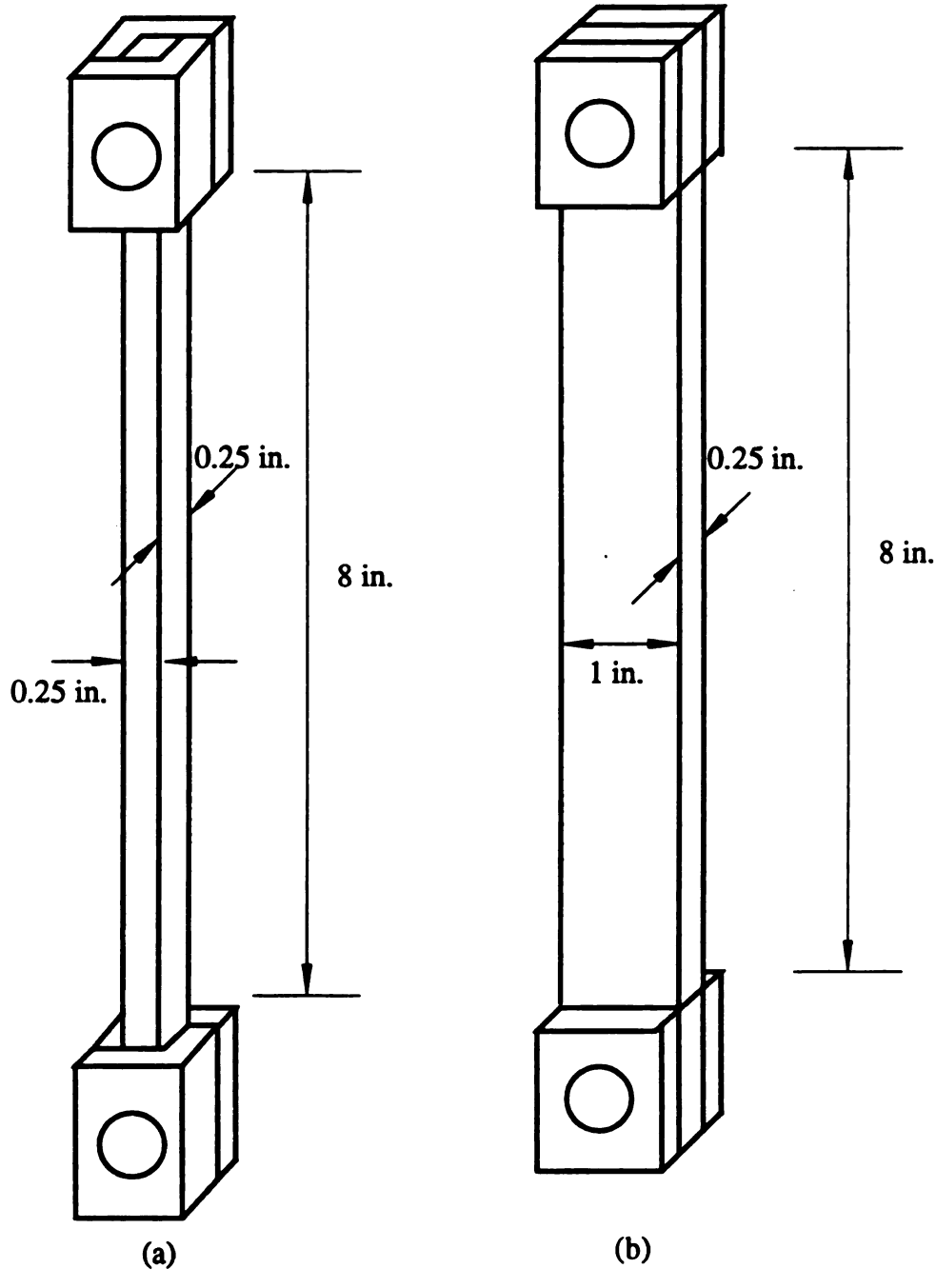

Figure 3-11 Dimensions of tension specimens of yellow-poplar (a) and MDF (b).

Figure 3-12 Device for measuring swelling stresses. Miniature load cell measures swelling force, clip gage in center measures length change of restrained specimens.

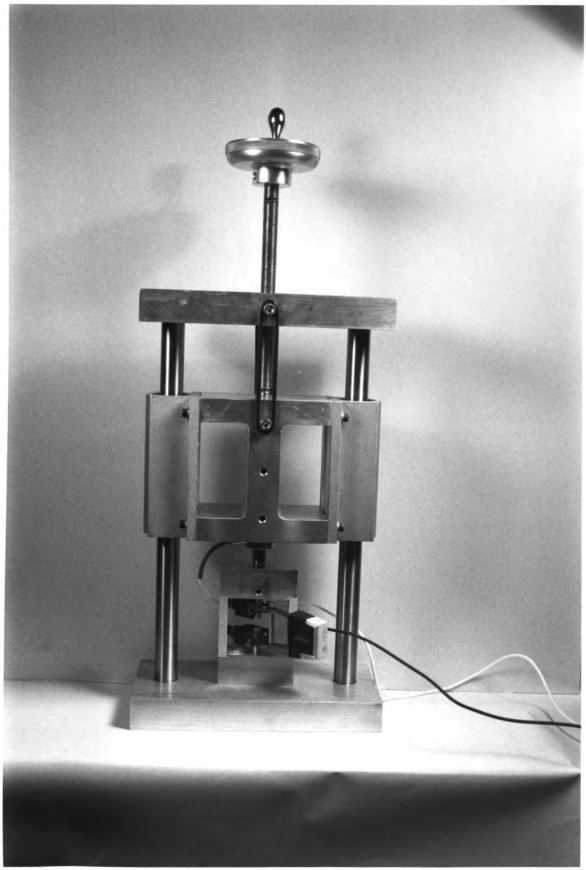

THIS PHOTOGRAPH
WAS PRODUCED BY
MSU / INSTRUCTIONAL
MEDIA CENTER
(517) 353-3960
MSU is an
Affirmative Action /
Equal Opportunity
Institution.

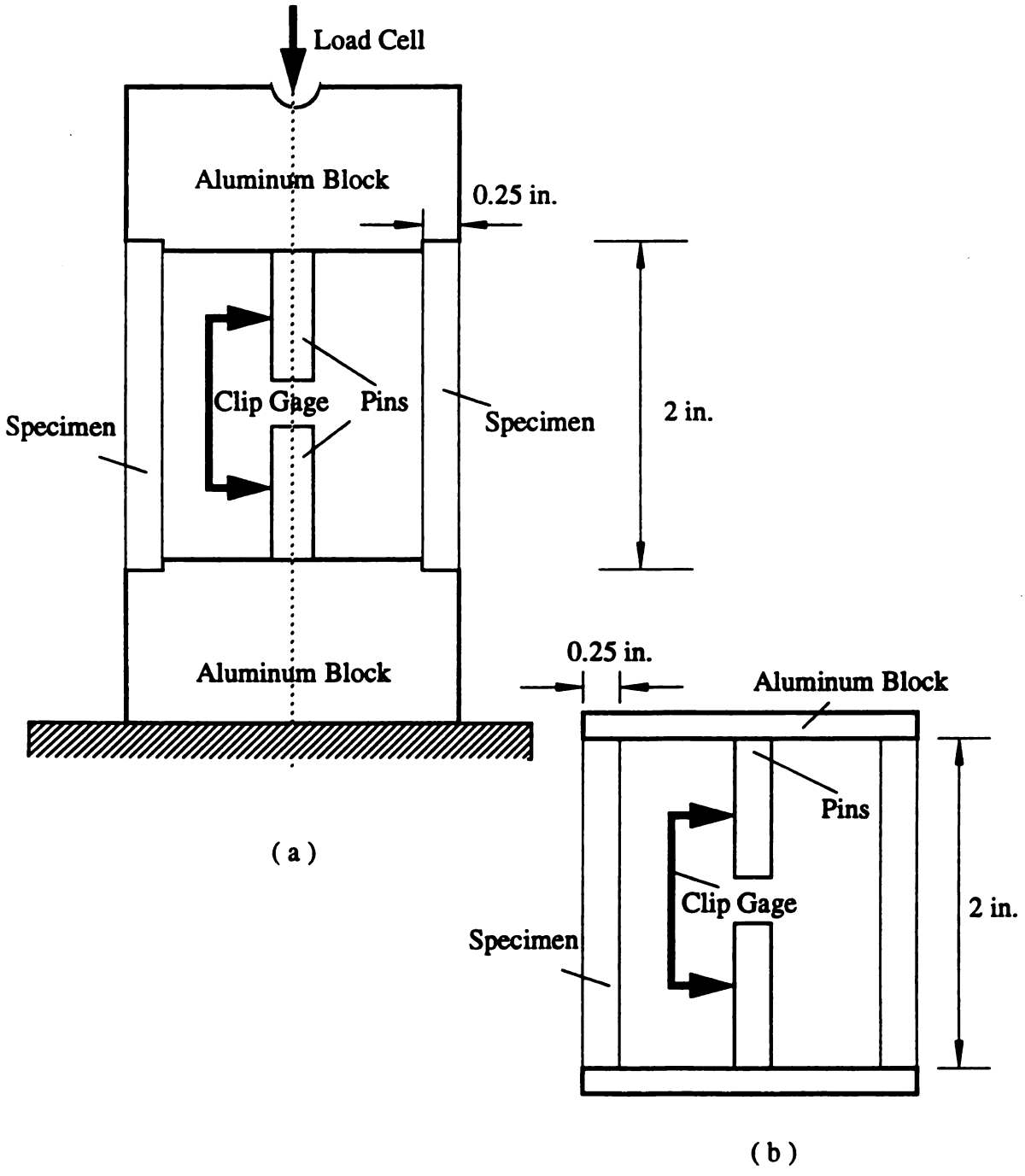

Figure 3-13 Drawing of specimen placement: (a) restrained swelling; (b) free hygroscopic expansion.

Figure 3-14 Restraining test setup. All measurements are simultaneously and continuously recorded by a data acquisition system.

THIS PHOTOGRAPH
WAS PRODUCED BY
MSU / INSTRUCTIONAL
MEDIA CENTER
(517) 353-3960

Action /
portunity

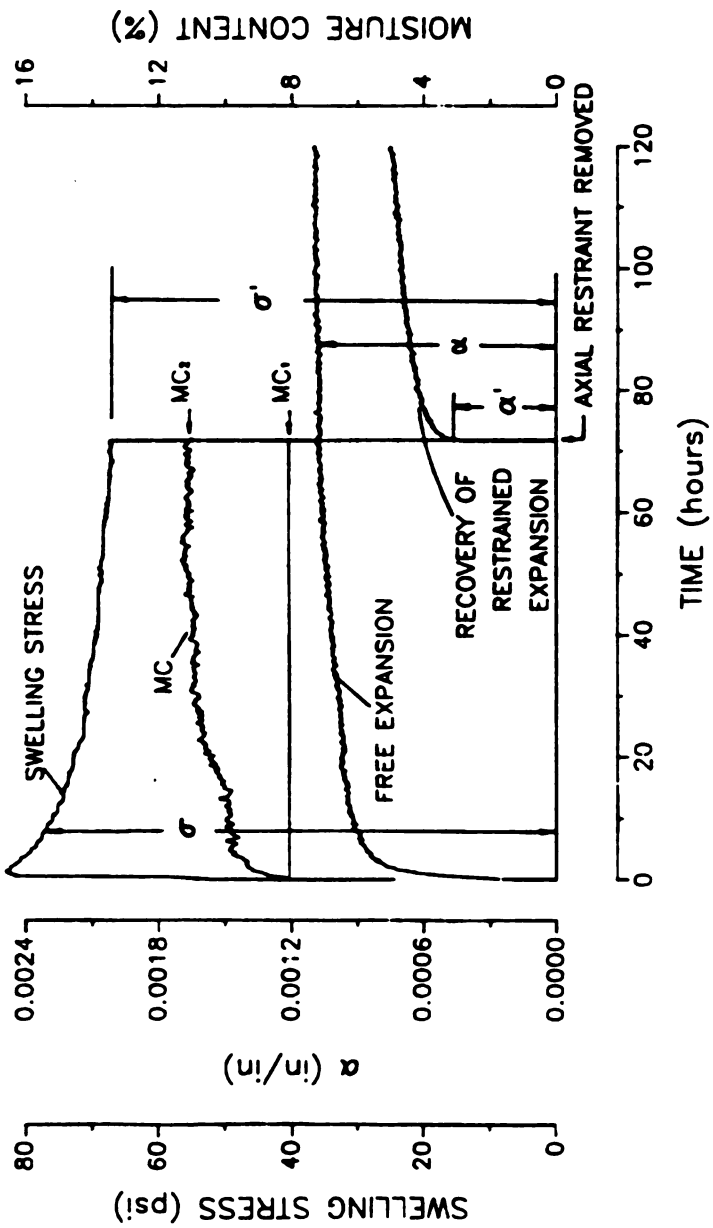

Figure 3-15 Record of restrained swelling test of MDF [43]. Specimens reached equilibrium at MC_2 after about 70 hours. Upon removal of restraint the instantaneous elastic recovery α' of the free expansion is determined. Swelling stress at that point is σ'.

CHAPTER IV
RESULTS AND ANALYSIS

4.1 General

In this chapter, the results of the tests of the mechanical and physical properties of the various materials used in the study are presented and discussed. This includes the measured warp of the unbalanced laminated beams exposed to various relative humidity conditions. These warp measurements are then compared with three analytical predictions of warp from:

- elastic beam equation
- inelastic beam equation (modified elastic beam equation)
- visco-elastic beam equation.

Finally, the practical application of the results to plywood and composite panel warping is discussed.

4.2. Yellow-Poplar

4.2.1 Results of Experiment

As illustrated in the previous chapter, a yellow-poplar sheet was fabricated in our laboratory. The two principal axis in the plane of the sheet are in the tangential and longitudinal directions. The sheet was made by edge gluing selected wood strips.

The density of the individual strips that were used for the yellow-poplar board was determined individually before edge gluing. The over-all density profile is plotted in Figure 4-1, where X on the horizontal axis denotes the distance from one edge of the panel, while L is the width of the panel. Each point represents the density of that particular strip. $X/L = 0$ corresponds to edge ① - ④ in Figure 3-2, and $X/L = 1$ corresponds to edge ② - ③. Twenty-six strips were used to form this panel. As can be seen, the density across the panel is quite uniform.

The experimental results of tension, compression, and hygroscopic expansion test in both longitudinal and tangential directions as well as the results of the restrained swelling tests are listed in Tables 4-1 through 4-5.

The MOE values show the typical effect of moisture content. The longitudinal values are considerably below the average MOE value in bending as listed in the Wood Handbook (MOE bending: 1580.0 ksi at 12% Moisture content). Tangential values are not listed. The measured hygroscopic expansion values, if converted to a change from green to oven dry (0 to 30 percent moisture content) are 0.1 percent longitudinally and 10.5

percent tangentially.

The longitudinal expansion value is not listed in the Wood Handbook. The listed tangential value is 8.2 percent. While these variations from the listed values seem large, the actual measured values are very consistent and have a relatively small standard deviations.

The results of the restrained swelling test in the tangential direction are summarized in Table 4-5 for the two relative humidity intervals 66 to 81 percent and 66 to 93 percent.

The elastic strain, ε_{elast}, is that portion of the restrained expansion which recovers instantly upon removing the restraint. It is this portion that sustains the swelling stress and thus contributes to the warping. The swelling stress σ' is the measured axial compressive stress at the end of the exposure period, at which time the specimen has reached moisture content equilibrium (weight constancy). The clamp is opened at this time and ε_{elast} is recorded.

It is interesting to note that the "deformation modulus" $E' = \sigma'/\varepsilon_{elast}$ is larger than the statically determined MOE at both 81 and 93 percent relative humidity. This is so because what is being measured is the equivalent of the stiffness of the elastic component of the Burger body alone.

It appears that the specimens become stiffer at the higher moisture content.

The elastic strain is about 25 percent of the total free expansion (or total compressive strain). This is true for both relative humidity conditions and also for many other specimens as shown by Keylwerth [21].

The 24 *inches* long laminated beams were conditioned in fish tanks charged with saturated salt solutions. Two exposure intervals were used: 66

to 81 and 66 to 93 percent relative humidity. Their center deflection was measured every day. The warping increased rapidly at first, then leveled off. After seven days the beams had reached equilibrium and the warping stabilized (Figure 4-2).

All these beams showed positive warp (concave) when viewed from the top (Table 4-4). It may be noted that compared with beam T-L which is severely unbalanced, the addition of a thin third layer in the tangential direction (T-L-T) does not balance the construction, substantially reduces the warp.

4.2.2 Theoretical Estimation of Warping

Three approaches were used for the theoretical estimation of the warping of the laminated beams:

—— elastic approach

Standard beam equation (Equation 2-13) with elastic inputs *MOE* and the free hygroscopic expansion α for both directions.

—— inelastic approach

Modified beam equation with *MOE* replaced by "deformation modulus" $E' = \sigma'/\varepsilon_{elast}$ and with free expansion α replaced by ε_{elast}.

These modification apply only to the tangential direction.

The longitudinal direction is treated as in the elastic approach.

—— visco-elastic approach

Swelling stress relaxation modulus and free expansion were used as inputs for the tangential direction.

Relaxation modulus is defined as the ratio of swelling stress to the free expansion value: $Y = \sigma'/\alpha$, as function of exposure time.

Static tension MOE and free expansion were used for the longitudinal direction.

The visco-elastic approach required the establishment of time functions for free expansion and for the relaxation modulus.

The experimentally obtained characteristics were subjected to a non linear regression analysis which yielded continuous time functions of free expansion and relaxation modulus.

The regression models are illustrated in Figures 4-3 and 4-4.

The final warping is the cumulative result of the warping calculated for small time intervals. One hour time elements provided sufficiently accurate results. Reducing the time element did not result in significant improvements.

Table 4-6 shows a summary of the inputs for the elastic and inelastic approaches. The inputs for the visco-elastic model are shown in Table 4-7. This approach was applied only to the two-layer laminates.

A summary of the results allowing a comparison of the theoretical

calculation with measured warping is given in Table 4-8.

It is apparent that the elastic approach leads to a substantial overestimate of the warp of the laminated wood beams of all constructions. The inelastic approach yields results that are very close to the measured warp. The visco-elastic approach results in a slight overestimate.

It is known that moisture content gradients develop in solid wood when exposure conditions are changed dramatically, i.e., portions of the wood near the surface reach equilibrium moisture content much sooner than the interior portions. Such moisture content gradients can have significant effects on swelling stress and on warp development. No allowance was made in this study for such effects. However, the cross-section of the lamina as well as of the short columns used in the restrained compression test were relatively small so disregarding the moisture content gradients may be justified.

Table 4-1 Modulus of elasticity in tension (ksi) of yellow-poplar in the longitudinal direction

Specimen ID	66%RH	81%RH	93%RH
L1	1366.969	1288.556	1196.713
L2	1236.557	1159.427	1080.540
L3	1236.564	1152.939	1055.610
L4	1213.704	1124.407	1039.997
AVG	1263.449	1181.332	1093.215
STD	69.850	73.083	70.990
C.V.	5.53%	6.19%	6.49%

Table 4-2 Modulus of elasticity in compression (ksi) of yellow-poplar in the tangential direction

Specimen ID	66%RH	81%RH	93%RH
C1	46.296	37.919	29.058
C2	45.029	37.055	27.045
C3	44.720	36.953	25.993
C4	49.404	41.445	31.226
C5	50.576	42.171	36.833
AVG	47.205	39.109	30.031
STD	2.643	2.506	4.297
C.V.	5.60%	6.41%	14.31%

Table 4-3 Properties of yellow-poplar

	66%RH	81%RH	93%RH
Moisture Content (%)	9.71	13.97	18.39
MOE tension longtudinal (ksi)	1263.45	1181.33	1093.22
MOE comp tangential (ksi)	47.21	39.11	30.03

	66-81%RH	66-93%RH
Free Hygroscopic Expansion Longitudinal (in/in)	0.00013	0.00025
Free Hygroscopic Expansion Tangential (in/in)	0.01492	0.02967
Free Hygroscopic Exp. Coefficient Longitudinal (%/%)	0.00305	0.00288
Free Hygroscopic Exp. Coefficient Tangential (%/%)	0.350	0.342

Table 4-4 Measured warping of yellow-poplar laminated beams over 24-inch span with initial condition of 66 percent RH

NO.	Beam ID	Thickness	81%RH	93%RH
1	L - T	0.257 0.257	+0.296	+0.644
2	T - L - T	0.0643 0.257 0.257	+0.279	+0.548
3	L - T - L	0.257 0.257 0.0643	+0.041	+0.081

Table 4-5 Results from restraint test of yellow-poplar

66 - 81%RH

Specimen ID	Elastic Strain ε_{elast} (in/in)	Swelling Stress σ' (psi)	Deformation Modulus E' (psi)	Free Expansion α (in/in)	$\varepsilon_{elast}/\alpha$
1	0.003937	155.56	39512.1	0.016019	24.58%
2	0.003199	131.78	41199.2	0.015349	20.84%
3	0.003649	157.68	43214.6	0.015362	23.75%
4	0.003218	137.90	42857.1	0.013227	24.33%
5	0.003262	151.21	46355.7	0.014461	22.56%
AVG	0.003453	146.82	42627.7	0.014884	23.21%
STD	0.000328	11.40	2551.6	0.001079	0.01538
C.V.	9.49%	7.76%	5.99%	7.25%	6.63%

66 - 93%RH

Specimen ID	Elastic Strain ε_{elast} (in/in)	Swelling Stress σ' (psi)	Deformation Modulus E' (psi)	Free Expansion α (in/in)	$\varepsilon_{elast}/\alpha$
1	0.006933	319.09	46026.5	0.027674	25.05%
2	0.007224	316.39	43794.6	0.033381	21.64%
3	0.008480	381.51	44990.7		
4	0.008381	375.55	44807.1	0.030392	27.58%
5	0.007576	314.13	41463.7	0.027230	27.82%
AVG	0.007719	341.33	44216.5	0.029669	24.76%
STD	0.000689	34.07	1730.6	0.002842	0.02808
C.V.	8.93%	9.98%	3.91%	9.58%	11.34%

Table 4-6 Calculated warping of yellow-poplar laminated beams over 24-inch span using elastic and inelastic approach

	Beam	Layer ID	Thickness ID	Elastic Approach[1)] MOE (psi)	Elastic Approach[1)] Expansion (in/in)	Elastic Approach[1)] Est.Warp (in)	Inelastic Approach[2)] Modulus (psi)	Inelastic Approach[2)] Expansion (in/in)	Inelastic Approach[2)] Est.Warp (in)	Meas.Warp (in)
66-81%RH		L1	0.257	1288556	0.00013		1288556	0.00013		
	L-T					1.0226			0.2758	0.296
		T1	0.257	39109	0.01492		42628	0.003453		
		T2	0.0643	39109	0.01492		42628	0.003453		
	T-L-T	L2	0.257	1159427	0.00013	0.8928	1159427	0.00013	0.2193	0.279
		T3	0.257	39109	0.01492		42628	0.003453		
		L4	0.257	1124407	0.00013		1124407	0.00013		
	L-T-L	T4	0.257	39109	0.01492	0.1460	42628	0.003453	0.0356	0.041
		L3	0.0643	1152939	0.00013		1152939	0.00013		
66-93%RH		L1	0.257	1196713	0.00025		1196713	0.00025		
	L-T					1.8359			0.6109	0.644
		T1	0.257	30031	0.02967		44217	0.007719		
		T2	0.0643	30031	0.02967		44217	0.007719		
	T-L-T	L2	0.257	1080540	0.00025	1.6146	1080540	0.00025	0.5262	0.548
		T3	0.257	30031	0.02967		44217	0.007719		
		L4	0.257	1039997	0.00025		1039997	0.00025		
	L-T-L	T4	0.257	30031	0.02967	0.2459	44217	0.007719	0.0900	0.081
		L3	0.0643	1055610	0.00025		1055610	0.00025		

1) Using MOEtension, α for tension layers; MOEcomp., α for compression layers

2) Using MOEtension, α for tension layers; Deformation modulus E', elastic strain for compression layers

Table 4-7 Visco-elastic warping prediction of yellow-poplar two-layer beams over 24-inch span

		66-81%RH	66-93%RH
Longitudinal Dir. Inputs	$MOE\,(psi)$	$E = 1288556\,(psi)$	$E = 1196713\,(psi)$
	Expansion (in/in)	$\alpha = 0.00013 - 0.00013e^{-0.1t}$	$\alpha = 0.00025 - 0.00025e^{-0.1t}$
	Thickness (in)	$T = 0.257\,(in)$	$T = 0.257\,(in)$
Tangential Dir. Inputs	Swelling Stress Rel. Mod. (psi)	$Y = 11571.21 + 27065.41e^{-0.1524058t}$ $(R^2 = 0.935)$	$Y = 11121.42 + 46689.71e^{-0.5402794t}$ $(R^2 = 0.986)$
	Expansion (in/in)	$\alpha = 0.01380079 - 0.01119413e^{-0.2199973t}$ $(R^2 = 0.993)$	$\alpha = 0.02820793 - 0.02694963e^{-0.168968t}$ $(R^2 = 0.998)$
	Thickness (in)	$T = 0.257\,(in)$	$T = 0.257\,(in)$
	Calculated Warp (in)	$0.3667\,(in)$	$0.7729\,(in)$
	Measured Warp (in)	$0.296\,(in)$	$0.644\,(in)$

Table 4-8 Comparison of estimated warping with measured warping for yellow-poplar laminated beams over 24-inch span

Condition Level	Beam ID	A Measured Warp (in)	B Elastic Estimated Warp (in)	B/A	C Inelastic Estimated Warp (in)	C/A	D Visco-elastic Estimated Warp (in)	D/A
	L - T	0.296	1.0226	3.45	0.2758	.93	0.3667	1.24
66-81%RH	T - L -T	0.279	0.8928	3.20	0.2193	.79	-	
	L - T - L	0.041	0.1460	3.56	0.0356	.87	-	
	L - T	0.644	1.8359	2.85	0.6109	.95	0.7729	1.20
66-93%RH	T - L -T	0.548	1.6146	2.95	0.5262	.96	-	
	L - T - L	0.081	0.2459	3.04	0.0900	1.11	-	
	Average			3.18		.94		1.22

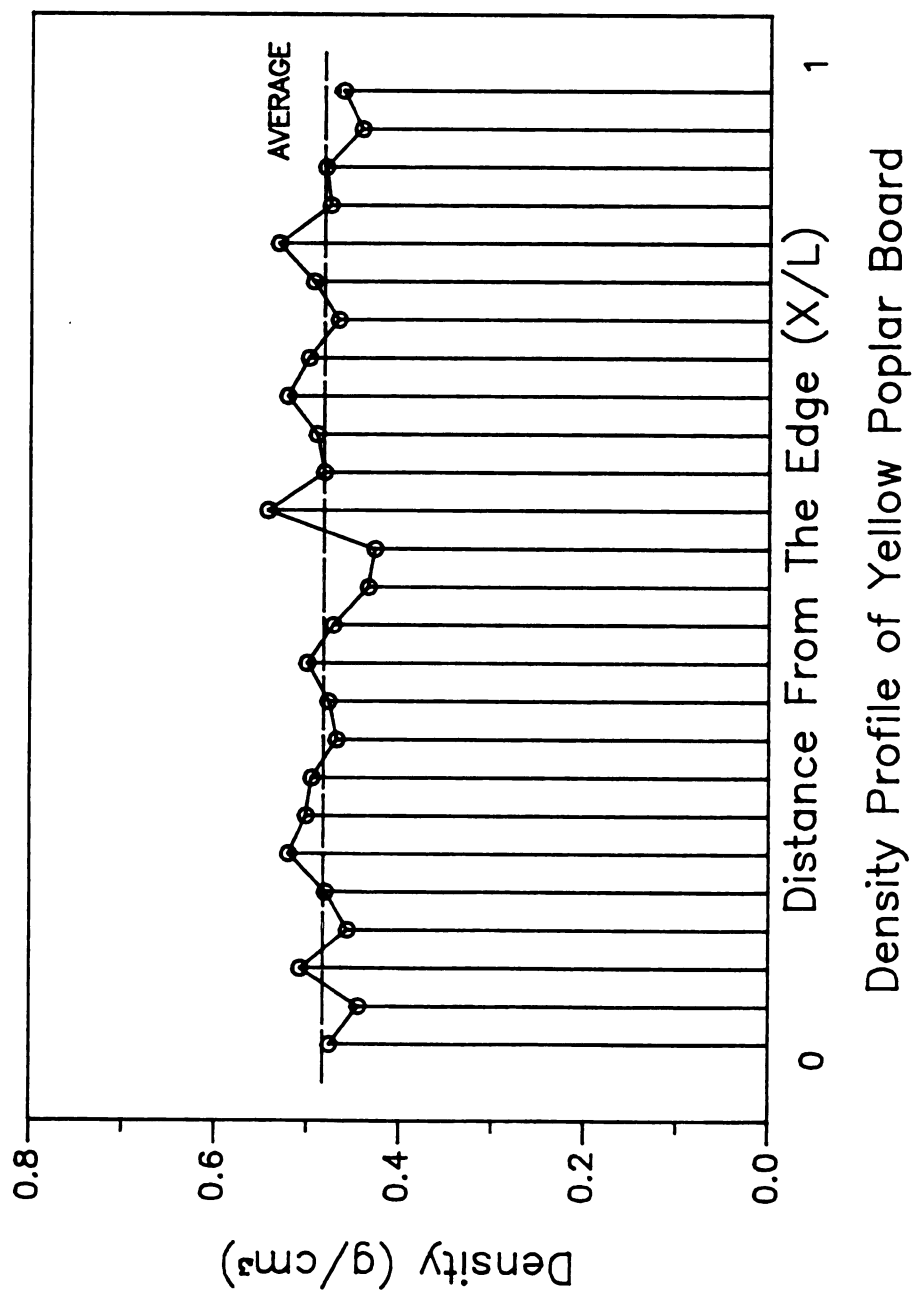

Figure 4-1 Density profile of yellow-poplar board.

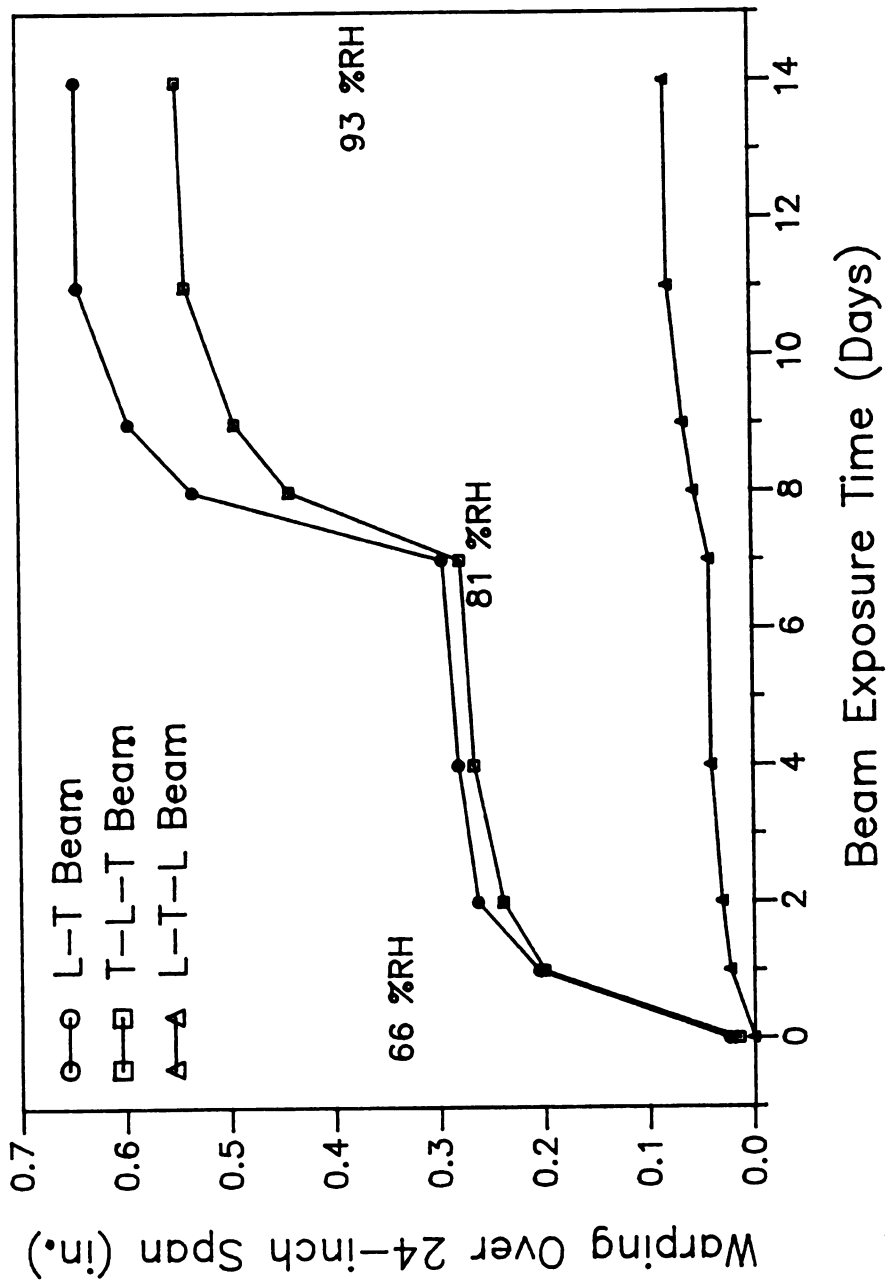

Figure 4-2 Measured warping of yellow-poplar beams.

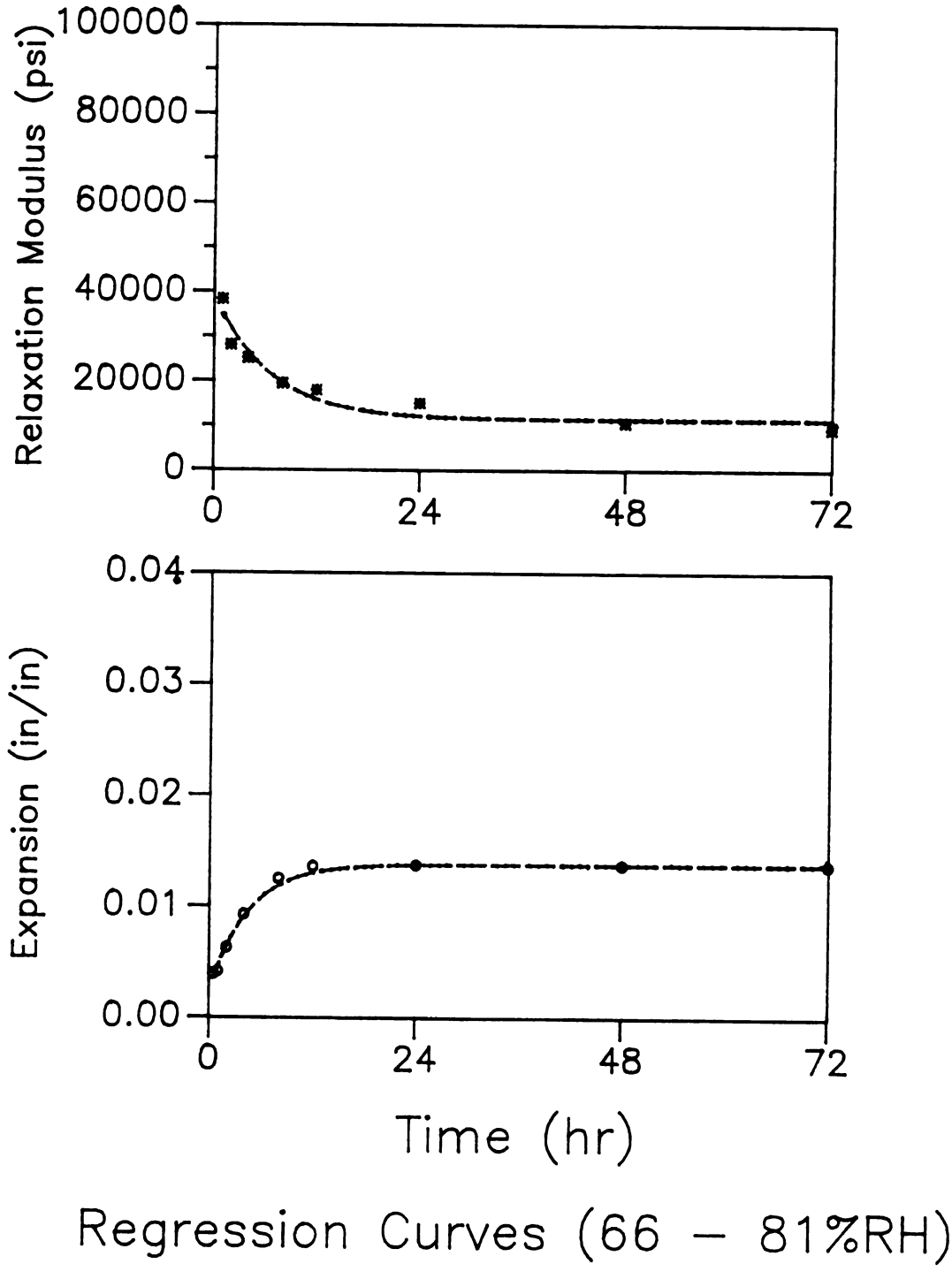

Figure 4-3 Nonlinear regression models of yellow-poplar for exposure interval of 66 - 81%RH.

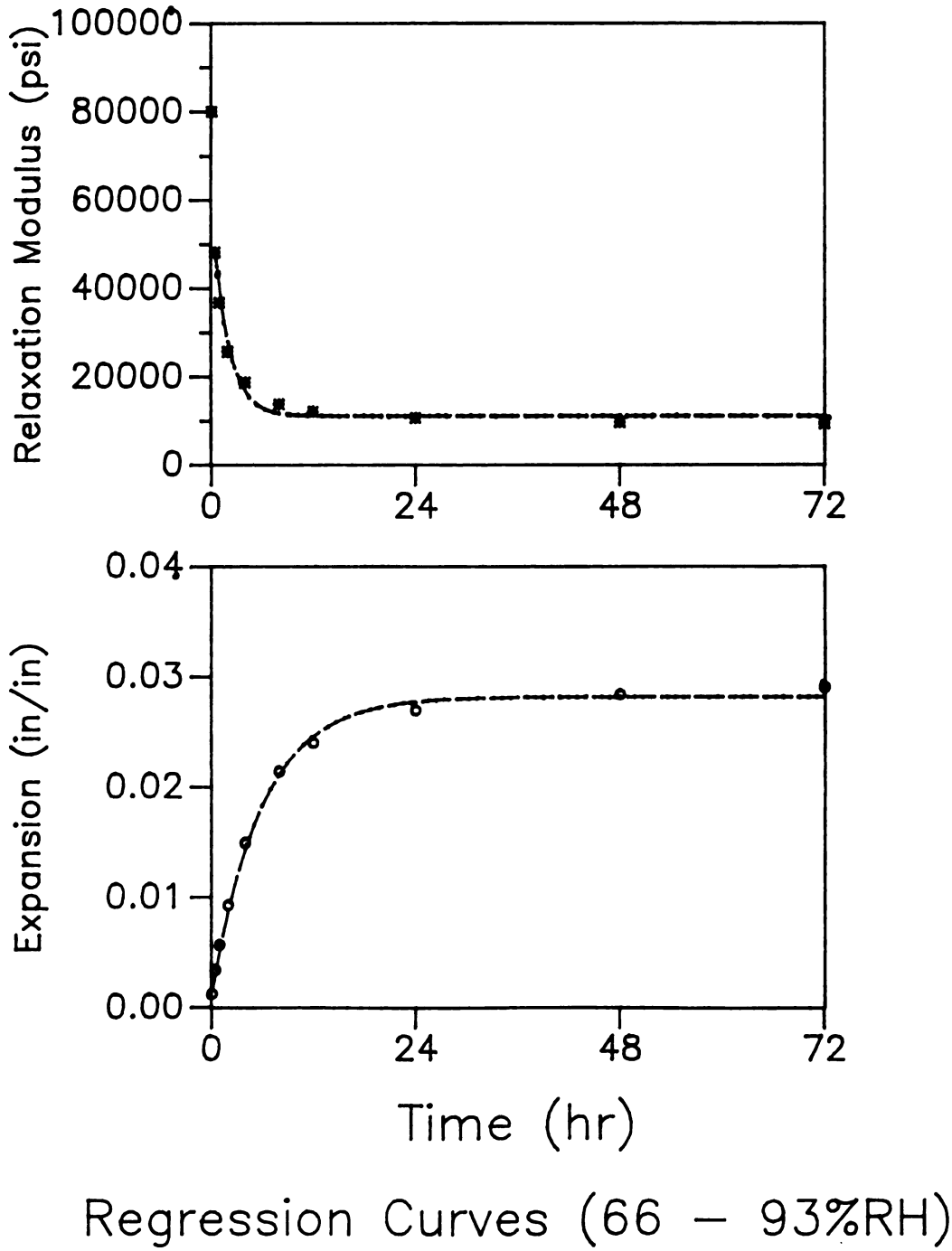

Figure 4-4 Nonlinear regression models of yellow-poplar for exposure interval of 66 - 93%RH.

4.3 MDF/PB

4.3.1 Results of Experiment

The test results from MDF and PB tests are presented in Table 4-9 to Table 4-11.

Results from the restrained swelling tests at various conditioning levels are tabulated in Table 4-10 and Table 4-11 for MDF and PB respectively.

The elastic portion of the total swelling stress in the case of MDF is near 40 percent for the exposure intervals 30 to 81 percent and 50 to 81 percent relative humidity and between 20 and 25 for exposure intervals 30 to 93 and 50 to 93. The corresponding values for particleboard are 20 and 25 percent.

This may be related to the fact that the pure compression of MDF is much lower than that of PB.

4.3.2 Theoretical Estimate of Warping

As in the case of the yellow-poplar laminate, three approaches were used for the theoretical determination of the warp of the composite beams.

— elastic approach

Standard beam equation (Equation 2-13) with MOE and free hygroscopic expansion α inputs for both materials (Table 4-12).

— inelastic approach

Modified beam equation for the condition of partial restraint as discussed in chapter II, Equation 2-47 to 2-50, (Table 4-13)

— inelastic approach

Modified beam equation with MOE replaced by "deformation modulus" $E' = \sigma'/\varepsilon_{elast}$ and with free expansion α replaced by ε_{elast} for both materials (Table 4-14).

— viscoelastic approach

This was based on the swelling stress relaxation moduli and the free expansion of both materials. The regression models are given in Table 4-15, 4-16 and Figure 4-5 to 4-7. The results are listed in Table 4-17 together with the other estimates for comparison.

This table shows that the elastic approach and the visco-elastic approach give results that are in very good agreement with the actual measured warping. The two inelastic approaches severely underestimating the warp. It thus appears that the composite boards behave much like elastic materials.

Table 4-9 Properties of MDF and PB

	30%RH	50%RH	81%RH	93%RH
Moisture Content of MDF(%)	6.80	7.19	11.81	15.80
Moisture Content of PB (%)	7.80	8.16	13.66	17.21
MOE tension of MDF (ksi)	-	-	430.052	231.144
MOE comp of PB (ksi)	217.296	198.157	123.175	94.131
	30-81%RH	**50-81%RH**	**30-93%RH**	**50-93%RH**
Free Hygroscopic Expansion of MDF (in/in)	0.002495	0.001810	0.003553	0.002583
Free Hygroscopic Expansion of PB (in/in)	0.005675	0.004338	0.009083	0.007100
Free Hygroscopic Expansion Coeff. of MDF (%/%)	0.0498	0.0392	0.0395	0.0300
Free Hygroscopic Expansion Coeff. of PB (%/%)	0.0968	0.0789	0.1045	0.0785
Warp of MDF/PB Beams	+0.81	+0.70	+1.66	+1.33

Table 4-10 Results from restraint test of MDF

30 - 81%RH

Specimen ID	Elastic Strain ε_{elast} (in/in)	Swelling Stress σ' (psi)	Deformation Modulus E' (psi)	Free Expansion α (in/in)	$\varepsilon_{elast}/\alpha$
1	0.000866	219.75	253853.4	0.002188	39.57%
2	0.001016	256.33	252406.9	0.002363	42.97%
3	0.001020	227.42	223046.4	0.002620	38.92%
4	0.001021	233.51	228716.9	0.002296	44.47%
5	0.001024	269.03	262810.0	0.002404	42.58%
6	0.000957	298.14	311382.2	0.002795	34.25%
7	0.000939	302.83	322647.5	0.002687	34.92%
8	0.001026	250.81	244368.4	0.002606	39.38%
AVG	0.000983	257.23	262404.0	0.002495	39.63%
STD	0.000058	31.15	36273.7	0.000212	0.037
C.V.	5.92%	12.11%	13.82%	8.50%	9.29%

50 - 81%RH

Specimen ID	Elastic Strain ε_{elast} (in/in)	Swelling Stress σ' (psi)	Deformation Modulus E' (psi)	Free Expansion α (in/in)	$\varepsilon_{elast}/\alpha$
1	0.000551	204.35	370578.0	0.002183	25.26%
2	0.000711	225.61	317399.1	0.002263	31.41%
3	0.000789	238.00	301697.0	0.001546	51.03%
4	0.000775	265.07	342232.5	0.001817	42.63%
5	0.000598	176.74	295733.3	0.001673	35.71%
6	0.000673	240.41	357464.5	0.001657	40.58%
7	0.000708	229.14	323828.8	0.001530	46.25%
AVG	0.000686	225.62	329847.6	0.001810	38.98%
STD	0.000087	28.23	28054.9	0.000299	0.089
C.V.	12.71%	12.51%	8.51%	16.50%	22.71%

Table 4-10 (continued)

30 - 93%RH

Specimen ID	Elastic Strain ε_{elast} (in/in)	Swelling Stress σ' (psi)	Deformation Modulus E' (psi)	Free Expansion α (in/in)	$\varepsilon_{elast}/\alpha$
1	0.000743	257.12	345976.1	0.003597	20.66%
2	0.000705	243.11	345000.0	0.003331	21.16%
3	0.000743	229.02	308167.3	0.003731	19.92%
4	0.000774	241.26	311606.1	0.003908	19.81%
5	0.000669	230.52	344491.2	0.003435	19.48%
6	0.000773	317.88	411341.0	0.003316	23.30%
AVG	0.000735	253.15	344430.3	0.003553	20.72%
STD	0.000041	33.29	37073.4	0.000236	0.014
C.V.	5.57%	13.15%	10.76%	6.65%	6.78%

50 - 93%RH

Specimen ID	Elastic Strain ε_{elast} (in/in)	Swelling Stress σ' (psi)	Deformation Modulus E' (psi)	Free Expansion α (in/in)	$\varepsilon_{elast}/\alpha$
1	0.000679	191.15	281685.1	0.002242	30.27%
2	0.000697	161.80	232246.2	0.002874	24.24%
3	0.000602	274.47	456025.0	0.002618	22.99%
4	0.000618	179.36	290024.3	0.002723	22.71%
5	0.000679	204.83	301840.4	0.002317	29.29%
6	0.000642	183.78	286042.2	0.002723	23.59%
AVG	0.000653	199.23	307977.2	0.002583	25.51%
STD	0.000038	39.48	76401.2	0.000250	0.034
C.V.	5.79%	19.81%	24.81%	9.68%	13.16%

Table 4-11 Results from restraint test of PB

30 - 81%RH

Specimen ID	Elastic Strain ε_{elast} (in/in)	Swelling Stress σ' (psi)	Deformation Modulus E' (psi)	Free Expansion α (in/in)	$\varepsilon_{elast}/\alpha$
1	0.001383	353.40	255548.2	0.005990	23.09%
2	0.001491	319.60	214415.1	0.005489	27.15%
3	0.001351	371.87	275241.3	0.005853	23.08%
4	0.001495	291.87	195213.0	0.006369	23.48%
5	0.001483	295.28	199110.4	0.006081	24.39%
6	0.001538	320.08	208169.2	0.005140	29.91%
7	0.001427	350.51	245642.9	0.005626	25.36%
8	0.001463	347.93	237772.0	0.004852	30.16%
AVG	0.001454	331.32	228889.0	0.005675	25.83%
STD	0.000062	29.02	28979.0	0.000504	0.029
C.V.	4.30%	8.76%	12.66%	8.88%	11.34%

50 - 81%RH

Specimen ID	Elastic Strain ε_{elast} (in/in)	Swelling Stress σ' (psi)	Deformation Modulus E' (psi)	Free Expansion α (in/in)	$\varepsilon_{elast}/\alpha$
1	0.000864	213.62	247355.9	0.004447	19.42%
2	0.001190	217.07	182438.7	0.004189	28.40%
3	0.001272	253.81	199500.7	0.003880	32.79%
4	0.001020	258.98	253939.4	0.004189	24.34%
5	0.001190	253.43	213001.4	0.004790	24.84%
6	0.001190	247.37	207907.6	0.004533	26.25%
7	0.001197	248.36	207546.6		
AVG	0.001132	241.80	215955.8	0.004338	26.01%
STD	0.000141	18.51	25713.5	0.000319	0.045
C.V.	12.42%	7.65%	11.91%	7.35%	17.13%

Table 4-11 (continued)

30 - 93%RH

Specimen ID	Elastic Strain ε_{elast} (in/in)	Swelling Stress σ' (psi)	Deformation Modulus E' (psi)	Free Expansion α (in/in)	$\varepsilon_{elast}/\alpha$
1	0.001929	441.27	228776.1	0.008766	22.00%
2	0.001914	466.38	243642.4	0.008747	21.88%
3	0.001839	350.58	190616.9	0.009900	18.58%
4	0.001907	415.45	217869.5	0.008491	22.46%
5	0.001748	358.81	205308.9	0.009223	18.95%
6	0.001742	416.15	238865.5	0.009370	18.59%
AVG	0.001846	408.11	220846.6	0.009083	20.41%
STD	0.000085	45.51	20353.5	0.000516	0.019
C.V.	4.58%	11.15%	9.22%	5.69%	9.22%

50 - 93%RH

Specimen ID	Elastic Strain ε_{elast} (in/in)	Swelling Stress σ' (psi)	Deformation Modulus E' (psi)	Free Expansion α (in/in)	$\varepsilon_{elast}/\alpha$
1	0.001395	236.75	169740.3	0.007509	18.57%
2	0.001518	259.57	170965.3	0.006126	24.78%
3	0.001317	228.18	173212.5	0.006340	20.78%
4	0.001523	253.69	166551.4	0.007147	21.31%
5	0.001321	259.91	196808.0	0.007707	17.14%
6	0.001693	273.05	161303.5	0.007772	21.78%
AVG	0.001461	251.86	173096.8	0.007100	20.73%
STD	0.000145	16.53	12328.6	0.000709	0.027
C.V.	9.95%	6.56%	7.12%	9.99%	12.84%

Table 4-12 Estimated warping of MDF/PB laminated beams over 30-inch span using elastic approach[1)]

Condition Level	Layer ID	Thickness (in)	Modulus (psi)	Expansion (in/in)	Est.Warp (in)	Meas.Warp (in)
30 - 81%RH	MDF	0.25	430052	0.002459	0.9659	0.81
	PB	0.25	123175	0.005675		
50 - 81%RH	MDF	0.25	430052	0.001810	0.7679	0.70
	PB	0.25	123175	0.004338		
30 - 93%RH	MDF	0.25	231144	0.003553	1.7709	1.66
	PB	0.25	94131	0.009083		
50 - 93%RH	MDF	0.25	231144	0.002583	1.4465	1.33
	PB	0.25	94131	0.007100		

1) Using MOEtension, α for MDF; MOEcomp., α for PB

Table 4-13 Estimated warping of MDF/PB laminated beams over 30-inch span using inelastic approach by partial restraint concept[1)]

Layer ID	Parameter	30 - 81%RH	30 - 81%RH	30 - 81%RH	30 - 81%RH
MDF	ε_{1elast} (in/in)	0.000983	0.000686	0.000735	0.000653
	E (psi)	430052	430052	231144	231144
	α (in/in)	0.002495	0.001810	0.003553	0.002583
	e_1	0.0008173	0.0006492	0.0026788	0.00171112
	ε'_{1elast}	0.000322152	0.000246124	0.0005538	0.0004324
PB	ε_{2elast} (in/in)	0.001454	0.001132	0.001846	0.001461
	E' (psi)	228889	215956	220846	173097
	α (in/in)	0.005675	0.004338	0.009083	0.007100
	e_2	0.00236273	0.0018788	0.0028512	0.00280588
	ε'_{2elast}	0.000605281	0.00049013	0.000579624	0.00057745
Estimated Warping (in)		0.1648	0.1442	0.4474	0.3335
Measured Warping (in)		0.81	0.70	1.66	1.33

1) Described in Section 2-5. ε'_{1elast}, ε'_{2elast}, e_1 and e_2 are calculated by Equation 2-47 to 2-50; substitute negative ε'_{1elast} and positive ε'_{2elast} as the expansion values in warping equation 2-13.

Table 4-14 Estimated warping of MDF/PB laminated beams over 30-inch span using inelastic approach [1)]

Condition Level	Layer ID	Thickness (in)	Deformation Modulus (psi)	Restrained Swelling (in/in)	Est.Warp (in)	Meas.Warp (in)
30 - 81%RH	MDF	0.25	262404	0.000983	0.1588	0.81
	PB	0.25	228889	0.001454		
50 - 81%RH	MDF	0.25	329848	0.000686	0.1488	0.70
	PB	0.25	215956	0.001132		
30 - 93%RH	MDF	0.25	344430	0.000735	0.3703	1.66
	PB	0.25	220847	0.001846		
50 - 93%RH	MDF	0.25	307977	0.000653	0.2670	1.33
	PB	0.25	173097	0.001461		

1) Using elastic strain and deformation modulus for both MDF and PB

Table 4-15 Regression models of hygroscopic expansion (in./in.) of MDF and PB

Rel. Hum.	MDF	Particleboard
30 - 81%	$\alpha = -0.001097703 \times e^{-0.07911654t} + 0.002334789$ ($R^2 = 0.853$)	$\alpha = -0.004285141 \times e^{-0.08775340t} + 0.005522294$ ($R^2 = 0.966$)
50 - 81%	$\alpha = -0.0008559854 \times e^{-0.0246812t} + 0.001931123$ ($R^2 = 0.906$)	$\alpha = -0.003311357 \times e^{-0.03710923t} + 0.004368760$ ($R^2 = 0.982$)
30 - 93%	$\alpha = -0.002112470 \times e^{-0.0629086t} + 0.003383037$ ($R^2 = 0.936$)	$\alpha = -0.007128240 \times e^{-0.06065341t} + 0.008802536$ ($R^2 = 0.974$)
50 - 93%	$\alpha = -0.001747302 \times e^{-0.06004222t} + 0.00254909$ ($R^2 = 0.970$)	$\alpha = -0.006263148 \times e^{-0.06763732t} + 0.007026246$ ($R^2 = 0.996$)

Table 4-16 Regression models of swelling stress relaxation moduli (psi) of PB and tension moduli of MDF

Rel. Hum.	MDF[1)]	Particleboard
30 - 81%	$Y = 430052$	$Y = 439538.6 \times e^{-0.4101544t} + 141734.3$ $(R^2 = 0.940)$
50 - 81%	$Y = 430052$	$Y = 331100.0 \times e^{-0.0831994t} + 88410.5$ $(R^2 = 0.957)$
30 - 93%	$Y = 231144$	$Y = 491405.3 \times e^{-0.2396595t} + 111467.2$ $(R^2 = 0.964)$
50 - 93%	$Y = 231144$	$Y = 575778.4 \times e^{-0.2459324t} + 112101.0$ $(R^2 = 0.939)$

1) *MOE* from tension test at end condition.

Table 4-17 Comparison of estimated warping with measured warping for MDF/PB laminated beams over 30-inch span

Condition Level	A Measured Warp (in)	B Elastic Estimated Warp (in)	B/A	C Inelastic Estimated[1)] Warp (in)	C/A	D Inelastic Estimated[2)] Warp (in)	D/A	E Visco-elastic Estimated Warp (in)	E/A
30 - 81%RH	0.81	0.9659	1.19	0.1648	.20	0.1588	.20	0.9913	1.22
50 - 81%RH	0.70	0.7679	1.10	0.1442	.21	0.1488	.21	0.6992	1.00
30 - 93%RH	1.66	1.7709	1.07	0.4474	.27	0.3703	.22	1.7676	1.07
50 - 93%RH	1.33	1.4465	1.09	0.3335	.25	0.2670	.20	1.4612	1.10
Average			1.13		.24		.21		1.10

1) Based on partial restraint concept, see Table 4-13
2) Using restraint properties for both MDF and PB, see Table 4-14

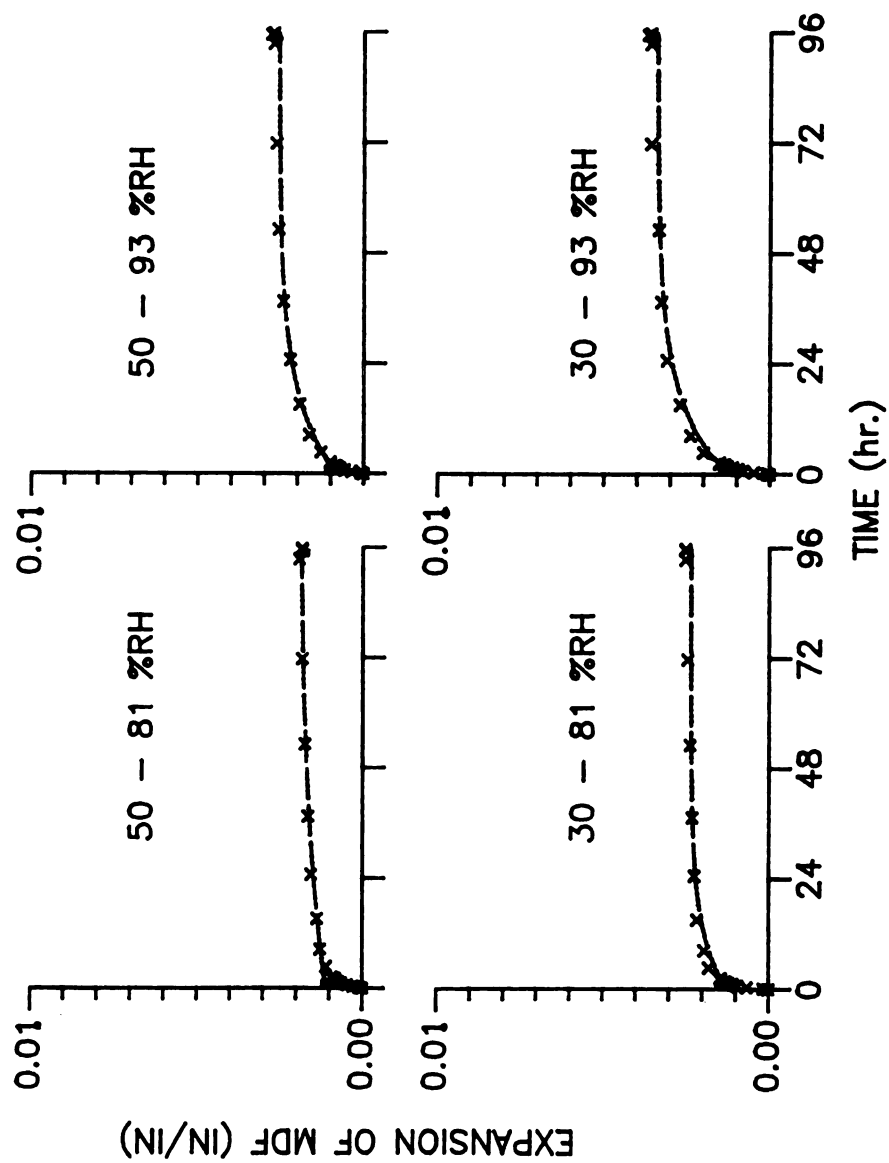

Figure 4-5 Nonlinear regression models of MDF expansion.

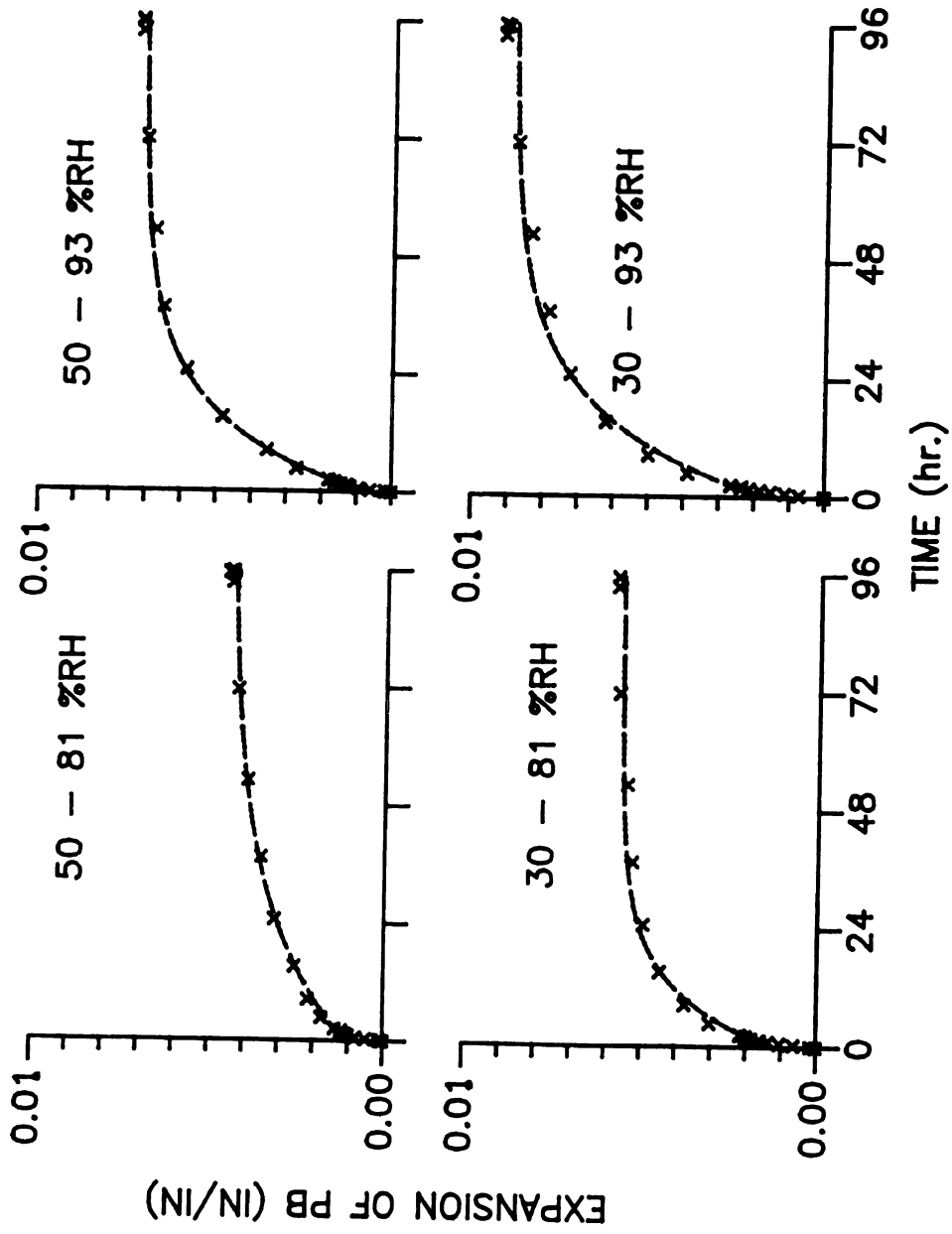

Figure 4-6 Nonlinear regression models of PB expansion

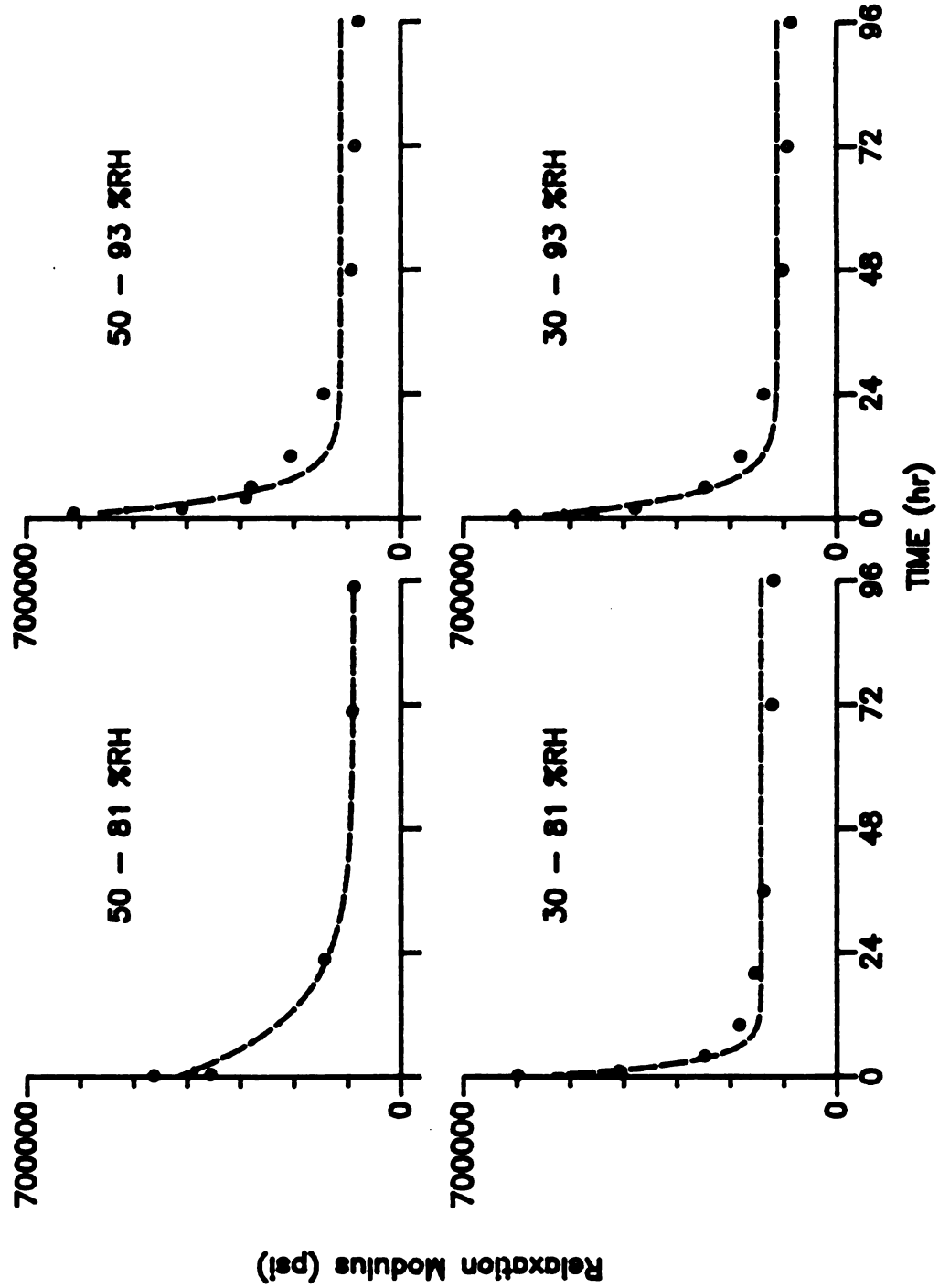

Figure 4-7 Nonlinear regression models of PB swelling stress relaxation modulus.

4.4 Application of Results to Plywood

It is clear from the results that the warping of cross-laminated solid wood cannot be predicted with a reasonable degree of accuracy by applying elastic beam equation. It can, however, be approximated remarkably well by either the modified elastic beam equation or by the visco-elastic approach. Of the two, the modified elastic approach is by far the easier one to use. Its success derives from the fact that a solid wood lamina can in the longitudinal direction be treated as an elastic material (high MOE and very small α) This results in almost complete expansion restraint in the transverse direction of adjacent layers (low MOE, large α). The model illustrated in Figure 2-15 is therefore applicable. Its application, however, requires the experimental determination of the deformation modulus and of the elastic strain component. There is evidence, however, that the elastic strain component may be a constant fraction of the free expansion for many species (see Keylwerth [21]). Also the deformation modulus is not drastically different from the statically determined MOE so that fairy reasonable results could possibly be obtained using inputs readily available for many species from the Wood Handbook [10].

It should be noted here, however, that these discussion and predictions are limited to the condition of increasing moisture contents and to one species (yellow-poplar).

Figure 4-8 illustrates the relationship between the warp measured on and calculated for narrow laminated beams and the warp of a square plate of the same construction.

In the following, the elastic and inelastic approximating of cross laminated solid wood is applied to the beams tested and to conventional plywood of various construction with the additional feature of including in the inputs the natural variation of these properties (see [47]).

The generated computer program creates random variables for each inputs controlled by arbitrary coefficients of variation. 200 runs were employed for each of the beam and plywood construction. The results are shown in the form of normal distribution curves of the warping, indicating the effect on warping of the natural variability of the input variables (Figure 4-9 to 4-14).

The computer model for the two yellow-poplar plywood sheets shown are average warp of zero. This is because the plywood is structurally balanced. The warp on each side of the average is due to natural variation in the input variable. (Figure 4-15 and 4-16).

The plywood sheets are constructed of 0.125-*inch* thick veneer sheets. Inputs and their assumed variations are shown in Table 4-20 and 4-21.

Also shown in Figure 4-15 and 4-16 is the effect of assuming property variability only in the faces and constant average properties in the core layers veneers and assumed property variability in all layers.

It is apparent that any variation of properties in the core layers has a negligible effect on the computed warping.

4.5 Application of Results to Wood Composites

The results clearly indicate that both MDF and PB behave like elastic materials. The reasons for this unexpected behavior are not clear.

It seems justified, therefore, to apply the elastic beam equation to materials consisting of or containing PB or MDF as substrates.

This is supported by experimental and theoretical results of warping study involving particleboard substrates and veneer or plastic overlays ([42] and [44]).

Table 4-18 Random run inputs for yellow-poplar beams at 66 - 81%RH interval

Elastic Approach

	Thickness (in)		Modulus (psi)		Expansion (in/in)	
ID	AVG	C.V.	AVG	C.V.	AVG	C.V
L - T						
L:	0.257	5%	1181332	6.19%	0.00013	8%
T:	0.257	5%	39109	6.41%	0.01492	8%
T - L - T						
T:	0.0643	5%	39109	6.41%	0.01492	8%
L:	0.257	5%	1181332	6.19%	0.00013	8%
T:	0.257	5%	39109	6.41%	0.01492	8%
L - T - L						
L:	0.257	5%	1181332	6.19%	0.00013	8%
T:	0.257	5%	39109	6.41%	0.01492	8%
L:	0.0643	5%	1181332	6.19%	0.00013	8%

Inelastic Approach

	Thickness (in)		Modulus (psi)		Expansion (in/in)	
ID	AVG	C.V.	AVG	C.V.	AVG	C.V
L - T						
L:	0.257	5%	1181332	6.19%	0.00013	8%
T:	0.257	5%	42628	5.99%	0.003453	9.49%
T - L - T						
T:	0.0643	5%	42628	5.99%	0.003453	9.49%
L:	0.257	5%	1181332	6.19%	0.00013	8%
T:	0.257	5%	42628	5.99%	0.003453	9.49%
L - T - L						
L:	0.257	5%	1181332	6.19%	0.00013	8%
T:	0.257	5%	42628	5.99%	0.003453	9.49%
L:	0.0643	5%	1181332	6.19%	0.00013	8%

Table 4-19 Random run inputs for yellow-poplar beams at 66 - 93%RH interval

Elastic Approach

	Thickness (in)		Modulus (psi)		Expansion (in/in)	
ID	AVG	C.V.	AVG	C.V.	AVG	C.V
L - T						
L:	0.257	5%	1093215	6.49%	0.00025	8%
T:	0.257	5%	30031	14.31%	0.02967	8%
T - L - T						
T:	0.0643	5%	30031	14.31%	0.02967	8%
L:	0.257	5%	1093215	6.49%	0.00025	8%
T:	0.257	5%	30031	14.31%	0.02967	8%
L - T - L						
L:	0.257	5%	1093215	6.49%	0.00025	8%
T:	0.257	5%	30031	14.31%	0.02967	8%
L:	0.0643	5%	1093215	6.49%	0.00025	8%

Inelastic Approach

	Thickness (in)		Modulus (psi)		Expansion (in/in)	
ID	AVG	C.V.	AVG	C.V.	AVG	C.V
L - T						
L:	0.257	5%	1093215	6.49%	0.00025	8%
T:	0.257	5%	44217	3.91%	0.007719	8.93%
T - L - T						
T:	0.0643	5%	44217	3.91%	0.007719	8.93%
L:	0.257	5%	1093215	6.49%	0.00025	8%
T:	0.257	5%	44217	3.91%	0.007719	8.93%
L - T - L						
L:	0.257	5%	1093215	6.49%	0.00025	8%
T:	0.257	5%	44217	3.91%	0.007719	8.93%
L:	0.0643	5%	1093215	6.49%	0.00025	8%

Table 4-20 Random run inputs for yellow-poplar 3-ply balanced beams using inelastic approach

66 - 81%RH

	Thickness (in)		Modulus (psi)		Expansion (in/in)	
ID	**AVG**	**C.V.**	**AVG**	**C.V.**	**AVG**	**C.V**
All layers have variability:						
L:	0.125	5%	1181332	6.19%	0.00013	8%
T:	0.125	5%	42628	5.99%	0.003453	9.49%
L:	0.125	5%	1181332	6.19%	0.00013	8%
Only face layers have variability:						
L:	0.125	5%	1181332	6.19%	0.00013	8%
T:	0.125	0%	42628	0.00%	0.003453	0%
L:	0.125	5%	1181332	6.19%	0.00013	8%

66 - 93%RH

	Thickness (in)		Modulus (psi)		Expansion (in/in)	
ID	**AVG**	**C.V.**	**AVG**	**C.V.**	**AVG**	**C.V**
All layers have variability:						
L:	0.125	5%	1093215	6.49%	0.00025	8%
T:	0.125	5%	44217	3.91%	0.007719	8.93%
L:	0.125	5%	1093215	6.49%	0.00025	8%
Only face layers have variability:						
L:	0.125	5%	1093215	6.49%	0.00025	8%
T:	0.125	0%	44217	0.00%	0.007719	0%
L:	0.125	5%	1093215	6.49%	0.00025	8%

Table 4-21 Random run inputs for yellow-poplar 5-ply balanced beams using inelastic approach

66 - 81%RH

	Thickness (in)		Modulus (psi)		Expansion (in/in)	
ID	AVG	C.V.	AVG	C.V.	AVG	C.V
All layers have variability:						
L:	0.125	5%	1181332	6.19%	0.00013	8%
T:	0.125	5%	42628	5.99%	0.003453	9.49%
L:	0.125	5%	1181332	6.19%	0.00013	8%
T:	0.125	5%	42628	5.99%	0.003453	9.49%
L:	0.125	5%	1181332	6.19%	0.00013	8%
Only face layers have variability:						
L:	0.125	5%	1181332	6.19%	0.00013	8%
T:	0.125	0%	42628	0.00%	0.003453	0%
L:	0.125	0%	1181332	0.00%	0.00013	0%
T:	0.125	0%	42628	0.00%	0.003453	0%
L:	0.125	5%	1181332	6.19%	0.00013	8%

66 - 93%RH

	Thickness (in)		Modulus (psi)		Expansion (in/in)	
ID	AVG	C.V.	AVG	C.V.	AVG	C.V
All layers have variability:						
L:	0.125	5%	1093215	6.49%	0.00025	8%
T:	0.125	5%	44217	3.91%	0.007719	8.93%
L:	0.125	5%	1093215	6.49%	0.00025	8%
T:	0.125	5%	44217	3.91%	0.007719	8.93%
L:	0.125	5%	1093215	6.49%	0.00025	8%
Only face layers have variability:						
L:	0.125	5%	1093215	6.49%	0.00025	8%
T:	0.125	0%	44217	0.00%	0.007719	0%
L:	0.125	0%	1093215	0.00%	0.00025	0%
T:	0.125	0%	44217	0.00%	0.007719	0%
L:	0.125	5%	1093215	6.49%	0.00025	8%

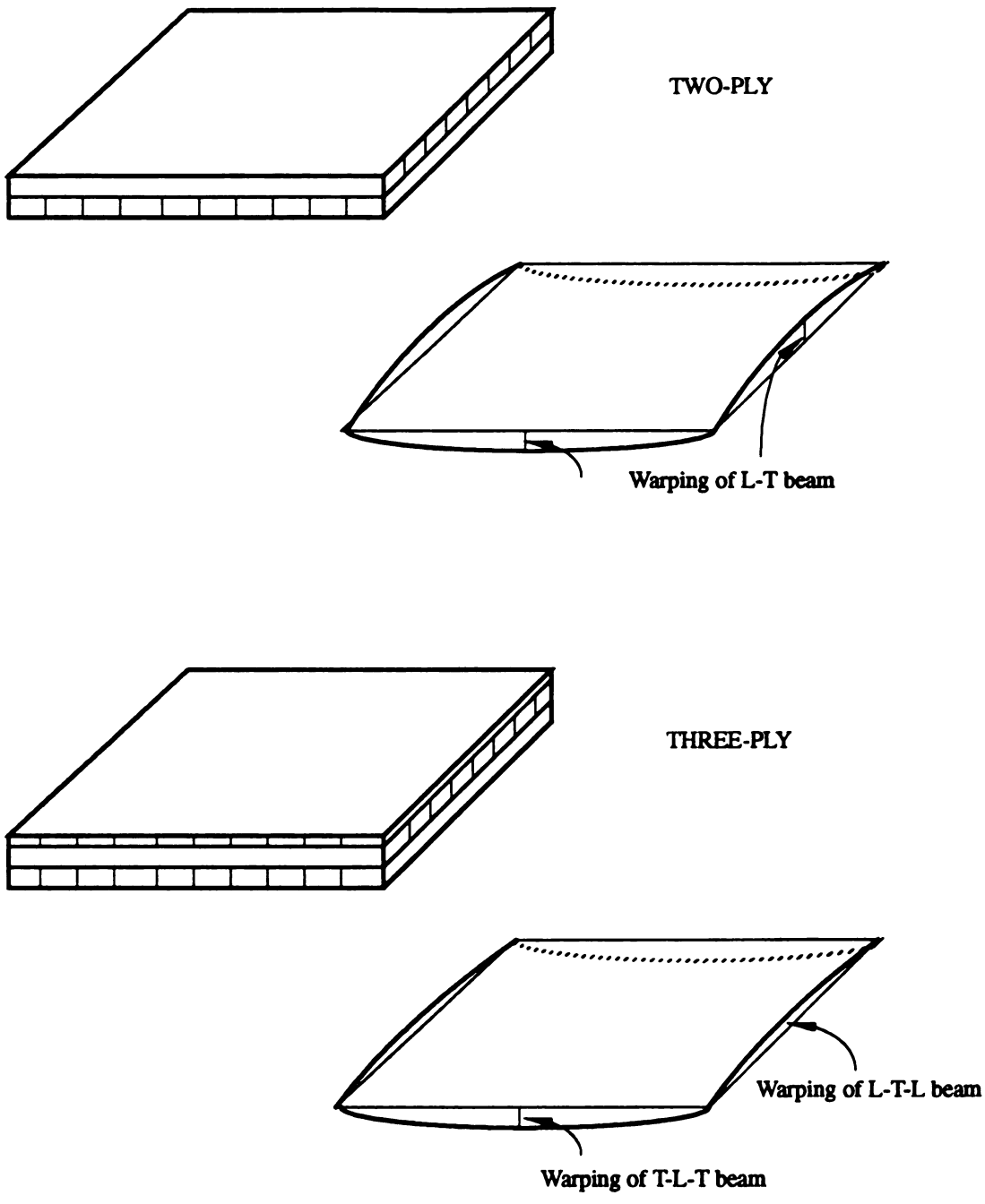

Figure 4-8 Implication to the warping of plywood

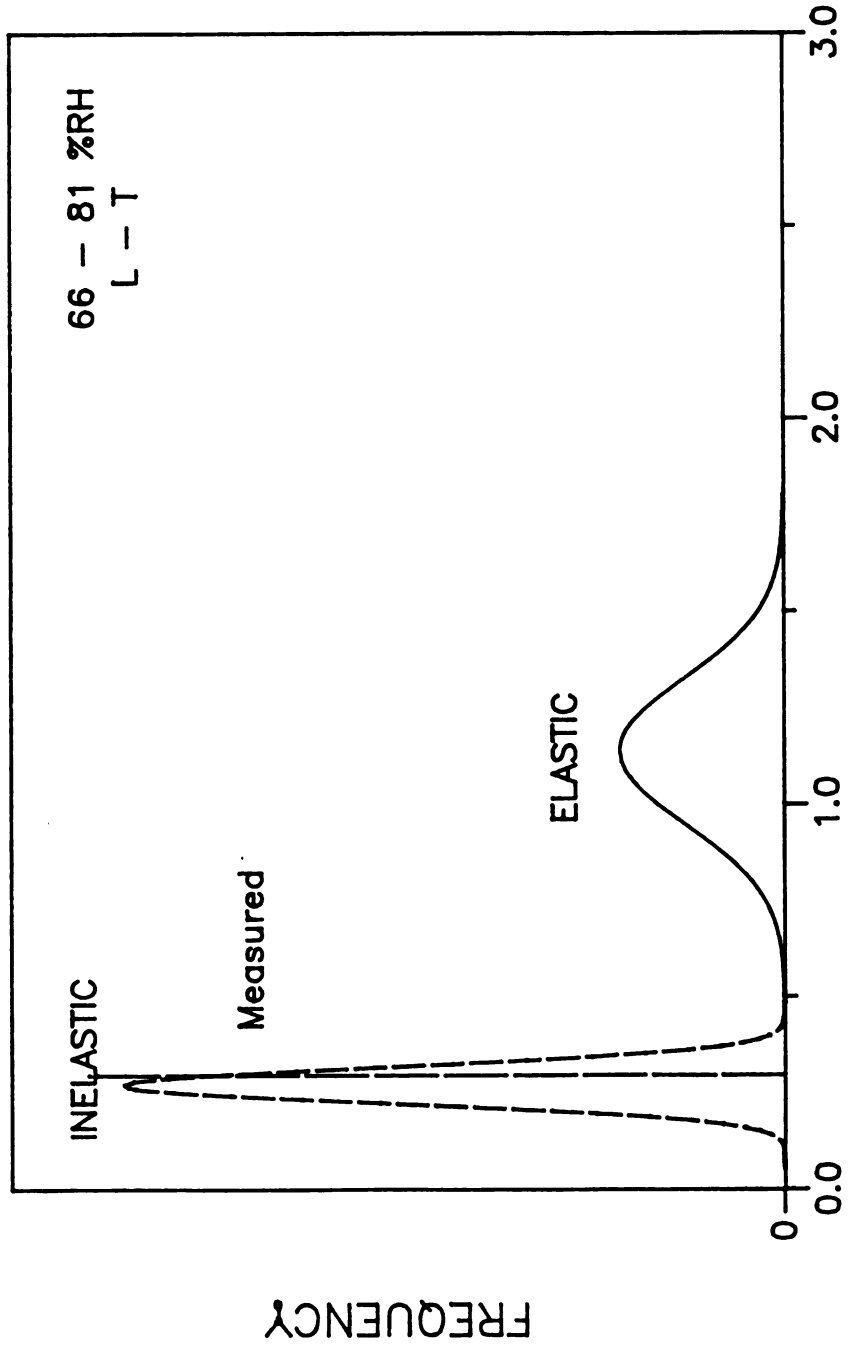

Figure 4-9 Estimated warping of yellow-poplar two-ply (L-T) beam from random run at the condition of 66 - 81%RH using elastic and inelastic approach

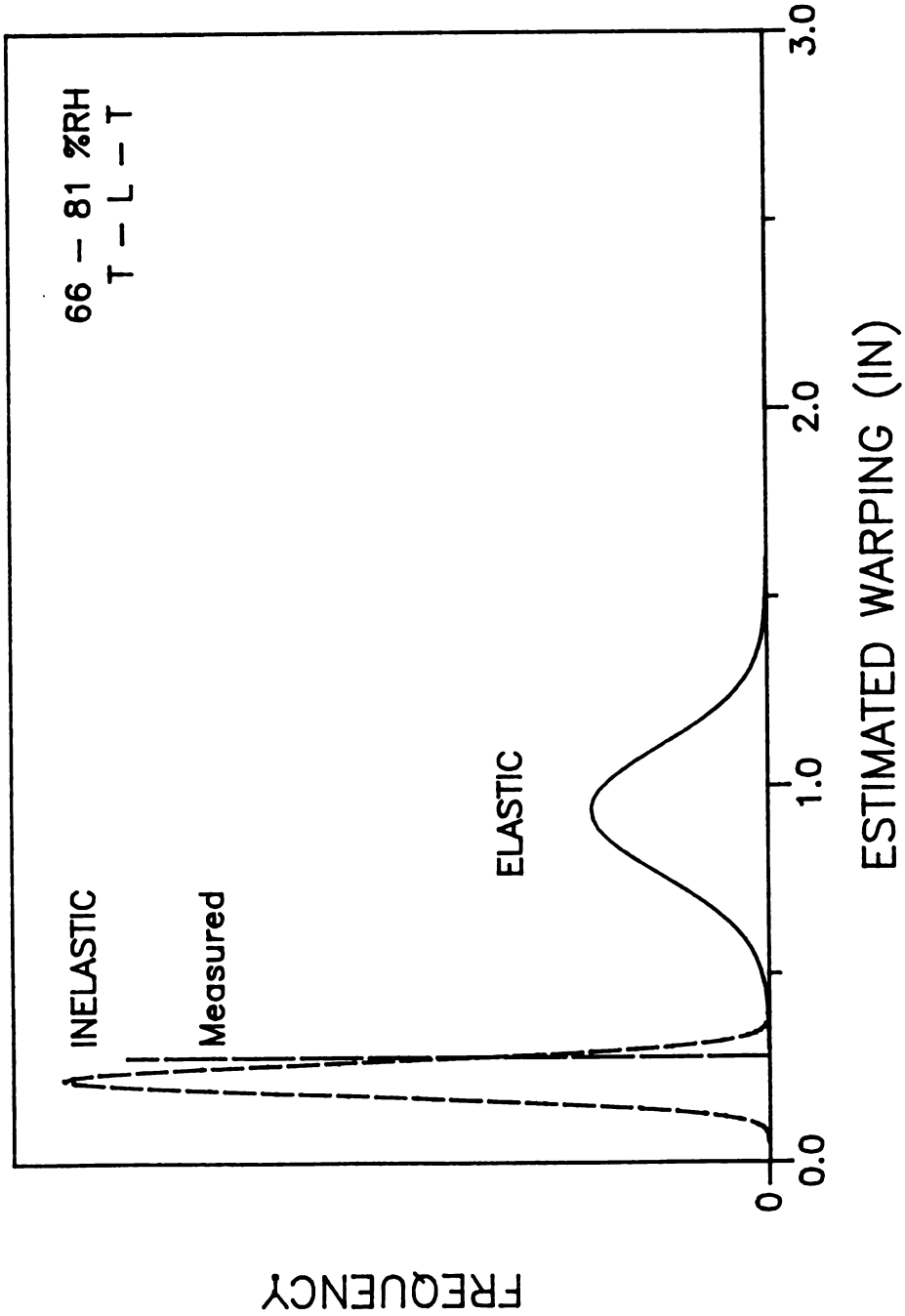

Figure 4-10 Estimated warping of yellow-poplar three-ply beam (T-L-T) from random run at the condition of 66 - 81%RH using elastic and inelastic approach

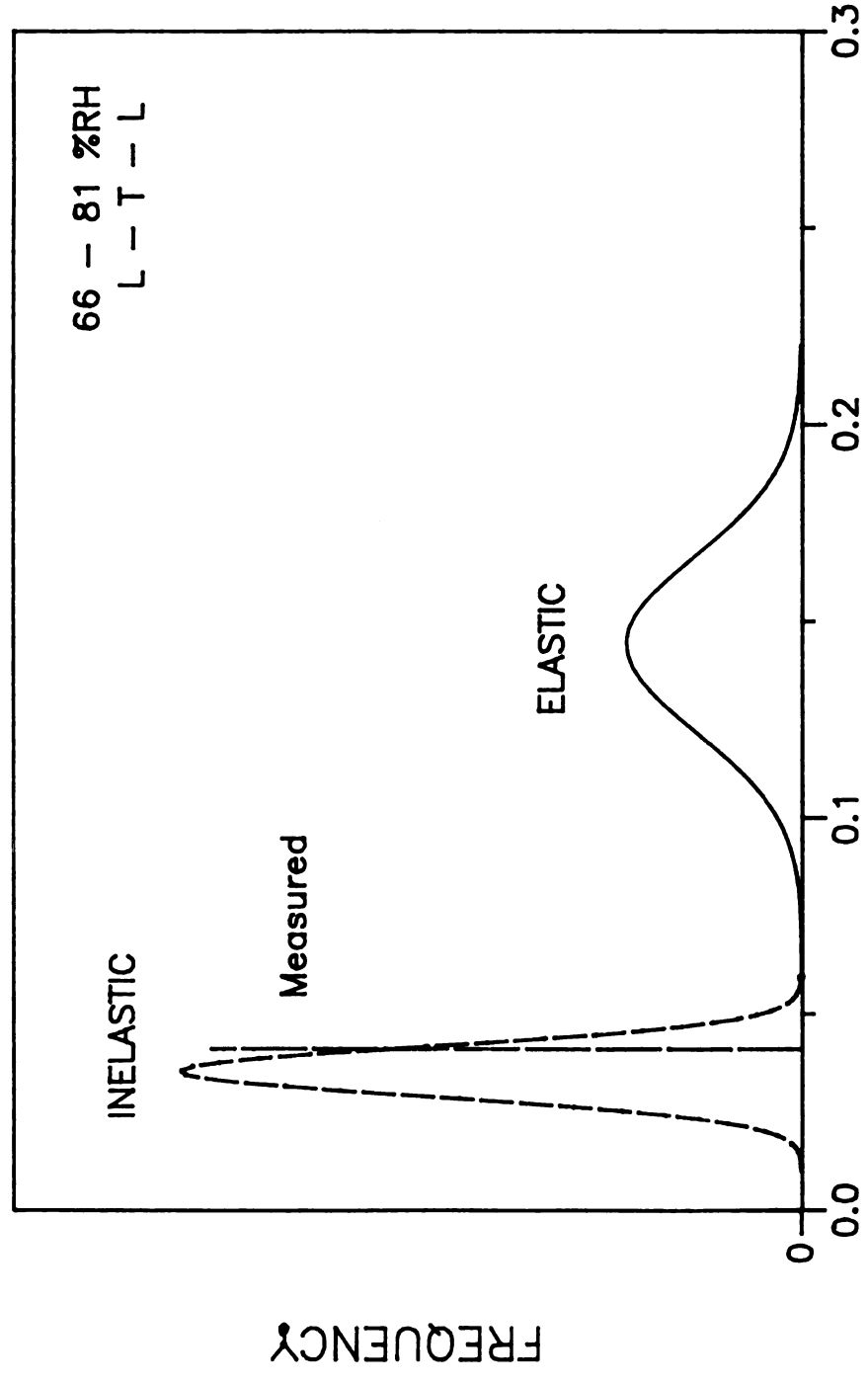

Figure 4-11 Estimated warping of yellow-poplar three-ply beam (L-T-L) from random run at the condition of 66 - 81%RH using elastic and inelastic approach

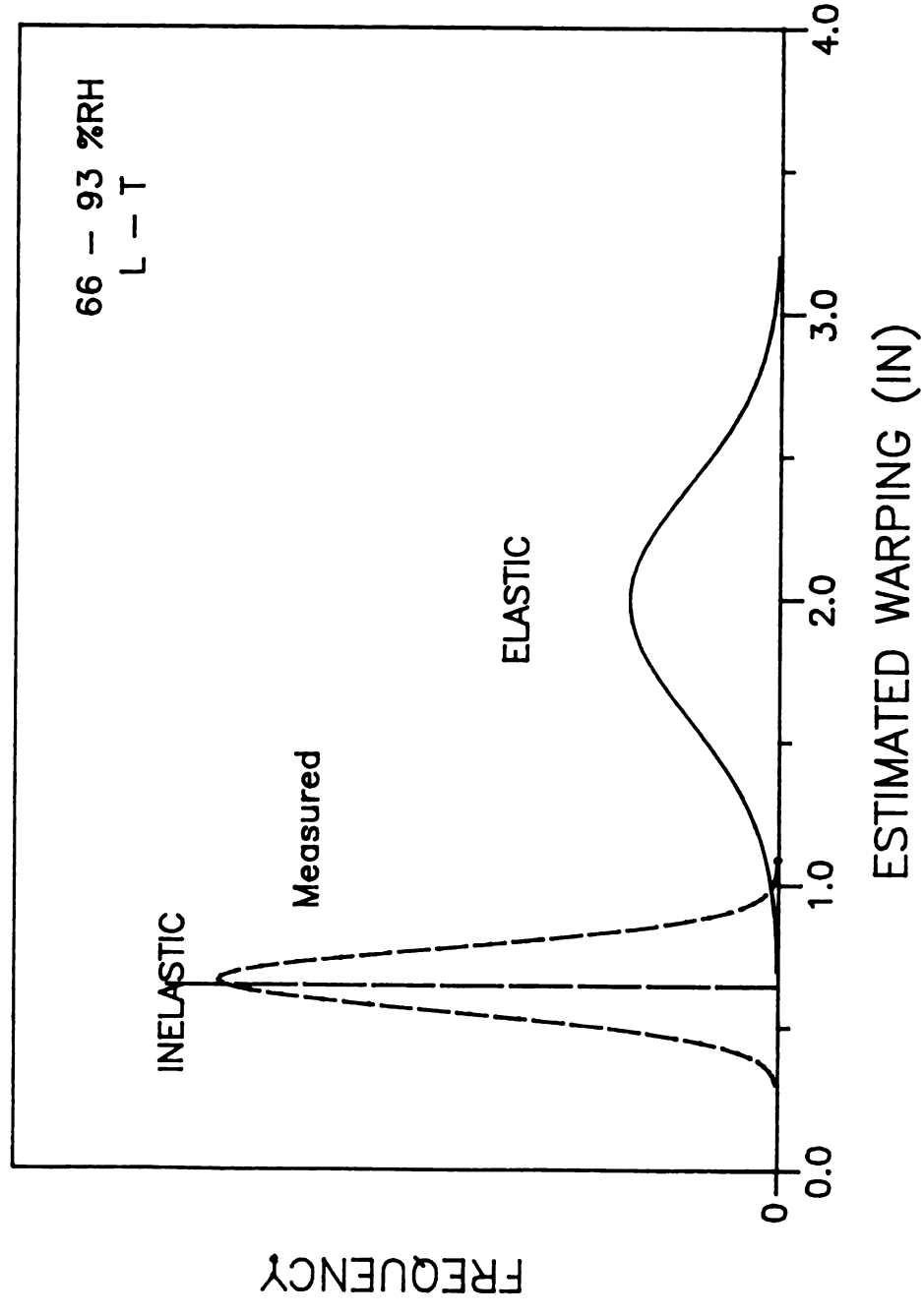

Figure 4-12 Estimated warping of yellow-poplar two-ply (L-T) beam from random run at the condition of 66 - 93%RH using elastic and inelastic approach

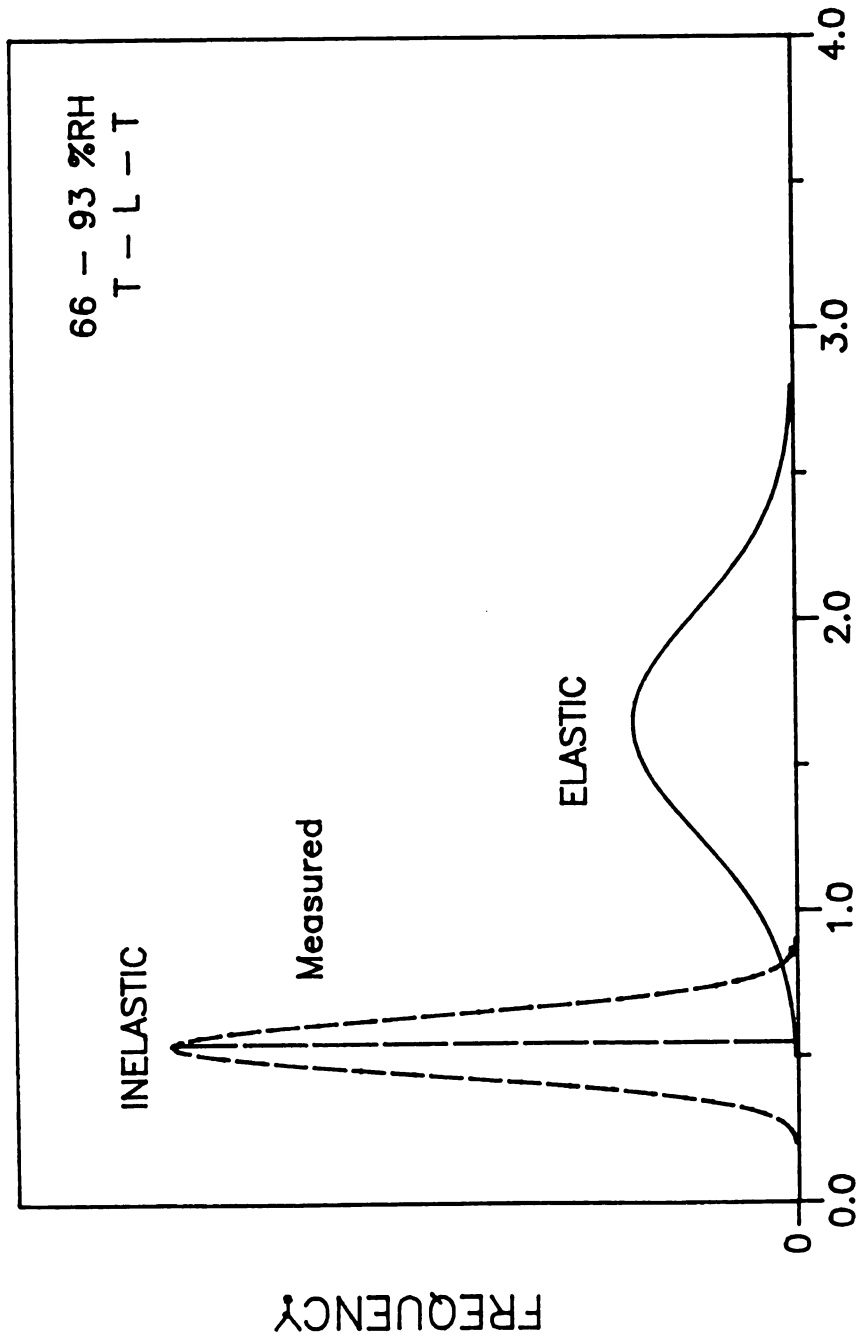

Figure 4-13 Estimated warping of yellow-poplar three-ply beam (T-L-T) from random run at the condition of 66 - 93%RH using elastic and inelastic approach

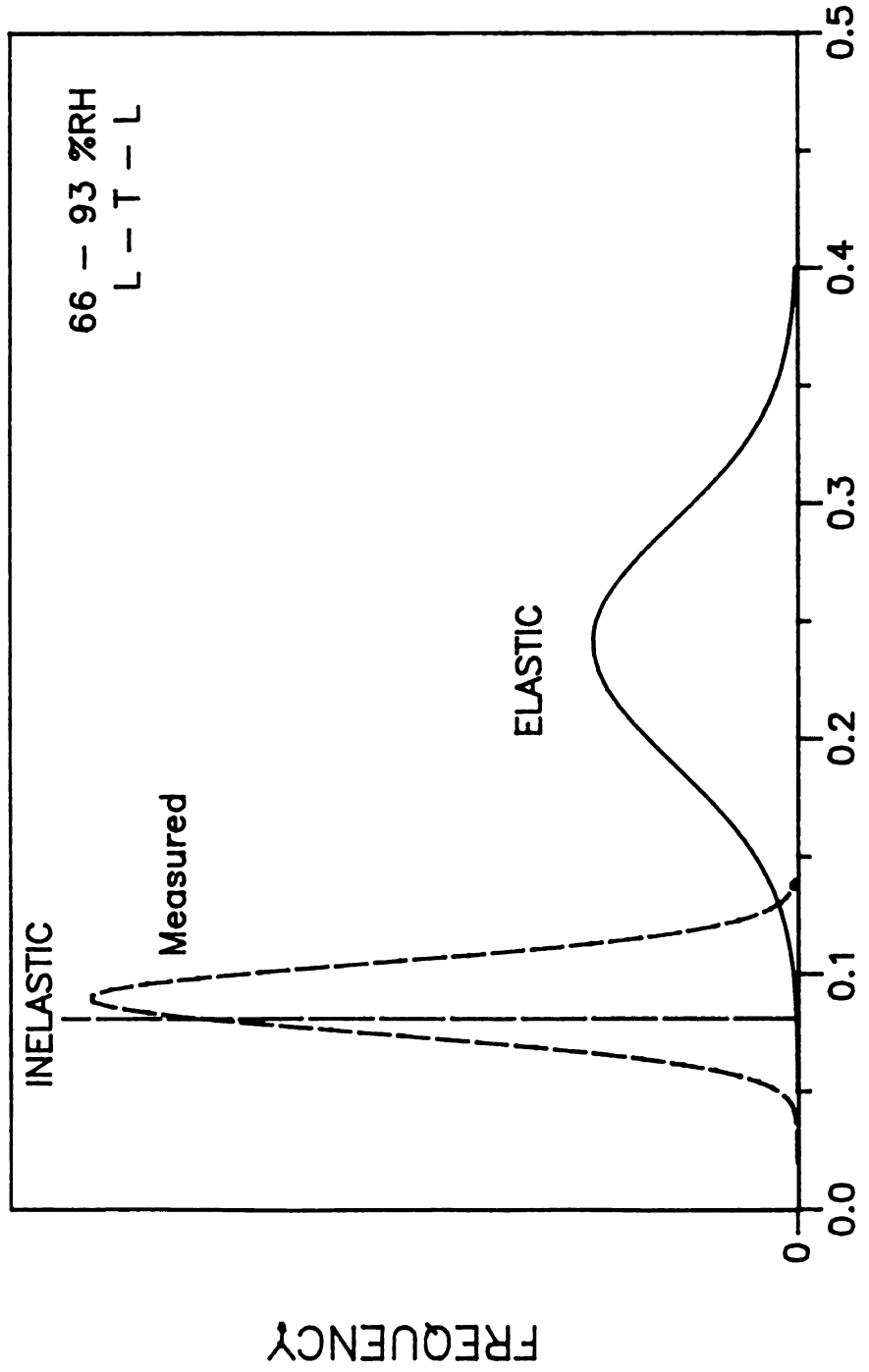

Figure 4-14 Estimated warping of yellow-poplar three-ply beam (L-T-L) from random run at the condition of 66 - 93%RH using elastic and inelastic approach

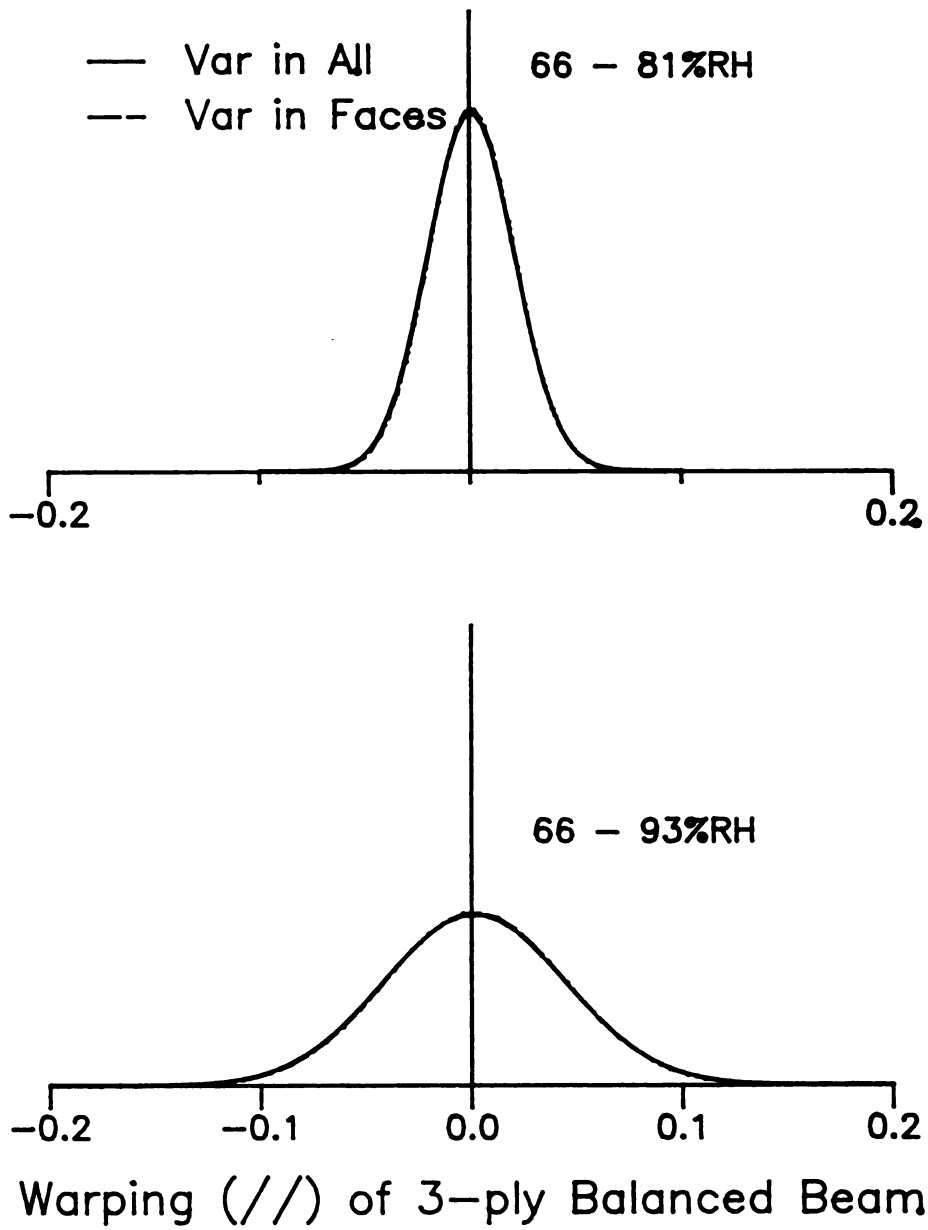

Figure 4-15 Estimated warping (in.) of three-ply balanced yellow-poplar beams with 48-inch span by introducing the variability on all layers and face layers.

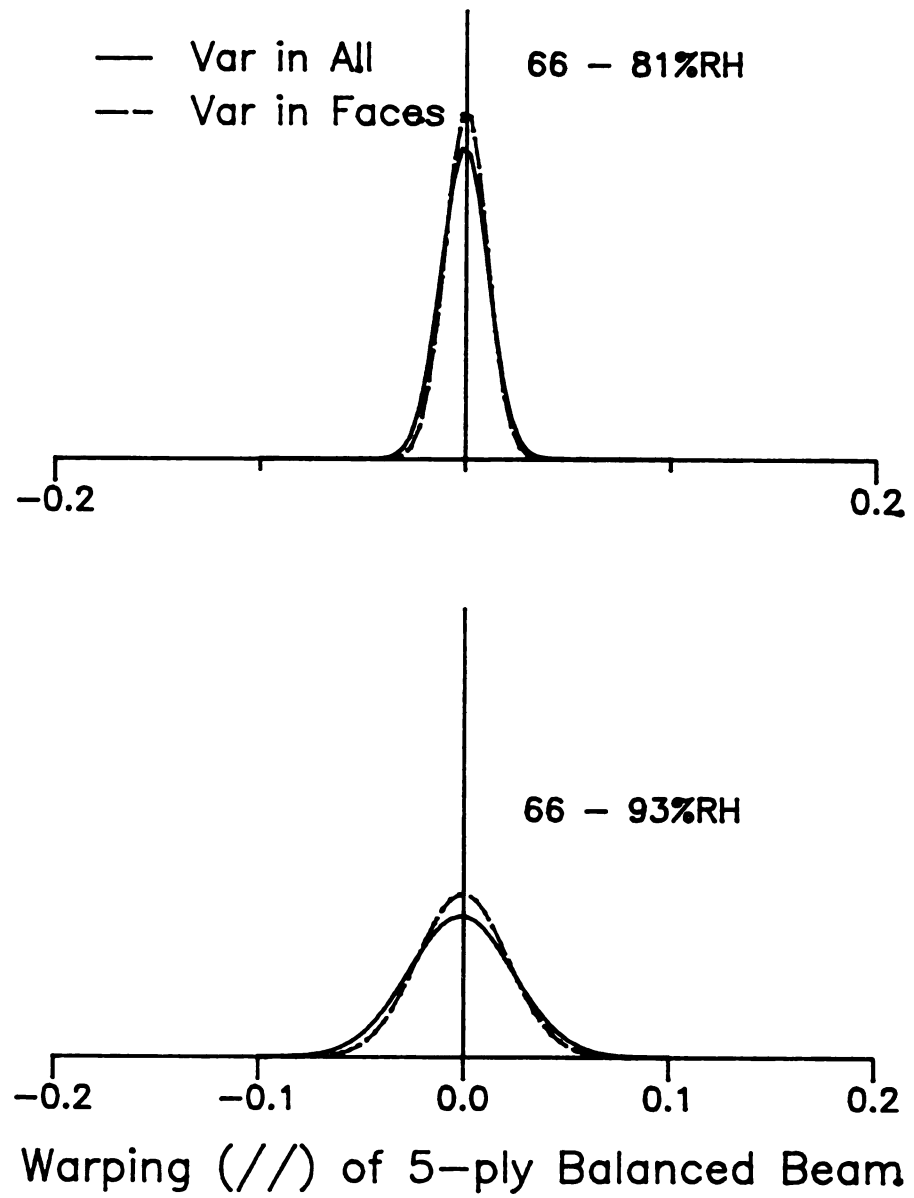

Figure 4-16 Estimated warping (in.) of five-ply balanced yellow-poplar beams with 48-inch span by introducing the variability on all layers and face layers.

CHAPTER V
SUMMARY AND CONCLUSION

All hygroscopic warping of panel materials made from solid wood or wood composites is due to the imbalance of ensuing swelling stresses over the cross section of the panel. This stress imbalance in turn is the result of an unsymmetrical distribution over the cross section of the combination of hygroscopic expansion characteristics and of the stiffness (modulus of elasticity). In the case of plywood, this distribution is discrete and can readily be investigated by tests described in this study. In the case of wood composites, the distribution of these characteristics is more gradual and less easy determined.

Given the above characteristics: hygroscopic expansion, modulus of elasticity and their spatial distribution over the cross section, the warp upon moisture content change can be calculated. The accuracy of the predicted warp is dependent to a large extent on how well the materials in question follows the assumption made by the theoretical analysis or on how well the theoretical treatment can be modified to accommodate the specific characteristics of the materials involved.

This study used essentially two approaches for the prediction of the warping of composite beams, namely the application of the standard equation

for the deformation of an elastic laminated beam including some modification to accommodate the less than elastic behavior of solid wood across the grain and a visco elastic approach which accounts for the time dependence of the mechanical characteristics of the materials involved.

The elastic equation is discussed in some detail in Appendix A. It is shown there that the warping of a two component beam, which could have more than two layers is proportional to the difference between the expansion value of the two components ($\alpha_2 - \alpha_1$) and is a nonlinear function of the moduli ratio (E_1/E_2).

The equation assumes that any restraint imposed by one layer on the hygroscopic expansion of another layer is transformed into elastic strain.

Our experiments show that this is not the case for solid wood in the cross grain direction.

These tests yielded results that allowed appropriate modification of the inputs to the above equation (inelastic approach), which greatly improved the accuracy of the predicted warp. The important modification is the reduction of the free hygroscopic expansion to about 25% of its measured value, which represents the elastic portion of the total free expansion, i.e., that portion that converts into elastic strain. The other less important modification is the calculation of a "deformation modulus", which, however, does not differ too much from the measured modulus of elasticity across the grain.

These results present the very attractive possibility of calculating the warp of plywood from listed values $E_{//}$ and $E_{\perp}$, and 1/4 of the free expansion. These values would, of course, have to be adjusted for a specific moisture content interval. But even if it was necessary to measure the free

expansion, it would be an easy test to perform. In the grain direction (longitudinal), the elastic assumption are valid and no modification are necessary.

The visco elastic approach in the case of solid wood laminates yielded very good results, but the generation of the necessary inputs is complicated and time consuming.

In the case of laminated composition boards, MDF and PB, the results were unexpected. It turned out that the beam equation fitted the warping problem very well without modification. Modification based on experiments resulted in considerable error of the estimates. This means that these materials act like elastic materials or more like solid wood in the grain direction (longitudinal).

This is supported by research on overlaid particleboard [42].

The following speculative explanation is offered. MDF and PB have far smaller expansion value than solid wood across the grain. Also the difference in their expansion values are very small so that the mutual restraint is relatively minor and the resulting stresses relatively small.

Further investigation of these phenomena would be desirable.

In any event, the warping of such laminate can well be calculated using standard inputs into the elastic beam equation.

In conclusion, the experiments appear to support the following statements:

— The uniaxial restraining of swelling stresses of wood across the grain is a viscoelastic process. Only a fraction of the total swelling restraint can be converted into elastic strain.

— The elastic portion of the free expansion across the grain of solid wood is about 25%.

— Along the grain, solid wood can be assumed to behave elastically under conditions prevailing in a laminate subjected to moisture content increase.

— Laminates consisting of composite boards behave "elastically" and their reaction to moisture content increase can be described by standard beam equations.

These results and conclusions will allow the formulation of relatively simple guidelines for the mathematical modeling of wood based laminates.

LIST OF REFERENCES

LIST OF REFERENCES

1. Alexopoulos, J. 1989. Effect of resin content on creep and other properties of waferboard. M. S. Thesis, Department of Forestry, University of Toronto. Toronto, Canada.

2. American Society for Testing and Materials (ASTM). 1991. Evaluating the properties of wood based fiber and particle panel materials. Method D1037 (04.09); Method of testing small clear specimens of timber. Method D143 (04.09). 1916 Race street, Philadelphia, PA 19103-1187.

3. Bodig, J. and B. A. Jayne. 1982. Mechanics of Wood and Wood Composites. Van Nostrand Reinhold Company Inc. 135 West 50th Street, New York, N.Y. 10020.

4. Buss, F. 1951. Study of effect of unbalanced construction of plywood. The Perkins glue line 2(7): 2-4. Febr. - March.

5. Chapra, S. C. and R. P. Canale. Numerical Methods for Engineers. McGraw-Hill, Inc. New York, NY.

6. Christensen, R. M. 1982. Theory of Viscoelasticity: An Introduction. 2nd ed. Academic Press. New York.

7. Ferry, J. D. 1970. Viscoelastic Properties of Polymers. John Wiley & Sons, Inc. New York, NY.

LIST OF REFERENCES (continued)

8. Flaggs, D. L. and F. W. Crossman. 1981. Analysis of the viscoelastic response of composite laminates during hygrothermal exposure. Journal of Composite Materials Vol. 15, pp21-40.

9. Flugge, W. 1967. Viscoelasticity. Blaisdell Publishing Company, A Division of Ginn and Company, Waltham, MA.

10. Forest Products Laboratory. Wood Handbook: Wood as an Engineering Materials. Agric. Handbook 72. Washington, DC. U.S. Department of Agriculture; rev. 1987. 466p.

11. Gatewood, B. E. 1957. Thermal Stresses. McGraw-Hill, Inc. New York, NY.

12. Haygreen, J., H. Hall, K-N. Yang, and R. Sawicki. 1975. Studies of flexural creep behavior in particleboard under changing humidity conditions. Wood and Fiber 7(2): 74-90.

13. Heebink, B. C., H. H. Haskell, and C. B. Norris. 1961. Warping characteristics of six panel constructions having decorative laminate faces. Forest Products Laboratory, Madison, WI. Unpublished report.

14. Heebink, B. C. and H. H. Haskell. 1962. Effect of heat and humidity on the properties of high pressure laminates. Forest Products Journal 20(11): 542-548.

15. Hetnarski, R. B. 1986. Thermal Stresses I. (Mechanics and mathematical methods) Elsevier Science Publishing Company, Inc. 52 Vanderbilt Avenue, New York, N.Y. 10017.

16. Hiziroglu, S. S. and O. Suchsland. 1991. Level of bending stresses in buckled sheathing composites. Forest Products Journal 41(2): 58-62.

LIST OF REFERENCES (continued)

17. Iwashita, M. and A. M. Stashevski. 1968. Studies on particle board (XI), Studies on overlaid particle board (2): The influence of physical properties of some Japanese particleboard and high pressure decorative laminates on the stability of overlaid boards. Bulletin of Japanese Government Forest Experiment Station in Meguro. No. 215: 1- 37.

18. Johns, D. J. 1965. Thermal Stress Analysis. Pergamon Press Inc., 122 East 55th Street, New York 22, N.Y.

19. Jones, R. M. 1975. Mechanics of Composite Materials. McGraw-Hill, Inc. New York, NY.

20. Karasudhi, P. 1991. Foundations of Solid Mechanics. Kluwer Academic Publishers, 101 Philip Drive, Norwell, MA 02061.

21. Keylwerth, R. 1962. Investigations on the free and restraint swelling —— Part II: Restraint swelling. Holz als Roh-und Werkstoff 20(8): 292-303. Translated by E. Pichler. Nal. Translation No. 6241B. USDA National Agricultural Lib. Beltsville, MD.

22. Keylwerth, R. 1962. Investigations on the free and restraint swelling —— Part I: Free swelling. Holz als Roh-und Werkstoff 20(7): 252-259. Translated by E. Pichler. Nal. Translation No. 6241A. USDA National Agricultural Lib. Beltsville, MD.

23. Kollmann, F. F. P., E. W. Kuenzi and A. J. Stamm. 1975. Principles of Wood Science and Technology II: Wood Based Materials. Springer-Verlag, New York Inc.

24. Leichti, R. J., R. H. Falk and T. L. Laufenberg. 1990. Prefabricated wood composite I-beams: A literature review. Wood and Fiber Science Vol. 22(1).

LIST OF REFERENCES (continued)

25. Laufenberg, T. L. 1982. Exposure effects upon performance of laminated veneer lumber and glulam materials. Forest Products Journal 32(5): 42-48.

26. McNatt, J. D., J. Youngquist and T. Xin. 1992. Physical and mechanical properties of laminating materials. U. S. Forest Products Lab. Madison, WI. Unpublished report.

27. McNatt, J. D. and M. O. Hunt. 1982. Creep of thick structural flakeboard in properties of wood. Forest Products Journal 32(5): 49-54.

28. Miller, D. G. and J. Benicak. 1967. Relation of creep to the vibrational properties of wood. Forest Products Journal 17(12): 36-39.

29. Maloney, T. M. 1986. Modern Particleboard and Dry Process Fiberboard Manufacturing. Miller Freedom Pub, Inc., San Francisco, CA.

30. Moslemi, A. 1964. Some aspects of the viscoelastic behavior of hardboard. Ph. D. dissertation, Department of Forest Products, Michigan State University, E. Lansing, MI.

31. Nielsen, A. 1972. Rheology of Building Materials. Document D6:1972. Nat. Swedish Institution. Bldg. Res. 213pp.

32. Norris, C. B. 1964. Warpage of laminated materials due to change in moisture content or temperature. Appendix in: Heebink, B. G., Kuenzi, E. W. and A. C. Maki. Linear movement of plywood and flakeboards as related to the longitudinal movement of wood. Forest Service Research Note FPL-073.

33. Panshin, A. J. and C. de Zeeuw. 1980. Textbook of Wood Technology. Volume 1. Fourth Ed. McGraw-Hill, Inc. New York, NY.

LIST OF REFERENCES (continued)

34. Pierce, C.B., and J. M. Dinwoodie. 1977. Creep in chipboard. Part I: Fitting 3- and 4-element response curves to creep data. Journal Material Science 12: 1955-1960.

35. Pipes, R. B., J. R. Vinson and T. W. Chou. 1976. On the hygrothermal response of laminated composite systems. Journal of Composite Materials Vol. 10, pp129-149.

36. Pipkin, A. C. 1986. Lectures on Viscoelasticity Theory. Springer-Verlag, New York Inc.

37. Schapery, R. A. 1967. Stress analysis of viscoelastic composite materials. Journal of Composite Materials Vol. 1, pp228-267.

38. Schniewind, A. P. 1968. Recent progress in the study of the rheology of wood. Wood Science and Technology 2(3): 188-206.

39. Sims, D. F. 1972. Viscoelastic creep and relaxation behavior of laminated composite plates. Ph.D. Dissertation, Department of Mechanical Engineering and the Solid Mechanics Center, Southern Methodist University, Dallas, Texas.

40. Springer, G. S. 1984. Environmental Effects on Composite Materials. Technomic Publishing Company, Inc. 851 New Holland Ave. Box 3535, Lancaster, PA 17604.

41. Stamm, A. J. 1964. Wood and Cellulose Science. The Ronald Press Co., New York, N.Y.

42. Suchsland, O., Y. Feng and D. Xu. 1993. The warping of laminated particleboard. Wood Science Series, No. 4. Department of Forestry, Michigan State University. East Lansing, MI.

LIST OF REFERENCES (continued)

43. Suchsland, O. and D. Xu. 1992. Determination of swelling stresses in wood-based materials. Forest Products Journal 42(5): 25-27.

44. Suchsland, O. 1990. How to analyze the warping of a furniture panel. Wood Science Series, No. 3. Department of Forestry, Michigan State University. East Lansing, MI.

45. Suchsland, O. 1990. Estimating the warping of veneered furniture panels. Forest Products Journal 40(9): 39-43.

46. Suchsland, O. and G. E. Woodson. 1986. Fiberboard Manufacturing Practices in the United States. USDA Forest Service, Agriculture Handbook No. 640.

47. Suchsland, O. and J. D. McNatt. 1985. On the warping of laminated wood panels. Michigan State University. East Lansing, MI.

48. Suchsland, O. 1976. Measurement of swelling forces with load cells. Wood Science. 8(3): 194-198.

49. Suchsland, O. 1974. Determination of small linear expansion coefficients from curvature of two-ply laminate strips. Forest Products Journal 24(4): 38-39.

50. Suchsland, O. 1970. Optical determination of linear expansion and shrinkage of wood. Forest Products Journal 20(6): 26-29.

51. Suchsland, O. 1965. Swelling stresses and swelling deformation in hardboard. Michgan Agriculture Experiment Station. Michgan State University, E. Lansing. Quarterly Bulletin 47(4): 591-605.

LIST OF REFERENCES (continued)

52. Timoshenko, S. P. and J. N. Goodier. 1951. Theory of Elasticity. 2nd. ed. McGraw-Hill, Inc. New York, NY.

53. Timoshenko, S. P. 1925. Analysis of bi-metal thermostats. J. of Optic. Soc. Amer.: 235-255.

54. Tong, Y. and O. Suchsland. 1993. Application of finite element analysis to panel warping. Holz ais Roh- und Werkstoff (51): 55-57.

55. Tsai, S. W. and T. H. Hahn. 1980. Introduction to Composite Materials. Techromic Pub.

56. Whitney, J. M. 1969. Analysis of heterogeneous anisotropic plates, Journal of Applied Mechanics Vol. 36, pp.261-266.

57. Xu, H. 1993. Application of a linear visco-elastic plate theory on hygroscopic warping of laminates. Ph. D. dissertation, .Department of Forestry, Michigan State University, E. Lansing, MI.

APPENDIX A

APPENDIX A

ON WARPING EQUATION FOR TWO-PLY BEAM

For a two-ply laminated beam, it can be derived that the center deflection W is proportional to the difference of the expansion value between the two layers. In fact, by letting

$$\begin{aligned} A_1 &= E_1(S_1^2 - S_0^2) \\ A_2 &= E_2(S_2^2 - S_1^2) \\ B_1 &= E_1 T_1 \\ B_2 &= E_2 T_2 \end{aligned} \tag{A-1}$$

Equation (2-13) leads to the center deflection of the beam over length L

$$W = \frac{L^2}{8R} = \frac{L^2}{8} \frac{\dfrac{\alpha_1 A_1 + \alpha_2 A_2}{A_1 + A_2} - \dfrac{\alpha_1 B_1 + \alpha_2 B_2}{B_1 + B_2}}{\dfrac{2\sum_1^2 E_i(S_i^3 - S_{i-1}^3)}{3\sum_1^2 E_i(S_i^2 - S_{i-1}^2)} - \dfrac{\sum_1^2 E_i(S_i^2 - S_{i-1}^2)}{2\sum_1^2 E_i T_i}} \tag{A-2}$$

The numerator in the above equation

$$\frac{\alpha_1 A_1 + \alpha_2 A_2}{A_1 + A_2} - \frac{\alpha_1 B_1 + \alpha_2 B_2}{B_1 + B_2} = \frac{(\alpha_1 - \alpha_2)\,(A_1 B_2 - A_2 B_1)}{(A_1 + A_2)\,(B_1 + B_2)}$$

$$= \frac{(E_1 E_2 (S_1^2 - S_0^2) T_2 - E_1 E_2 (S_2^2 - S_1^2) T_1)}{\sum_1^2 E_i (S_i^2 - S_{i-1}^2) \sum_1^2 E_i T_i} (\alpha_1 - \alpha_2) \qquad \text{(A-3)}$$

Therefore, the difference of the expansion value between the two layers is proportional to the center deflection, that is

$$W = \frac{L^2 C}{8} (\alpha_1 - \alpha_2) \qquad \text{(A-4)}$$

where C is a constant for given dimension and moduli of the materials determined by

$$C = \frac{E_1 E_2 (S_1^2 - S_0^2) T_2 - E_1 E_2 (S_2^2 - S_1^2) T_1}{\left(\frac{2\sum_1^2 E_i (S_i^3 - S_{i-1}^3)}{3\sum_1^2 E_i (S_i^2 - S_{i-1}^2)} - \frac{\sum_1^2 E_i (S_i^2 - S_{i-1}^2)}{2\sum_1^2 E_i T_i} \right) \sum_1^2 E_i (S_i^2 - S_{i-1}^2) \sum_1^2 E_i T_i} \qquad \text{(A-5)}$$

It can be shown that W is also a function of E_1/E_2 , T_1/T_2 and a reference thickness, say T_2.

By letting $T_2 = T$ and $T_1 = cT_2 = cT$

one get $S_0 = 0$

$$S_1 = T_1 = cT$$

$$S_2 = T_1 + T_2 = (c+1)T$$

$$S_1^2 - S_0^2 = c^2T^2$$

$$S_2^2 - S_1^2 = (2c+1)T^2 \qquad \text{(A-6)}$$

$$S_1^3 - S_0^3 = c^3T^3$$

$$S_2^3 - S_1^3 = (3c^2+3c+1)T^3$$

The center deflection may be expressed as

$$W = \frac{L^2}{8R} = \frac{L^2}{8} \frac{\dfrac{\alpha_1 E_1 c^2 T^2 + \alpha_2 E_2 (2c+1) T^2}{E_1 c^2 T^2 + E_2 (2c+1) T^2} - \dfrac{\alpha_1 E_1 cT + \alpha_2 E_2 T}{E_1 cT + E_2 T}}{\dfrac{2 (E_1 c^3 T^3 + E_2 (3c^2+3c+1) T^3)}{3 (E_1 c^2 T^2 + E_2 (2c+1) T^2)} - \dfrac{E_1 c^2 T^2 + E_2 (2c+1) T^2}{2 (E_1 cT + E_2 T)}}$$

$$= \frac{L^2}{8T} \frac{\dfrac{\alpha_1 \beta c^2 + \alpha_2 (2c+1)}{\beta c^2 + (2c+1)} - \dfrac{\alpha_1 \beta c + \alpha_2}{\beta c + 1}}{\dfrac{2 (\beta c^3 + (3c^2+3c+1))}{3 (\beta c^2 + (2c+1))} - \dfrac{\beta c^2 + (2c+1)}{2 (\beta c + 1)}} \qquad \text{(A-7)}$$

or

$$W = \frac{D}{T} = \frac{D}{T_2} \qquad \text{(A-8)}$$

$$W = f(E_1/E_2, T_1/T_2) \frac{(\alpha_1 - \alpha_2) L^2}{T_2} \qquad \text{(A-9)}$$

where D is a function of β ($= E_1/E_2$) and c ($= T_1/T_2$), and is a constant for given materials.

The relationship between W and E_1/E_2 , $\alpha_1 - \alpha_2$ can be extended to any two-component multi-layer laminated beams.

The effect of E_1/E_2 and T_1/T_2 on W is not linear. Certain combination of these two would leads to maximum warping. In order to find

out E_1/E_2 ratio at a point when warping reaches to the maximum for certain T_1/T_2 , rewrite Equation (A-7) as

$$W = \frac{6L^2}{8T} \frac{(\beta c+1)(\alpha_1 \beta c^2 + \alpha_2 (2c+1)) - (\beta c^2 + (2c+1))(\alpha_1 \beta c + \alpha_2)}{4(\beta c+1)(\beta c^3 + (3c^2+3c+1)) - 3(\beta c^2 + (2c+1))(\beta c^2 + (2c+1))}$$

$$= \frac{3L^2}{4T} \frac{(\beta c+1)(\alpha_1 \beta c^2 + \alpha_2 (2c+1)) - (\beta c^2 + 2c+1)(\alpha_1 \beta c + \alpha_2)}{4(\beta c+1)(\beta c^3 + 3c^2+3c+1) - 3(\beta c^2 + 2c+1)^2}$$

$$= \frac{3L^2 (\alpha_2 - \alpha_1) c(1+c)}{4T} \frac{\beta}{4(\beta c+1)(\beta c^3 + 3c^2+3c+1) - 3(\beta c^2 + 2c+1)^2}$$

To get a β value when warping reaches the extreme, consider T , c be constants. Take the first partial derivative of W respect to β , and set to zero, solve for β ,

$$\frac{\partial W}{\partial \beta} = 0 \qquad \text{(A-10)}$$

Only the numerator needs to be zero. Therefore, we have

$$4(\beta c+1)(\beta c^3 + 3c^2+3c+1) - 3(\beta c^2 + 2c+1)^2$$

$$-\beta [4c(\beta c^3 + 3c^2+3c+1) + 4c^3(\beta c+1) - 6c^2(\beta c^2 + 2c+1)] = 0$$

After manipulating, we get

$$4(\beta c^3 + 3c^2 + 3c + 1) - 4\beta c^3(\beta c + 1) + (\beta c^2 + 2c + 1)(3\beta c^2 - 6c^2\beta - 3) = 0$$

This can be simplified as

$$1 - \beta^2 c^4 = 0 \qquad \text{(A-11)}$$

or take the positive root, when $\beta = \frac{1}{c^2}$, warping reaches the maximum. In other words,

$$\left.\frac{E_1}{E_2}\right|_{w=max} = \left(\frac{T_2}{T_1}\right)^2 \qquad \text{(A-12)}$$

When $T_1/T_2 = 1$, the thickness of both layers are the same, the maximum warping occurs if E_1/E_2 reaches 1.

Equation (A-12) implies that one should avoid to use a E_1/E_2 value which leads to maximum warping if desired. For instance, if the structure requires $T_1/T_2 = \frac{1}{3}$, the maximum warping occurs when a value of $E_1/E_2 = 9$. Either $E_1/E_2 > 9$ or $E_1/E_2 < 9$ would reduce the warp.

APPENDIX B

APPENDIX B

COMPUTER PROGRAM OF

VISCO-ELASTIC BEAM THEORY

```
      PROGRAM NONLWARP
C     ************************************************
C     * AK, BK, CK, DK, AFK, BTK ARE CONSTANTS FROM   *
C     * FREE HYGROSCOPE EXPANSION REGRESSION:         *
C     * EPH = A + B * T ** AF                         *
C     * Y = C + D * EXP(BT * T)                       *
C     * K USED FOR DIFFERENT LAYERS                   *
C     ************************************************
C     IMPLICIT REAL*8 (A-H,O-Z)
      DIMENSION AK(2),BK(2),CK(2),DK(2),AFK(2),BTK(2),
     + H(2),S(3)
      DIMENSION ST(2),F(2),E(2),SE(2),SN(2,2),SNI(2,2)
      DIMENSION EP(100),RK(100),EPHO(2)
      OPEN (UNIT = 1, FILE = 'input',STATUS = 'OLD')
      OPEN (UNIT = 2, FILE = 'output',STATUS = 'NEW')
C     ++++++++INITIALIZE++++++++++
      WRITE (2,230)
      DO 10 I = 1,2
      READ (1,200) AK(I),BK(I),CK(I),DK(I),AFK(I),
     + BTK(I),H(I)
      WRITE (2,240) AK(I),BK(I),CK(I),DK(I),AFK(I),
     + BTK(I),H(I)
200   FORMAT(' ',7F15.12)
10    CONTINUE
      READ (1,210) AL,DT
      WRITE (2,220) AL,DT
210   FORMAT(' ',2F10.5)
220   FORMAT(//' ','SPAN LENGTH: ',F7.1,//' ',
     + 'DT = ',F7.3)
230   FORMAT(' ',5X,'AK(I)',7X,'BK(I)',7X,'CK(I)',7X,
     + 'DK(I)',5X,'AFK(I)',5X,'BTK(I)',5X,'H(I)'/)
240   FORMAT(/' ',2F12.9,2F12.1,2F10.6,F10.2)
```

```
      S(1) = 0.
      S(2) = H(1)
      S(3) = H(1) + H(2)
      EP(1) = 0.
      RK(1) = 0.
      RKI = 0.
      TT = 168.
      DO 5 K = 1,2
5     EPHO(K) = 0.
C     ++++++++CALCULATE++++++++++
      NT = INT(TT/DT)
      DO 80 M = 1, NT
      DO 20 K = 1, 2
      E(K) = 0.
      F(K) = 0.
20    CONTINUE
      DO 70 N = 1, M
      AYT = 0.
      BYT = 0.
      DYT = 0.
      HNT = 0.
      HMT = 0.
      T = N * DT
      T1 = (N-1) * DT
      T2 = T - T1
      DO 50 K = 1, 2
      A = AK(K)
      B = BK(K)
      C = CK(K)
      D = DK(K)
      AF = AFK(K)
      BT = BTK(K)
      IF (N.EQ.1) THEN
      EPHI = EPHO(K)
      ELSE
      EPHI = A + B * T1 ** AF
      END IF
      EPH = A + B * T ** AF
      DEP = (EPH - EPHI)/DT
      Y = C + D * EXP(BT * T2)
      AY = Y * (S(K+1) - S(K))
      BY = Y * (S(K+1)**2 - S(K)**2)/2
      DY = Y * (S(K+1)**3 - S(K)**3)/3
      HN = Y * (S(K+1) - S(K)) * DEP
      HM = Y * (S(K+1)**2 - S(K)**2)/2 * DEP
      AYT = AYT + AY
```

```
      BYT = BYT + BY
      DYT = DYT + DY
      HNT = HNT + HN
      HMT = HMT + HM
50    CONTINUE
      IF (N.EQ.M) GO TO 100
      E(1) = E(1) + AYT * EP(N) + BYT * RK(N)
      E(2) = E(2) + BYT * EP(N) + DYT * RK(N)
100   F(1) = F(1) + HNT
      F(2) = F(2) + HMT
70    CONTINUE
      DO 60 I = 1, 2
60    ST(I) = F(I) - E(I)
      SN(1,1) = AYT
      SN(1,2) = BYT
      SN(2,1) = BYT
      SN(2,2) = DYT
      CALL INVERSE (SN,SNI)
      CALL MULTIPL (SNI,ST,SE)
      EP(M) = SE(1)
      RK(M) = SE(2)
      RKI = RKI + RK(M) * DT
      EPI = EPI + EP(M) * DT
80    CONTINUE
      W = RKI * AL**2 / 8.
      WRITE (2,250) W,EPI
250   FORMAT (//' ','WARPING OVER 30 INCH: ',F7.4,//
     + ' ','NORMAL EXPANSION: ',F9.7)
      END
C
C
      SUBROUTINE INVERSE(SN,SNI)
      DIMENSION SN(2,2),SNI(2,2)
      DO 10 I = 1, 2
      DO 10 J = 1, 2
      SNI(I,J) = 0.
10    CONTINUE
      DETM = SN(1,1)*SN(2,2)-SN(1,2)*SN(2,1)
      SNI(1,1) = SN(2,2)/DETM
      SNI(2,2) = SN(1,1)/DETM
      SNI(1,2) = - SN(1,2)/DETM
      SNI(2,1) = - SN(2,1)/DETM
      RETURN
      END
C
C
```

```
      SUBROUTINE MULTIPL(AM,BM,CM)
      DIMENSION AM(2,2),BM(2),CM(2)
      DO 10 I = 1, 2
10    CM(I) = 0.
      DO 20 I = 1, 2
      DO 20 J = 1, 2
      CM(I) = CM(I) + AM(I,J) * BM(J)
20    CONTINUE
      RETURN
      END
```

APPENDIX C

APPENDIX C

COMPUTER PROGRAM OF

WARPRAND

```
      PROGRAM WARPRAND
C     ****************************************************
C     THE PROGRAM CALCULATES THE WARPING OF A MULTILAYER
C     BEAM
C     USING ELASTIC THEORY WITH DEFINED MEAN AND COEFF. OF
C     VAR.
C     ****************************************************
      PARAMETER (LTEMP = 10, NRAND = 1000)
      DIMENSION MOE(LTEMP),THICK(LTEMP),EXPAN(LTEMP),
     + CVMOE(LTEMP),CVTHICK(LTEMP),CVEXPAN(LTEMP),
     + STDMOE(LTEMP),STDTHICK(LTEMP),STDEXPAN(LTEMP),
     + MOER(NRAND,LTEMP),THICKR(NRAND,LTEMP),
     + EXPANR(NRAND,LTEMP), + WARP(NRAND
      REAL*8 MOE, MOER
      OPEN(UNIT = 1, FILE = 'input', STATUS = 'OLD')
      OPEN(UNIT = 2, FILE = 'output', STATUS = 'OLD')
C
C     INPUT NO. OF LAYERS, LENGTH OF THE BEAM (IN), NO. OF
C     RANDOM RUN
C
      READ (1, *) NLAYER, ALENGTH, NR
      WRITE (2, 1) NLAYER, ALENGTH, NR
C
      DO 10 I = 1, NLAYER
      MOE(I) = 0.
      THICK(I) = 0.
      EXPAN(I) = 0.
      CVMOE(I) = 0.
      CVTHICK(I) = 0.
      CVEXPAN(I) = 0.
      STDMOE(I) = 0.
      STDTHICK(I) = 0.
      STDEXPAN(I) = 0.
10    CONTINUE
```

```
C       INPUT MOE(PSI), THICK(IN), EXPAN(IN/IN), CV(%) FOR
C       EACH LAYER
        DO 20 I = 1, NLAYER
        READ (1, *) MOE(I), CVMOE(I), THICK(I), CVTHICK(I),
     +  EXPAN(I), CVEXPAN(I)
        STDMOE(I) = CVMOE(I) * MOE(I) / 100.
        STDTHICK(I) = CVTHICK(I) * THICK(I) / 100.
        STDEXPAN(I) = CVEXPAN(I) * EXPAN(I) / 100.
        WRITE (2, 5) MOE(I), THICK(I), EXPAN(I),
     +  CVMOE(I), CVTHICK(I), CVEXPAN(I),
     +  STDMOE(I), STDTHICK(I), STDEXPAN(I)
20      CONTINUE
        DO 40 N = 1, NR
        S = 0.
        SS = 0.
        SUMI = 0.
        SUMJ = 0.
        SUMK = 0.
        SUML = 0.
        SUMM = 0.
        DO 30 I = 1, NLAYER
        R1 = RAND(ARGUMENT) - 0.5
        MOER(N,I) = R1 * STDMOE(I) / 0.258 + MOE(I)
        R2 = RAND(ARGUMENT) - 0.5
        THICKR(N,I) = R2 * STDTHICK(I) / 0.258 + THICK(I)
        R3 = RAND(ARGUMENT) - 0.5
        EXPANR(N,I) = R3 * STDEXPAN(I) / 0.258 + EXPAN(I)
        SS = S
        S = S + THICKR(N, I)
        D = MOER(N,I) * (S**3 - SS**3)
        E = MOER(N,I) * (S**2 - SS**2)
        F = MOER(N,I) * THICKR(N,I)
        G = MOER(N,I) * EXPANR(N,I) * (S**2 - SS**2)
        H = MOER(N,I) * EXPANR(N,I) * THICKR(N,I)
        SUMI = SUMI + D
        SUMJ = SUMJ + E
        SUMK = SUMK + F
        SUML = SUML + G
        SUMM = SUMM + H
30      CONTINUE
        RADIUS = ((2*SUMI)/(3*SUMJ)-SUMJ/(2*SUMK))/
     +  ((SUML/SUMJ) - (SUMM/SUMK))
        WARP(N) = ALENGTH ** 2 / (8 * RADIUS)
40      CONTINUE
        WRITE (2,6)
        DO 50 N = 1, NR
```

```
50      WRITE (2,*) (MOER(N,I), I = 1,NLAYER)
        WRITE (2,7)
        DO 60 N = 1, NR
60      WRITE (2,*) (THICKR(N,I), I = 1,NLAYER)
        WRITE (2,8)
        DO 70 N = 1, NR
70      WRITE (2,*) (EXPANR(N,I), I = 1,NLAYER)
        WRITE (2,9)
        DO 80 N = 1, NR
80      WRITE (2,*) WARP(N)
1       FORMAT (' ','NO. OF LAYER: ',I5/'LENGTH OF BEAM:',
     +  F5.0/'NO. OF RANDOM RUNS: ',I5/)
5       FORMAT (' ',15X,'MOE(I)',5X,'THICKNESS(I)',5X,
     +  'EXPANSION(I)',/2X,'MEAN: ',F13.2,F13.3,3X,F13.6
     +  /2X,'C.V.(%):',2F13.3,F16.3/2X,'STD: ', 2F13.3,
     +  3X, F13.6/)
6       FORMAT (' ',/12X,'MOE (1)',12X,'MOE (2)',12X,
     +  'MOE (3)'/)
7       FORMAT (' ',/9X,'THICK(1)',9X,'THICK(2)',
     +  9X,'THICK(3)'/)
8       FORMAT (' ',/9X,'EXPAN(1)',9X,'EXPAN(2)',9X,
     +  'EXPAN(3)'/)
9       FORMAT (' ',/5X,'WARP'/)
        END
```